

# Visbreaking of Oilsands Bitumen between 150 and 300 °C

by

Lina Maria Yañez Jaramillo

A thesis submitted in partial fulfillment of the requirements for the degree of

Master of Science

in

Chemical Engineering

Department of Chemical and Materials Engineering  
University of Alberta

© Lina Maria Yañez Jaramillo, 2016

## ABSTRACT

Visbreaking is described as a mild thermal cracking, low conversion process, which industrially operates in the temperature range of 430 to 490 °C. Conversion is limited by the onset of coke formation. The main objective of visbreaking in conventional oil refineries is to reduce the viscosity of the fuel oil without causing oil instability. When visbreaking is applied to the upgrading of Canadian oil sands bitumen, the objective is to reduce the bitumen viscosity to facilitate pipeline transport. It was reported that bitumen viscosity could be decreased by two orders of magnitude by visbreaking in the temperature range 340 to 400 °C. These observations suggested that it might be possible to decrease bitumen viscosity without much cracking conversion, which provided justification for exploring even milder visbreaking conditions. The objective of this study was to determine and understand the changes in the properties of oil sands bitumen over time when the bitumen was exposed to temperatures in the range 150 to 300 °C for 1 to 8 hours. The study employed Cold Lake bitumen and it was found that the change in viscosity with time was not monotonous and was influenced by both temperature and reaction time. It was possible to reduce bitumen viscosity by two orders of magnitude over the temperature range 250 to 300 °C. A discontinuity in the viscosity behaviour was observed between 200 and 250 °C. At 200 °C and lower temperatures there was no improvement in viscosity. It was postulated that free radical addition reactions were responsible for the observed increase in viscosity. It is also worthwhile pointing out that hydrogen disproportionation was evident even at 150 °C.

**Keywords:** Visbreaking, viscosity, oil sands bitumen

## **Dedication**

To my mom and my aunt for all their love and support

## Acknowledgements

I would like to thank Professor Arno de Klerk for his patience and support during these two years, for giving me the opportunity to join his research group, an amazing research group. I have learnt a lot not only about my research but life...

I want to thank my labmates for their help and company but specially to Natalia Montoya, her advices and friendship have been invaluable. Special thanks to my friends back home for making me laugh with their stories and jokes. I have always felt closer to home! And my best friend, Stefania, for being always there, every time that I have needed support or just some silly times.

I would also like to thank Adrian, Babi, for his company all these years. I think I would not have seen so many versions of myself without your help.

Finally, I want to acknowledge the funding provided by the Canadian Government through the Helmholtz-Alberta Initiative (HAI). Thanks to Canada, a wonderful country, for this experience.

## Table of Contents

<b>1. INTRODUCTION.....</b>	<b>1</b>
<b>1.1 INTRODUCTION.....</b>	<b>1</b>
<b>1.2 OBJECTIVE .....</b>	<b>2</b>
<b>1.3 SCOPE OF WORK.....</b>	<b>2</b>
<b>2. LITERATURE REVIEW.....</b>	<b>5</b>
<b>2.1 GEOLOGY OF BITUMEN .....</b>	<b>5</b>
<b>2.2 ORIGIN OF PETROLEUM .....</b>	<b>5</b>
<b>2.2.1 Canadian Oil Sands.....</b>	<b>8</b>
<b>2.3 RELEVANCE OF GEOLOGY TO THE PRESENT WORK .....</b>	<b>9</b>
<b>2.4 COMPOSITION OF OIL SAND .....</b>	<b>9</b>
<b>2.5 COMPOSITION OF BITUME .....</b>	<b>10</b>
<b>2.5.1 SARA fractions .....</b>	<b>11</b>
<b>2.5.2 Proton nuclear magnetic resonance (<sup>1</sup>H NMR) spectroscopy .....</b>	<b>12</b>
<b>2.5.3 Fourier transform infrared (FT-IR) spectroscopy .....</b>	<b>13</b>
<b>2.6 SOME IMPORTANT PROPERTIES.....</b>	<b>13</b>
<b>2.6.1 Density .....</b>	<b>13</b>
<b>2.6.2 Viscosity .....</b>	<b>15</b>
<b>2.6.3 Refractive Index.....</b>	<b>15</b>
<b>2.6.4 Relevance of composition and properties to the present work .....</b>	<b>15</b>
<b>2.7 UPGRADING TECHNOLOGIES .....</b>	<b>16</b>
<b>2.7.1 Visbreaking.....</b>	<b>17</b>
<b>2.7.2 Why should bitumen be upgraded? .....</b>	<b>20</b>
<b>3. VISBREAKING OF OIL SANDS BITUMEN AT 300 °C.....</b>	<b>25</b>
<b>3.1 INTRODUCTION .....</b>	<b>25</b>
<b>3.2 EXPERIMENTAL.....</b>	<b>25</b>
<b>3.2.1 Materials.....</b>	<b>25</b>
<b>3.2.2 Equipment and procedure .....</b>	<b>26</b>
<b>3.2.3 Analyses .....</b>	<b>28</b>

<b>3.3</b>	<b>RESULTS</b> .....	29
<b>3.3.1</b>	<b>Material Balance</b> .....	29
<b>3.3.2</b>	<b>Products characterization</b> .....	31
<b>3.3.2.1</b>	<b>Viscosity</b> .....	31
<b>3.3.2.2</b>	<b>Refractive Index</b> .....	33
<b>3.3.2.3</b>	<b><sup>1</sup>H NMR</b> .....	35
<b>3.3.2.4</b>	<b>Density</b> .....	36
<b>3.3.2.5</b>	<b>FT-IR</b> .....	38
<b>3.3.2.6</b>	<b>Asphaltene content</b> .....	39
<b>3.3.2.7</b>	<b>Gas Chromatography</b> .....	39
<b>3.3.2.8</b>	<b>Solid content</b> .....	40
<b>3.4</b>	<b>DISCUSSION</b> .....	41
<b>3.4.1</b>	<b>Viscosity-Measurement temperature relationship</b> .....	41
<b>3.4.2</b>	<b>Viscosity-Residence time relationship</b> .....	43
<b>3.4.3</b>	<b>Effects of hydrogen disproportionation</b> .....	44
<b>3.4.4</b>	<b>Refractive Index-Density relationship</b> .....	46
<b>3.4.5</b>	<b>FT-IR Hints</b> .....	47
<b>3.4.6</b>	<b>Gaseous product contribution</b> .....	47
<b>3.4.7</b>	<b>Solid product contribution</b> .....	48
<b>3.5</b>	<b>CONCLUSIONS</b> .....	49
<b>4.</b>	<b>VISBREAKING OF OIL SANDS BITUMEN AT 250 °C</b> .....	52
<b>4.1</b>	<b>INTRODUCTION</b> .....	52
<b>4.2</b>	<b>EXPERIMENTAL</b> .....	52
<b>4.2.1</b>	<b>Materials</b> .....	52
<b>4.2.2</b>	<b>Equipment and procedure</b> .....	52
<b>4.2.3</b>	<b>Analyses</b> .....	53
<b>4.3</b>	<b>RESULTS</b> .....	53
<b>4.3.1</b>	<b>Material Balance</b> .....	53
<b>4.3.2</b>	<b>Products characterization</b> .....	54
<b>4.3.2.1</b>	<b>Viscosity</b> .....	55
<b>4.3.2.2</b>	<b>Refractive Index</b> .....	56
<b>4.3.2.3</b>	<b><sup>1</sup>H NMR</b> .....	58
<b>4.3.2.4</b>	<b>Density</b> .....	59

4.3.2.5	FT-IR .....	61
4.3.2.6	Asphaltene content .....	62
4.3.2.7	Gas Chromatography .....	63
4.3.2.8	Solid content .....	64
4.4	DISCUSSION .....	65
4.4.1	Temperature effects .....	65
4.4.2	Consequences of residence time .....	66
4.4.3	Spectroscopy hints .....	67
4.4.4	Gas products .....	69
4.4.5	Solid products .....	69
4.5	CONCLUSIONS .....	70
5.	VISBREAKING OF OIL SANDS BITUMEN AT 200 °C .....	73
5.1	INTRODUCTION .....	73
5.2	EXPERIMENTAL .....	73
5.2.1	Materials .....	73
5.2.2	Equipment and procedure .....	74
5.2.3	Analyses .....	74
5.3	RESULTS .....	74
5.3.1	Material Balance .....	74
5.3.2	Product characterization .....	76
5.3.2.1	Viscosity .....	76
5.3.2.2	Refractive Index .....	77
5.3.2.3	<sup>1</sup> H NMR .....	79
5.3.2.4	Density .....	80
5.3.2.5	FT-IR .....	82
5.3.2.6	Asphaltene content .....	83
5.3.2.7	Gas Chromatography .....	84
5.3.2.8	Solid content .....	84
5.4	DISCUSSION .....	85
5.4.1	Viscosity – Temperature relationship .....	85
5.4.2	Influence of reaction time .....	86
5.4.3	NMR results .....	88
5.4.4	The relationship between Density and Refractive Index .....	89

5.4.5	FT-IR .....	90
5.4.6	Gaseous products .....	90
5.4.7	Solid products .....	90
5.5	CONCLUSIONS .....	91
6.	VISBREAKING OF OIL SAND BITUMEN AT 150 °C .....	93
6.1	INTRODUCTION .....	93
6.2	EXPERIMENTAL .....	93
6.2.1	Materials .....	93
6.2.2	Equipment and procedure .....	93
6.2.3	Analyses .....	94
6.3	RESULTS .....	94
6.3.1	Material Balance .....	94
6.3.2	Product characterization .....	95
6.3.2.1	Viscosity .....	95
6.3.2.2	Refractive Index .....	97
6.3.2.3	<sup>1</sup> H NMR .....	98
6.3.2.4	Density .....	99
6.3.2.5	FT-IR .....	101
6.3.2.6	Asphaltene content .....	102
6.3.2.7	Gas Chromatography .....	103
6.3.2.8	Solid content .....	104
6.4	DISCUSSION .....	105
6.4.1	Viscosity changes .....	105
6.4.2	Impact of reaction time .....	106
6.4.3	Compositional changes .....	107
6.4.4	FT-IR .....	109
6.4.5	Gaseous and solid products .....	109
6.5	CONCLUSIONS .....	110
7.	CONCLUSIONS .....	112
7.1	INTRODUCTION .....	112
7.2	MAJOR CONCLUSIONS .....	112
7.3	FUTURE WORK .....	114
7.4	PRESENTATIONS .....	115

**BIBLIOGRAPHY** ..... 117

<b>TABLE</b>	<b>LIST OF TABLES</b>	<b>PAGE</b>
<i>Table 2.1</i>	<i>Typical Crude Oil pipeline specification [31]</i>	<i>21</i>
<i>Table 3.1</i>	<i>Characterization of Cold Lake Bitumen</i>	<i>26</i>
<i>Table 3.2</i>	<i>Mass balance (wt %) for visbreaking reactions at 300 °C and initial pressure of 4 MPa for different reaction times</i>	<i>30</i>
<i>Table 3.3</i>	<i>Product yield (wt%) for visbreaking reactions at 300 °C and initial pressure of 4 MPa for different reaction times</i>	<i>30</i>
<i>Table 3.4</i>	<i>Viscosity data performed to Visbreaking products under 300 °C and initial pressure 4 MPa</i>	<i>32</i>
<i>Table 3.5</i>	<i>Refractive Index measurements performed on visbreaking products after 300 °C and initial pressure 4 MPa reaction</i>	<i>33</i>
<i>Table 3.6</i>	<i>Density measurements performed on visbreaking products after 300 °C and internal pressure 4 MPa reaction and different reaction times</i>	<i>38</i>
<i>Table 3.7</i>	<i>Gas products associated to pyrolysis of bitumen after reaction at 300 °C and initial pressure 4 MPa</i>	<i>40</i>
<i>Table 3.8</i>	<i>Experimental viscosity values for 300 °C visbreaking products at different measurement temperatures calculated by Eq. 1.</i>	<i>42</i>
<i>Table 4.1</i>	<i>Mass balance (wt %) for visbreaking reactions at 250 °C and initial pressure of 4 MPa for different reaction times</i>	<i>53</i>
<i>Table 4.2</i>	<i>Product yield (wt%) for visbreaking reactions at 250 °C and initial pressure of 4 MPa for different reaction times</i>	<i>54</i>
<i>Table 4.3</i>	<i>Viscosity of visbreaking products after reaction at 250 °C and initial pressure of 4 MPa</i>	<i>55</i>
<i>Table 4.4</i>	<i>Refractive Index measurements performed on visbreaking products after 250 °C and internal pressure 4 MPa reaction</i>	<i>58</i>
<i>Table 4.5</i>	<i>Density measurements performed at four different temperatures: 20, 30, 40 and 60 °C to visbreaking products after reaction at 250 °C</i>	<i>61</i>
<i>Table 4.6</i>	<i>Gaseous products generated during visbreaking under 250 °C and an initial pressure of 4 MPa</i>	<i>64</i>

Table 5.1	<i>Overall Mass Balance (wt %) for Visbreaking Reactions at 200 °C and Constant Pressure (4 MPa) for different reaction times</i>	75
Table 5.2	<i>Product yield (wt%) for visbreaking reactions at 200 °C and initial pressure of 4 MPa for different reaction times</i>	75
Table 5.3	<i>Viscosity data from measurements performed to Visbreaking products under 200 °C and initial pressure 4 MPa</i>	76
Table 5.4	<i>Refractive Index measurements performed on visbreaking products after 200 °C and initial pressure 4 MPa reaction</i>	79
Table 5.5	<i>Density measurements performed at four different temperatures: 20, 30, 40 and 60 °C to visbreaking products after reaction at 200 °C</i>	82
Table 5.6	<i>Gas products associated to pyrolysis of bitumen at 200 °C</i>	84
Table 6.1	<i>Mass Balance (wt %) for Visbreaking Reactions at 150 °C and Constant Pressure (4 MPa) for different reaction times</i>	94
Table 6.2	<i>Product yield (wt%) for visbreaking reactions at 150 °C and initial pressure of 4 MPa for different reaction times</i>	95
Table 6.3	<i>Viscosity data from measurements performed to Visbreaking products under 150 °C and initial pressure 4 MPa</i>	96
Table 6.4	<i>Refractive Index measurements performed on visbreaking products after 150 °C and internal pressure 4 MPa reaction</i>	98
Table 6.5	<i>Density measurements performed at four different temperatures: 20, 30, 40 and 60 °C to visbreaking products after reaction at 150 °C</i>	101
Table 6.6	<i>Gas products associated to pyrolysis of bitumen at 150 °C</i>	104

<b>FIGURE</b>	<b>LIST OF FIGURES</b>	<b>PAGE</b>
Figure 2.1	<i>Products expected from the oil maturation. This plot was adapted from [3].</i>	7
Figure 2.2	<i>Influence of the deposition time and depth in hydrocarbons generated [3].</i>	7
Figure 2.3	<i>Formation charts involve in the Canadian oil sands deposits. [5]</i>	9
Figure 2.4	<i>Typical scheme of oil sands [6]. The oil sand microstructure is from Takamura, K., Can. J. Chem. Eng. 1982 60, 538-545.</i>	10
Figure 2.5	<i>SARA fractionation</i>	11
Figure 2.6	<i>NMR spectrum with typical aromatic and aliphatic proton regions. Adapted from [9].</i>	12
Figure 2.7	<i>Comparison of water and bitumen Density-Temperature relationship [19].</i>	14
Figure 2.8	<i>Typical process scheme for a coil visbreaker [28].</i>	19
Figure 2.9	<i>Typical process scheme for soaker visbraker [28]</i>	19
Figure 3.1	<i>Batch reactor system used for visbreaking reactions.</i>	27
Figure 3.2	<i>Images taken of 1h, 4h and 8h reaction solids in SEM. Reaction conditions: 300 °C and 4 MPa.</i>	31
Figure 3.3	<i>Viscosity of visbreaking products obtained under 300 °C, initial pressure of 4 MPa and reaction time varying between 1 and 8 hours. Measurements were performed at four different temperatures: 20, 30, 40 and 60 °C.</i>	32
Figure 3.4	<i>Viscosity result for raw Cold Lake Bitumen.</i>	33
Figure 3.5	<i>Refractive Index results for Visbreaking Products at 300 °C, initial pressure of 4 MPa and different reaction times: a) Refractive index vs Time; and b) Refractive index vs Measurement Temperature.</i>	34
Figure 3.6	<i>NMR results of visbroken products after 300 °C, initial pressure of</i>	36

4 MPa and different times: a) NMR spectra for pyrolysis products;  
b) % Aliphatic protons vs Time.

Figure 3.7	Density of visbreaking products obtained under 300 °C, initial pressure of 4 MPa and different reaction times: a) Density vs Time; and b) Density vs Measurement Temperature	37
Figure 3.8	FTIR spectra for pyrolysis products after 300 °C, initial pressure of 4 MPa and different times reaction.	38
Figure 3.9	Asphaltene content for visbreaking products by n-pentane precipitation following the ASTM D6560 standard test method. The value at 0 h is for the bitumen feed.	39
Figure 3.10	Solid content in pyrolysis products after reaction at 300 °C. The value at 0 h refers to the feed material.	41
Figure 3.11	Viscosity of visbreaking products after 300 °C, internal pressure of 4 MPa along different residence times using Eq. (2).	42
Figure 3.12	Viscosity measurements of the pyrolysis products under 300 °C and 4 MPa at different residence time reaction.	43
Figure 3.13	Area under the curve extracted from the NMR spectra, comparing the amount of the type of proton found in visbroken samples after 300 °C reaction	45
Figure 4.1	Viscosity of visbreaking products obtained under 250 °C, initial pressure of 4 MPa and reaction time varying between 1 and 8 hours	55
Figure 4.2	Refractive Index results for Visbreaking Products at 250 oC, initial pressure of 4 MPa and different reaction times: a) Refractive index vs Time; and b) Refractive index vs Measurement Temperature.	57
Figure 4.3	NMR results of visbroken products after 250 °C, initial pressure of 4 MPa and different times: a) NMR spectra for pyrolysis products; b) % Aliphatic protons vs Time	59
Figure 4.4	Density of visbreaking products obtained under 250 °C, initial pressure of 4 MPa and different reaction times: a) Density vs Time; and b) Density vs Measurement Temperature.	60
Figure 4.5	FTIR spectra for pyrolysis products after 250 °C, initial pressure of 4 MPa and different times reaction	62

Figure 4.6	<i>Asphaltene content for visbreaking products by ASTM D6560. 0 h refers to Raw Cold Lake bitumen</i>	63
Figure 4.7	<i>Solid content in pyrolysis products after reaction at 250 °C</i>	65
Figure 4.8	<i>Viscosity of visbreaking products after 250 °C and 4 MPa along different residence times based on Eq. 1</i>	66
Figure 4.9	<i>Area under the curve extracted from the NMR spectra, comparing the different the amount of the type of proton found for visbreaking products obtained at 250 °C reaction</i>	68
Figure 5.1	<i>Viscosity of visbreaking products obtained under 200 °C, initial pressure of 4 MPa and reaction time varying between 1 and 8 hours</i>	76
Figure 5.2	<i>Refractive Index results for Visbreaking Products at 200 °C, initial pressure of 4 MPa and different reaction times: a) Refractive index vs Time; and b) Refractive index vs Measurement Temperature</i>	78
Figure 5.3	<i>NMR results of visbroken products after 200 °C, initial pressure of 4 MPa and different times: a) NMR spectra for pyrolysis products; b) % Aliphatic protons vs Time</i>	80
Figure 5.4	<i>Density of visbreaking products obtained under 200 °C, initial pressure of 4 MPa and different reaction times: a) Density vs Time; and b) Density vs Measurement Temperature</i>	81
Figure 5.5	<i>FTIR spectra for pyrolysis products after 200 °C, initial pressure of 4 MPa and different times reaction</i>	83
Figure 5.6	<i>Asphaltene content for visbreaking products by ASTM D6560</i>	83
Figure 5.7	<i>Solid content in pyrolysis products after reaction at 200 °C</i>	85
Figure 5.8	<i>Viscosity of visbreaking products after 200 °C and 4 MPa along different residence times based on the ASTM relationship</i>	86
Figure 5.9	<i>Viscosity measurements performed at 1.2 s<sup>-1</sup> to visbreaking products under 200 °C and initial pressure of 4 MPa</i>	87
Figure 5.10	<i>Area under the curve extracted from the NMR spectra, comparing the amount of the type of proton found in visbroken samples after 200 °C reaction</i>	88

<i>Figure 6.1</i>	<i>Viscosity of visbreaking products obtained under 150 °C, initial pressure of 4 MPa and reaction time varying between 1 and 8 hours. Measurements were performed at four different temperatures: 20, 30, 40 and 60 °C</i>	96
<i>Figure 6.2</i>	<i>Refractive Index of visbreaking products obtained under 150 °C, initial pressure of 4 MPa and reaction time varying between 1 and 8 hours. Measurements were performed at four different temperatures: 20, 30, 40 and 60 °C</i>	97
<i>Figure 6.3</i>	<i>NMR results of visbreaking products obtained under 150 °C, initial pressure of 4 MPa and reaction time varying between 1 and 8 hours</i>	99
<i>Figure 6.4</i>	<i>Density of visbreaking products obtained under 150 °C, initial pressure of 4 MPa and reaction time varying between 1 and 8 hours. Measurements were performed at four different temperatures: 20, 30, 40 and 60 °C</i>	100
<i>Figure 6.5</i>	<i>FT-IR results of visbreaking products obtained under 150 °C, initial pressure of 4 MPa and reaction time varying between 1 and 8 hours</i>	102
<i>Figure 6.6</i>	<i>Asphaltene content of visbreaking products obtained under 150 °C, initial pressure of 4 MPa and reaction time varying between 1 and 8 hours</i>	103
<i>Figure 6.7</i>	<i>Solid content of visbreaking products obtained under 150 °C, initial pressure of 4 MPa and reaction time varying between 1 and 8 hours</i>	105
<i>Figure 6.8</i>	<i>Viscosity of visbreaking products after 150 °C and 4 MPa along different residence times calculated through the ASTM relationship</i>	106
<i>Figure 6.9</i>	<i>Area under the curve extracted from the NMR spectra, comparing the amount of the type of proton found in visbroken samples after 150 °C reaction</i>	108

# 1. INTRODUCTION

## 1.1 INTRODUCTION

Canada has one of the largest oil reserves in the world, more than 90 % of them correspond to oil sands. Bitumen, the oil part in oil sands, is considered the heaviest fraction of petroleum. It is composed of aromatic, naphthenic and paraffinic hydrocarbons, but it is also rich in oxygen, nitrogen, sulfur and heteroatoms and contains some traces of metals. It is characterized by its poor fluidity, appearing semi-solid at ambient conditions and it is dark brown in color. Its Conradson Carbon Residue (CCR) content is high and its H/C ratio is low compared to most conventional crude oils.

Due to its geological origin and geographical (environmental) conditions, oil recovery from the Canadian oil sands deposits cannot employ conventional methods. Transportation of the recovered bitumen by pipeline is not possible because of its high viscosity (over  $10^3$  Pa.s at 20 °C) and that is why some form of dilution or treatment is required. An improvement in bitumen properties is necessary to facilitate pipeline transport.

In order to upgrade bitumen, several technologies have been developed. The oldest method came to the market around 1930s and it has been widely employed. Visbreaking (viscosity breaking), as it is called, is a mild thermal cracking process conducted typically at 430 to 490 °C, which avoids coking reactions [1]. The nature of this upgrading method is based on the cleavage of some molecular bonds. Thermal conversion leads mainly to homolytic bond scission and the resulting reactions follows free-radical chemistry. In a thermal cracking process the reactions are time and temperature dependent. However, oil sands bitumen does not follow a typical behaviour and the operating conditions can be less severe [2].

Visbreaker technologies can be divided into two types: a) soaker visbreaking and b) coil visbreaking. Both differ in temperature and residence time conditions. On one side, soaker visbreaking uses lower temperatures and longer residence times. On the other side, coil visbreaking works at higher temperatures but shorter residence times [3]. The stability of the visbroken products, which refers to its tendency to form a second phase, will limit the severity of

this process [4] and ways to suppress coking is important [5]. In crude oil refineries the main objective is to reduce viscosity and pour point without causing fuel instability in order to meet N° 6 fuel oil specifications. When visbreaking is applied to oil sands bitumen, the purpose is mainly to decrease the viscosity and thereby improve the fluidity of the oil. Since visbreaking uses mild cracking conditions, this will favor an increase in liquid product yield with less gas. Coke suppression could maximize the conversion and increase the yield of lighter liquid products [6].

Previous works in this field [2] have found that carrying out visbreaking under a lower temperature will cause an improvement on the products which could be a consequence of a better selectivity compared with those obtained under more severe conditions. This unexpected behaviour could be considered as the main motivation for this work, trying to understand those changes that bitumen experienced due to visbreaking and the influence of its operation conditions.

From a practical engineering point of view, it was of interest to establish to what extent the visbreaking temperature could be decreased while still decreasing viscosity without an impractical increase in residence time. As the temperature is decreased it was anticipated that less thermal cracking would take place, which would reduce the loss of material to gas, but at the same time it could undermine the ability to decrease product viscosity.

From an academic point of view, it was of interest to explore a temperature range of operation, from 150 to 300 °C, which has not been explored much. Even though low temperatures may not lead to practical benefit, material processes at higher temperatures must still pass through the lower temperature range during heating. Hence, the academic justification had some practical value too.

## **1.2 OBJECTIVE**

The objective of this work was to study and understand the changes over time when oil sands bitumen was exposed to temperatures in the range 150 to 300 °C.

## **1.3 SCOPE OF WORK**

In order to have an idea about bitumen behaviour and changes that could be expected, it was necessary to read proper literature related to this work. Chapter 2 will talk about the influence of

geology on bitumen composition, upgrading techniques and the motivation for upgrading bitumen.

The experimental section will comprise Chapter 3-6. Every chapter will talk about one set of experiments performed in batch mode. Every chapter will vary the reaction time; however, temperature will be changed from chapter to chapter.

The set of experiments previously mentioned are described:

- a) From previous works [2][7], it was found that a reduction on temperature will lead some changes that may improve bitumen properties. The first set corresponds to those experiments carried out at 300 °C, an initial pressure of 4 MPa and a variation of reaction time between 1 and 8 hours. This work is presented in Chapter 3. Big changes and a high conversion was not expected due to the low temperature. This temperature was selected, because it represents borderline thermal cracking conditions.
- b) In Chapter 4 the temperature was lowered to 250 °C for the second set of experiments. These experiments were performed with an initial pressure of 4 MPa and reaction time was varied between 1 and 8 hours. This temperature was selected because it represents the highest practical temperature that can be achieved by high pressure (4 MPa) steam without employing a furnace for feed heating. This temperature is also below the temperature threshold for thermal and it was anticipated that only the most labile bonds would dissociate at this temperature.
- c) Response of bitumen after a thermal cracking at 250 °C could show interesting changes, or not. A further decrease in temperature would indicate whether the same behavior persists. Chapter 5 will discuss the results obtained from visbreaking at 200 °C, 4 MPa and a reaction time in the range of 1-8 hours.
- d) Chapter 6 will be the last experimental section. Experiments were carried out at 150 °C, an initial pressure of 4 MPa and reaction time that varied between 1 and 8 hours. This temperature is so low that thermal bond dissociation can almost completely be ruled out. This investigation served as control, since it would reveal changes inherent to bitumen when the fluidity is sufficiently increased to allow free liquid phase movement.

Lastly, in order to conclude the investigation and consider the results obtained in all the experimental sections, overall conclusions will be presented in Chapter 7. All the changes observed due to reaction time and temperature variations are discussed in this chapter.

### Literature cited

[1] Speight, J. G. Visbreaking: A technology of the past and the future. *Scientia Iranica* **2012**, *19* (3), 569-573.

[2] Wang, L.; Zachariah, A.; Yang, S.; Prasad, V.; De Klerk, A. Visbreaking oilsands-derived bitumen in the temperature range of 340-400 °C. *Energy Fuels* **2014**, *28*, 5014-5022.

[3] Speight, J.G. *The Chemistry and Technology of Petroleum*, 4th ed.; Taylor & Francis Group: Boca Raton, FL, 2007.

[4] McKetta, J. J. *Petroleum Processing Handbook*; M. Dekker: New York, 1992.

[5] Gary, J. H.; Handwerk, G. E. *Petroleum Refining: Technology and Economics*, 5ed; Taylor & Francis Group: Boca Raton, FL, 2007, p. 111-115.

[6] Zachariah, A.; Wang, L.; Yang, S.; Prasad, V.; De Klerk, A. Suppression of coke formation during bitumen pyrolysis. *Energy Fuels* **2013**, *27*, 3061-3070.

[7] Wang, L. Low temperature visbreaking. MSc thesis, University of Alberta, Edmonton, AB, Canada, 2013.

## **2. LITERATURE REVIEW**

### **2.1 GEOLOGY OF BITUMEN**

It is very important and interesting to know which processes were involved in petroleum formation. Most of the oil reservoirs are formed in agreement with it; however, every reservoir will have specific characteristics due to the environmental and depositional processes.

### **2.2 ORIGIN OF PETROLEUM**

Petroleum is an organic substance, it basically consists of carbon-hydrogen molecules but it can also be accompanied by sulfur, oxygen and nitrogen in smaller quantities. Petroleum can be found in three different phases: gas, liquid and semi-solid. The gas phase is referred to as natural gas, which comprises of the smallest hydrocarbons ( $C_1$ - $C_5$ ). Liquid phase, or oil, will cover a wide range of hydrocarbons, including some asphaltene molecules. On the other side, the semi-solid phase consists of larger hydrocarbon molecules and complex asphaltene structures [1].

Petroleum reservoirs are spread around the world. However, these deposits will vary from place to place based on the geological and environmental conditions. Some similarities can be found between conventional crude oil reservoirs, but heavy oil and bitumen deposits will differ. In general, petroleum is formed in sedimentary basins. Sediments will accumulate in subsided areas; over geological time, they will develop layers that will solidify into sedimentary rocks due to high pressures and temperatures. The presence of the remains of plants or microorganisms is decisive for petroleum generation.

Petroleum is the result of a perfect combination of high temperatures and millions of years. The source of the organic matter determines the proportion of natural gas and crude oil. Organic material can be terrestrial (humic) or aquatic (sapropelic) in origin. Humic is linked to continental sediments and it is characterized by a low hydrogen content. In humic material the amount of nitrogen and oxygen are relatively high. This kind of material is considered a gas-prone, which means that a large amount of gas will be produced instead of oil. On the other side, sapropelic organic material will show high hydrogen content, which is derived from spores, cuticles and similar plant constituents. In contrast with the humic organic material, sapropelic organic material will tend to generate oil instead of gas [2].

Hydrocarbon generation will be influenced by temperature, time and pressure. Oil and gas are the result of a succession of chemical reaction, they will obey Arrhenius equation (Eq. 1).

$$k = Ae^{E_a/RT} \quad (1)$$

Where k is the rate constant, A is the pre-exponential factor (independent of temperature),  $E_a$  is the activation energy of the reaction, R is the universal constant and T is the temperature in Kelvins.

The dependency with temperature is obvious. However, when petroleum formation is considered as a chemical reaction, timing and burial pressure will also affect the final product. It is not going to be the same having a source rock heated at certain temperature for one year than for millions of years [3]. The transformation ratio of the organic matter will be affected by temperature and time, the influence of temperature will be exponential while the influence of time will be linear [3]. Figure 2.1 will show the relationship between temperature and burial. This figure is a modified version in order to show the equivalency in depth and temperature to define an immature, mature and post-mature of sediments. In the first place, immature sediments are the ones located below 60 °C and around 1.2 km depth. In this region, a biochemical gas will be produced. Between 60 and 120 °C and 1.2 – 3.5 km, it will be the region where the oil and wet gas will be generated. Lastly, the post-mature region occurs when the deposit temperature is 120 °C or more and 3.5 km or deeper. Dry gas will be produced in this area.

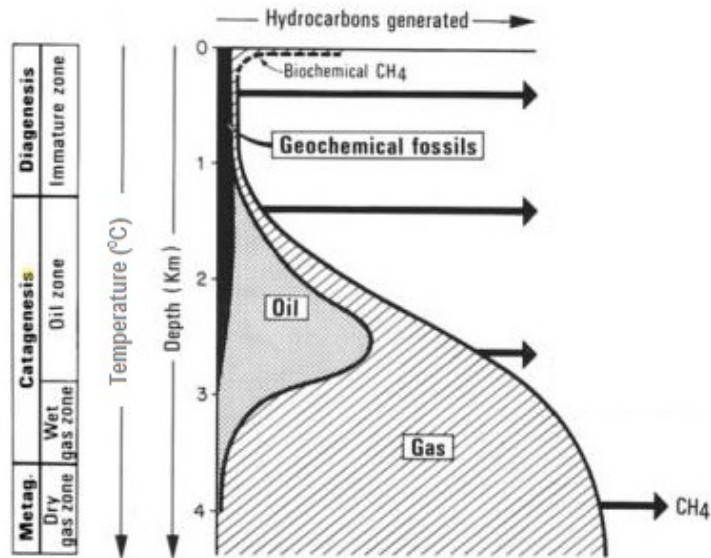


**Figure 2.1.** Products expected from the oil maturation. This plot was adapted from [3].

Figure 2.2 show the influence of the deposition time. A recent deposition will require a higher temperature to be degraded to the same extent as an older deposit. This shows that there is a relationship between time and temperature, as is to be expected from a chemical reaction.

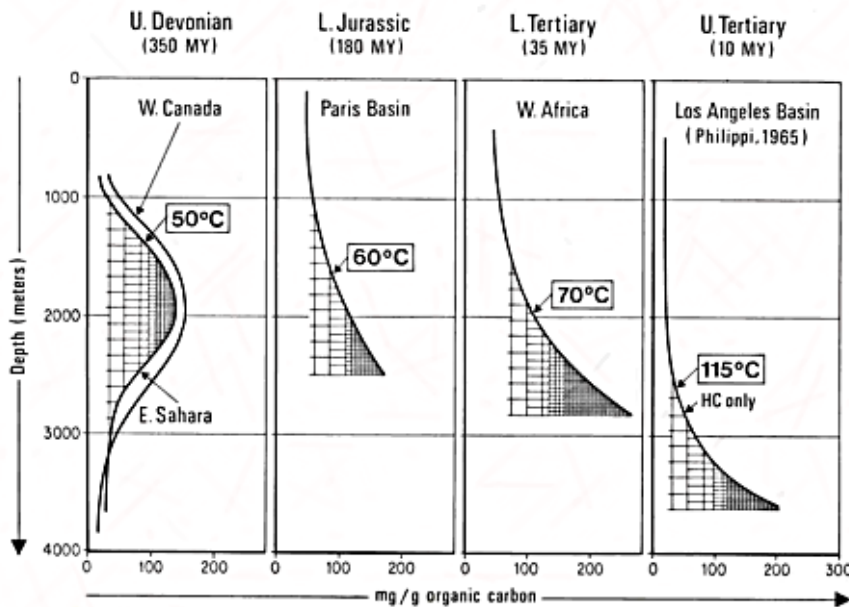


**Figure 2.2.** Influence of the deposition time and depth in hydrocarbons generated [3].

Knowing the conditions required for the organic matter transformation, it is necessary to explain how the formation process of a reservoir takes place. Since petroleum density is generally lower than water density, it could fill pores, voids and cracks in the source rock. This density difference will be the driving force for petroleum migration until it gets trapped into sealed reservoirs. When petroleum migrates, but it does not find a non-porous cap rock to act as a trap, it will keep flowing until it gets to the atmosphere, or an overlying water which will result in a loss of lighter hydrocarbons, water washing and biodegradation [1]. It is important to mention that the permeability and porosity will determine the proper migration of the petroleum. They could be considered the most important properties in a reservoir.

### **2.2.1 Canadian Oil Sands**

One of the largest oil reserves in the world is located in the Western Canadian Sedimentary Basin (WCSB), it occupies mainly British Columbia and Alberta area but it also has areas in Saskatchewan and Manitoba. Lower Cretaceous and Upper Devonian strata constitute the bitumen deposits. Three main deposits can be distinguished: Athabasca (Wabasca), Cold Lake and Peace River. The geology of the formations is shown in Figure 2.3.

Athabasca deposit is located in northeast Alberta, its geological formation comprises of several formations such as McMurray, Clearwater, Grand Rapids and Wabiskaw and it is considered the largest single accumulation of oil in the world [4]. It contains continental as well as marine sediments, and compared with the other deposits, Athabasca shows a very uniform and mature mineralogy that consists of quartz, feldspar and rock fragments.

Cold Lake deposits are formed by McMurray and Clearwater formations and the upper and lower Grand Rapids. It is characterized by fine to medium grains of quartz sand and it is dominated by a fluvial facies. Besides, it also contains coastal sandstones and marine shale deposits [5]. The Peace River area is the third largest deposit of the Alberta oil sands deposits [6]. It is formed by the Cretaceous Gething and Bluesky formation. Due to a water sand layer in this structure, enhanced recovery methods like steam injection are favoured [7].

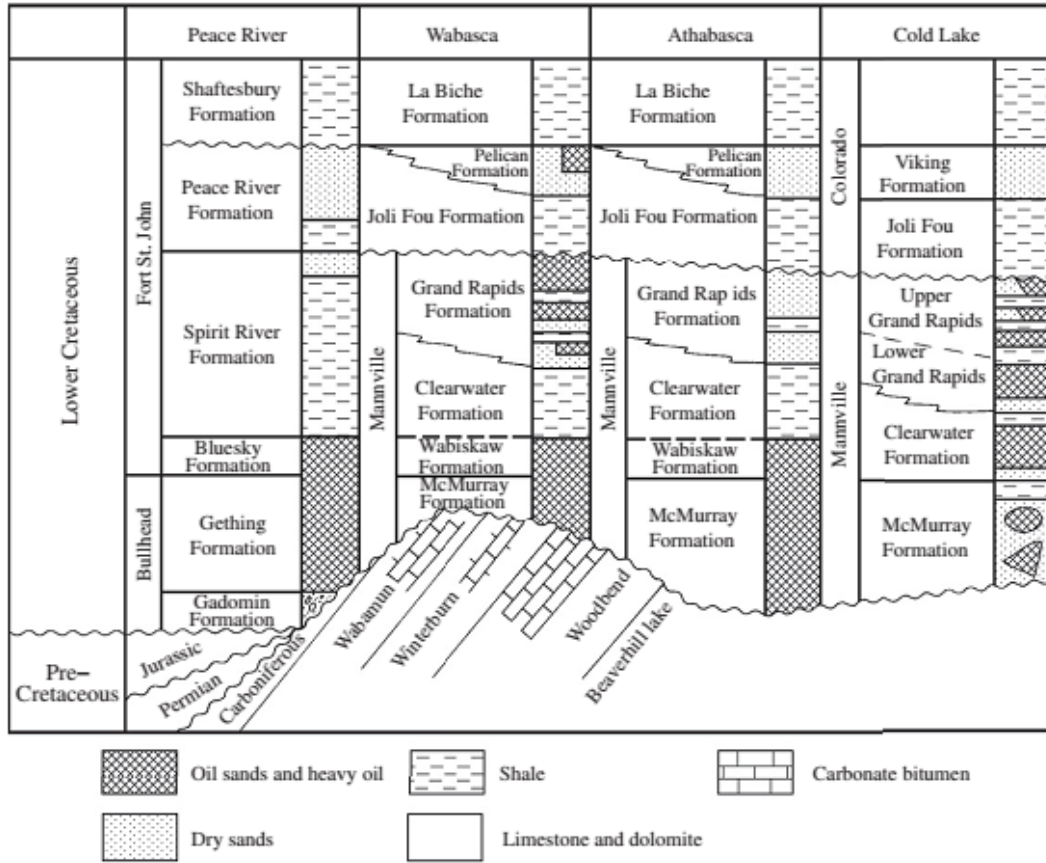


**Figure 2.3.** Formation charts involve in the Canadian oil sands deposits. [5]

### 2.3 RELEVANCE OF GEOLOGY TO THE PRESENT WORK

Bitumen behaviour reflects the geological composition and processes behind it. There are two factors that will affect the character of a crude: the nature of the source material and the original deposition environment [8]. A “young” crude oil is related with young formations, they are defined by a low gravity, high boiling point with a very small amount of gasoline, significant amounts of nitrogen and oxygen-containing compounds and high viscosity. Canadian oil sands fit in that description even though, they were not formed in a recent formation. In these cases, the deposition environment will determine the resulting crude.

### 2.4 COMPOSITION OF OIL SANDS

Oils sands are formed by bitumen, sand, fines, clays, salts, water, chemisorbed gases and colloids which makes it a very complex multiphase system [7]. Bitumen usually cements the

unconsolidated clastic sand grains (broken piece of older rock), this is commonly the result of shallow depths which can cause drilling and completion problems [9].

Regarding the reservoir rock properties, the porosity for the Athabasca deposits varies between 25 and 40 % without much changes. It was also found that there is an inverse relationship between water and bitumen content. When the water content is low, the bitumen reaches the highest saturation. On the other hand, fines follow a linear relationship with water which means that a higher water content will represent a high fines concentration. As a consequence, the bitumen recovery method will lose efficiency, because the fines will decrease the permeability of the rock by obstructing the porous structure and reducing bitumen flow rate.

Figure 2.4 shows a hypothetical diagram presented in [6], a thin water layer can be identified and it is called connate water. It cannot be reduced and it represents less than 5 %. The stability of this layer is due to a pressure generated by repulsive and attractive forces, as a result of the electrical double layer and London-Van der Waals interactions.

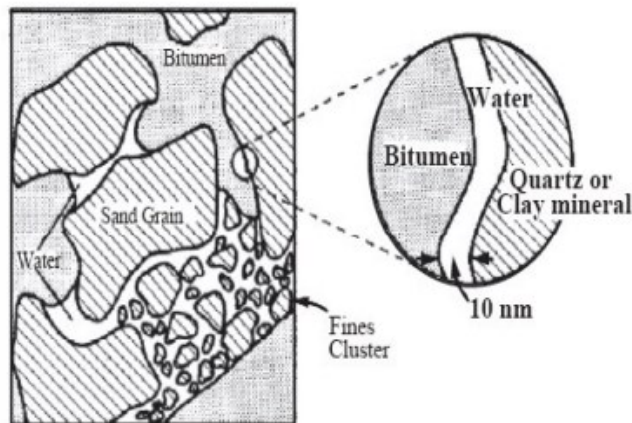


**Figure 2.4.** Typical scheme of oil sands [6]. The oil sand microstructure is from Takamura, K., Can. J. Chem. Eng. 1982 60, 538-545.

## 2.5 COMPOSITION OF BITUMEN

Bitumen is seen as the heaviest form of petroleum, it is characterized by its dark brown color, its high viscosity, its semisolid appearance and its high content of nitrogen, sulfur, oxygen and other

heteroatoms. The high viscosity (greater than  $10^4$  mPa.s) and high density (higher than  $1$  g/cm<sup>3</sup>) gives an idea about its behaviour [7].

As a form of petroleum, it is possible to recognize three main types of hydrocarbons: paraffins (acyclic alkanes), naphthenes (cycloalkanes) and aromatics (benzene and its derivatives). The proportion of each type affects the density and it will determine if it is light or a heavy crude. In the case of bitumen, naphthenes and aromatics dominate the composition. This chemical composition determines the nature of the expected products after an upgrading treatment.

### 2.5.1 SARA fractions

In order to characterize bitumen, one of the common methods is to fractionate it into saturates, aromatics, resins and asphaltenes. This procedure is found in ASTM D-2007. It is based on the solubility properties of each fraction [10]. A flow diagram is shown in Figure 2.5.

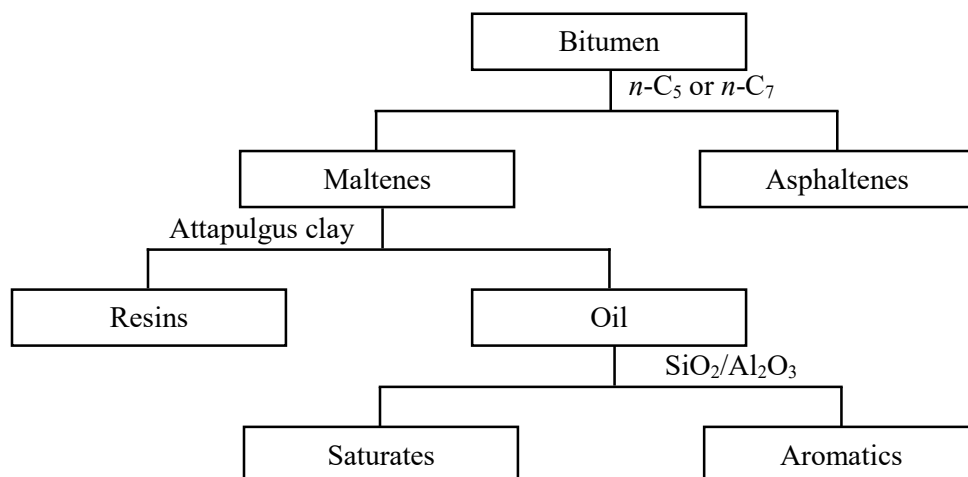


**Figure 2.5.** SARA fractionation.

Initially, asphaltenes are precipitated through the ASTM D6560-12 [11], *n*-pentane or *n*-heptane can be used for this purpose. In this work asphaltenes were determined using *n*-pentane only. The precipitation with *n*-pentane results in two fractions, one corresponds to asphaltenes (precipitate) and the other one is named maltenes (*n*-pentane soluble). Using chromatography, the *n*-pentane solution can be separated. An Attapulgus clay is used for this objective. As a result, resins are adsorbed onto the clay and a non-adsorbed fraction is collected that is called “oils”. This last solution will be separated using a silica/alumina column into two fractions, one

is going to adsorbed is called aromatics and the fraction that is not adsorbed is named saturates. In this study only the asphaltenes fraction was determined, because fluidity was of interest and the asphaltenes may affect fluidity.

### 2.5.2 Proton nuclear magnetic resonance ( $^1\text{H}$ NMR) spectroscopy

Nuclear Magnetic Resonance (NMR) is related to the atomic nuclei response to magnetic fields. The interaction of an external magnetic field with the spinning magnetic nuclei will generate measurable signal [12]. NMR spectroscopy has been widely utilised since its discovery in 1940s to determine organic compounds structure. It has also used for reservoir characterization since 1950s. Nowadays, the NMR logging tools have been developed to evaluate petroleum reservoirs [13].

Structural information is usually obtain through NMR. Figure 2.6 shows a spectra to present two types of protons that could be identified by NMR:

- Aromatic protons ( $\text{H}_{\text{aro}}$ )
- Aliphatic protons ( $\text{H}_{\text{ali}}$ )

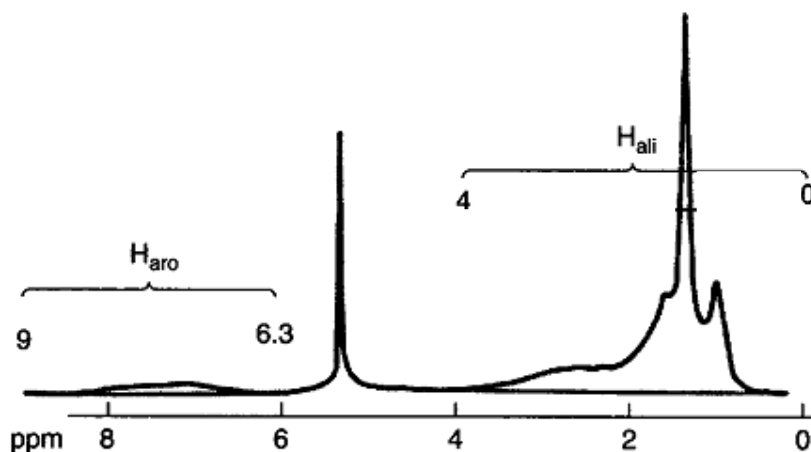


**Figure 2.6.** NMR spectrum with typical aromatic and aliphatic proton regions. Adapted from [9].

The identification of these kind of protons could be used to quantify the ratio between them. In that way, any changes experienced in bitumen structures may be identified by the variation on this ratio. Besides, the region related to aliphatic protons can be used to determine different types

of protons such as primary aliphatic ( $\sim 0.9$  ppm), secondary aliphatic ( $\sim 1.3$  ppm) and benzylic protons ( $\sim 2.3$  ppm) [14].

### **2.5.3 Fourier transform infrared (FT-IR) spectroscopy**

Infrared spectroscopy has been considered an useful tool to identify molecular structures. It is based on the light absorption of covalent bonds in molecules [15]. Every type of bond will absorb the light with a different intensity and frequency, this makes the chemical functionalities possible. Bitumen spectrum has to be analyzed very careful because some interferences can be observed e.g. band absorptions overlapping, shift of wave number due to dimer formation, electron withdrawing neighboring groups and conjugation, or structural geometry of the studied functional group and its neighborhood [15].

Some important peaks were identified. The stretch of the methyl C-H bond could be found at  $\sim 2970$   $\text{cm}^{-1}$  or  $2872$   $\text{cm}^{-1}$  depending on the asymmetric or symmetric stretch respectively. Methylene C-H stretch absorption can be observed in  $2926$  or  $2853$   $\text{cm}^{-1}$  if it is asymmetric or symmetric correspondingly. These bands suggest the aliphatic nature of those functional group [16]. The  $700$  to  $900$   $\text{cm}^{-1}$  region can confirm that, characteristic bands related to C-H and aromatic C-H out-of-plane bending modes can be found [17]. Additional to those bands, between  $\sim 1465$  and  $1380$   $\text{cm}^{-1}$  the aliphatic methyl and methylene groups show absorption bands as a consequence of the vibrational bending.

## **2.6 SOME IMPORTANT PROPERTIES**

As part of the bitumen characterization, some properties could give information about the formation process, as well as the changes and products expected when bitumen is subjected to upgrading processes.

### **2.6.1 Density**

Density is defined as mass per unit volume. Density will vary according to the bitumen composition. In general, aromaticity will increase bitumen density. But another factors can increase it, i.e. molecular weight, polarity, asphaltene content, and the presence of sulfur, nitrogen, oxygen and some traced metals.

In oil industry, it is important to consider two more quantities:

- Specific gravity (SG) which is the ratio of the density of a substance to the density of a reference substance, usually water at a specific temperature.
- Degrees American Petroleum Institute (API) gravity, it is a measure of how light or heavy is a petroleum liquid is and it is a unit of measure often employed in the oil industry.

API gravity can be calculated through Equation (2)

$$^{\circ}\text{API} = \frac{141.5}{\text{SG of oil at } 15.6^{\circ}\text{C}} \quad (2)$$

API gravity varies between 5° for dense bitumens and around 45° for light crudes.

Bitumen density is temperature dependent, this is related with the coefficient of expansion and it could be considered very important since petroleum products are sold by volume [18]. Figure 2.7 will show a comparison between water and bitumen density in relation to measurement temperature [19].

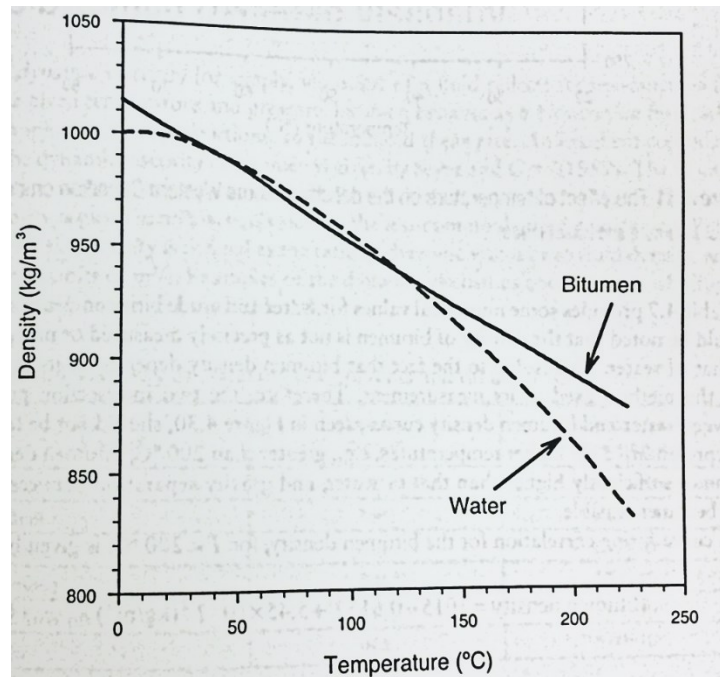


**Figure 2.7.** Comparison of water and bitumen Density-Temperature relationship [19].

Equation (3) [20] can be used to calculate bitumen density,

$$\rho_T = \rho_0 - 0.62T \quad (3)$$

Where  $\rho_T$  and  $\rho_0$  are density [kg/m<sup>3</sup>] at T [K] and 0°C (273 K) respectively.

### 2.6.2 Viscosity

Viscosity can be explained as the resistance of a fluid to flow. It is the results of the internal friction into the fluid respect an external force, e.g. shear rate. A low viscosity could be a consequence of thig molecules where the friction between molecules can be small, allowing the fluid to flow. Also, it can be represented as the ratio between the shear stress and the shear rate.

Conventional recovery technologies and pipeline transportation cannot be used for bitumen due to its high viscosity. Viscosity is extremely temperature dependent and it will decrease with increasing temperature. This dependence can be determined by fitting Equation (4) to the experimental data. This equation is found on the ASTM D341 standard and it is given by

$$\ln[\ln(\mu)] = a_1 + a_2 \ln(T) \quad (4)$$

Where  $\mu$  is viscosity [mPa.s], T is temperature [K],  $a_1$  and  $a_2$  are adjustable parameters.

This behaviour is typical of liquids. Equation (4) expresses viscosity as a function of shear stress and shear rate, it is shown in Equation (5)

$$\mu = \frac{\sigma}{\gamma} \quad (5)$$

Where  $\mu$  is viscosity [Pa.s],  $\sigma$  is the shear stress [Pa] and  $\gamma$  is the shear rate [s<sup>-1</sup>]. Raw bitumen exhibits mild non-Newtonian behavior [7], which means that an increase in shear force will subtly decrease its frictional resistance.

### 2.6.3 Refractive Index

Refractive index is the ratio of the velocity of the light propagation in vacuum respect to a given medium. It can vary with molecular size and structure. A small value in refractive index suggests the presence of paraffinic compounds. On the other hand, high values are related with aromatic compounds. Knowing that, refractive index may be used as an indicator of the degree of upgrading [7] for similar boiling range fractions.

### 2.6.4 Relevance of composition and properties to the present work

Oil sands bitumen is characterized by its high viscosity which is mainly a consequence of its composition. For bitumen and heavy oil engineering, this is considered the most important

transport property because it will be used in calculations and estimations of different transport properties [15]. Viscosity at low temperatures generates a particular interest since it could limit product shipment and pumping calculations.

Density is generally affected by the size and composition of the different compounds found in bitumen, it means density will be correlated with molar mass. Small changes in density are important because based on the density, bitumen and heavy oils are graded and priced. Viscosity and density have a direct relationship, this means that an increase in density will result in an increase in viscosity.

The response of refractive index is also related with the sample composition, it will affect by the molecular size and structure of the compounds found in bitumen. Subtle changes in refractive index are common and they cannot be neglected since they will help to analyze or try to analyze the differences in bitumen composition.

## **2.7 UPGRADING TECHNOLOGIES**

As it was mentioned before, bitumen has a high viscosity and a low H/C ratio. Due to its own characteristics, an upgrading treatment is required either to be transport or to obtain high-value products. There are four main challenges [21] associated with the upgrading and ultimate refining of bitumen:

- Reduce viscosity. A decrease in this property will mean an improvement in fluidity, this is crucial for recovery and transportation purposes.
- A higher H/C ratio. The low ratio in bitumen is due to the varied and complex nature of bitumen. This is the result of a high content of aromatic and naphthenic compounds that makes harder to meet the specification.
- Heteroatom reduction. The high content of sulfur, nitrogen and oxygen makes the refinery process harder. Heteroatoms also contribute to aggregation, which influences fluidity and fouling. In particular, specifications about sulfur are rigorous for transportation fuels.
- Decrease the boiling point distribution. To achieve this, a molecular size reduction of bitumen compounds is required. Just 20 % of the molecules in bitumen distil in the distillate range. The distillation curve expressed in terms of normal boiling point

temperature of bitumen indicate that bitumen consists of more higher boiling material that is found in benchmark crude oils, such as West Texas Intermediate (WTI).

Several technologies have been developed in order to upgrade bitumen. Choosing a suitable technology will depend on some important factors [22]:

- Crude oil price
- Level of impurities
- Upgraded oil quality objective
- Refinery process scheme

Upgrading processes can be classified as hydrogen addition and carbon rejection technologies [23]. The first category will increase of the H/C ratio due to the reaction development with hydrogen added to the system; some of the processes are hydrocracking, hydrovisbreaking and the donor solvent liquefaction. On the other hand, carbon rejection technologies are based on a redistribution of hydrogen in order to increase the H/C ratio of one fraction at the expense of decreasing the H/C ratio of another fraction. The processes that can be found in this category are: visbreaking, steam cracking and coking.

Of these different residue upgrading processes, only visbreaking is relevant to the current study.

### **2.7.1 Visbreaking**

Visbreaking (or viscosity breaking) was developed for the first time at the beginning of the twentieth century. It is a mild thermal cracking process, which is usually focused on the reduction of fuel oil viscosity to meet the specifications. It is considered a low-cost and low-severity process which has made it widely used around the world.

For this technology, conversion is not the main objective, it reaches around 20 to 30 % conversion to liquids in the transportation fuel boiling range [24][25]. Under this mild conditions, the liquid yield is favoured as well as the boiling point is decreased and the fluidity is improved through a viscosity reduction. It also allows a decreasing in gas and coke production.

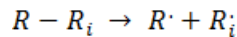
A typical visbreaking operation ranges are 430-490 °C and 0.5-1.2 MPa with significant short reaction times (1-15 min). It is considered a simple process. Vacuum residue is pumped to a furnace that is designed for these mild conditions which are controlled to avoid the formation of

coke during the thermal cracking reaction. During visbreaking operation, many reactions take place in parallel [26]:

- Cracking of the side chains attached to cycloparaffin or aromatic rings or close to them. Chains are either removed or shortened.
- Cracking of resins to lighter products
- Cracking of naphthenic rings (above 480 °C)

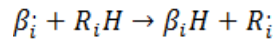
Thermal cracking follows free-radical chemistry, it shows three basic steps [24][27]:

- Initiation: Free radicals are formed through the cleavage of C-C bonds.

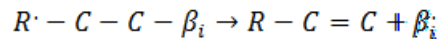


- Propagation: Hydrogen transfer, decomposition and creation of new free radicals, isomerization, cyclization and condensation will take place.

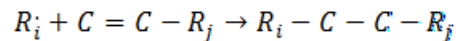
Hydrogen Abstraction



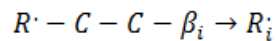
$\beta$ -Scission



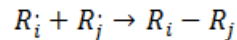
Radical addition



Radical rearrangement



- Termination: Two free radicals form a new bond.



Two types of visbreaking can be found in the industry [28]:

- Coil visbreaking: It is characterized by a high temperature operation with short residence times. A process scheme is shown in Figure 2.8.

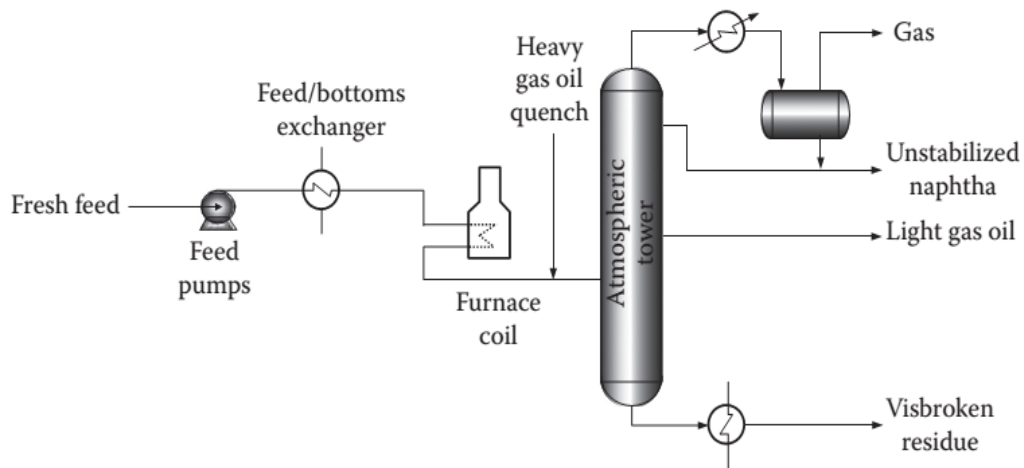
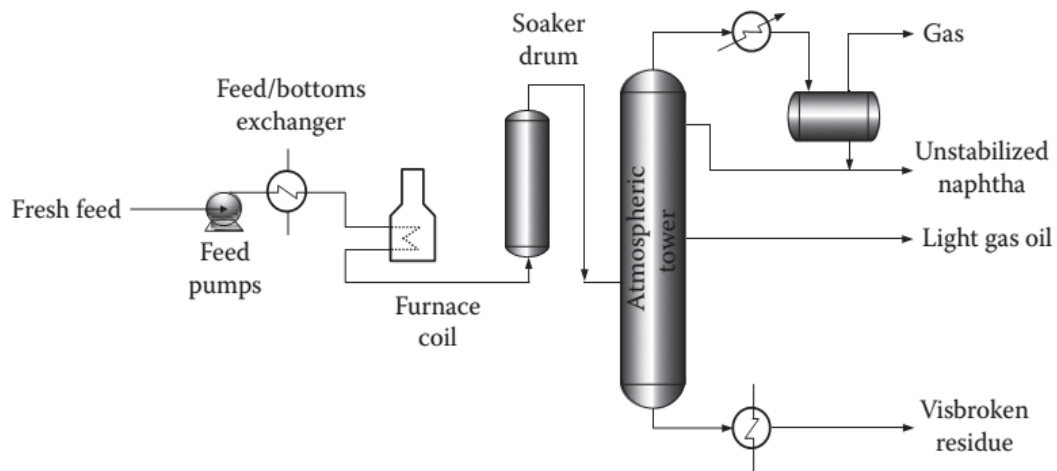


**Figure 2.8.** Typical process scheme for a coil visbreaker [28].

- Soaker visbreaking: It works at low temperature and high residence times. Most of the reaction occurs in a reaction drum or soaker. A typical process scheme is shown in Figure 2.9.



- **Figure 2.9.** Typical process scheme for soaker visbreaker [28]

They differ in the reaction conditions, temperature and residence time. However, the yields obtained and the conversion could be very similar. Fuel consumption is lower in soaker visbreaker, but it requires one additional process vessel compared to a coil visbreaker.

Visbreaking, as a thermal process, shows the limitation typical of this kind of technology which is the product instability. Using low pressures in visbreaking could produce olefins, they are very unstable and tend to undergo secondary reactions, forming gums [29].

In order to improve or modify the performance of this process, some factors should be taken in account: feed properties, temperature, pressure, and residence time. Feed characteristics will depend on the crude oil origin and the extent of topping. It can be affected by the asphaltene content (a high content in this kind of molecules will reduce the conversion), softening point (it could make the feed more susceptible to visbreaking), the Conradson carbon content (an increasing in this value will mean a tendency to increase the coking rate), viscosity (it could decrease with a higher severity). Temperature will vary according to the type of visbreaking used. Higher temperatures tend to form more coke and to reduce the selectivity. Residence time will show a close relationship with temperature. A long residence time will be the result of a low temperature.

### **2.7.2 Why should bitumen be upgraded?**

The oil sands and heavy oil reserves around the world are a significant fraction of the total oil reserves. Around 2 % of the crude oil production comes from the Canadian oil sands. However, the recovery process can be very energy intensive. Most of the Canadian deposits (~ 90 %) lie deep below the surface which make the recovery by a mining process not suitable. In situ recovery technology is required, such as SAGD (Steam-Assisted Gravity Drainage). SAGD consists in series of wells that are drilled into the deposit that allow the injection steam and promote bitumen migration by draining [30]. This is one type of in situ bitumen recovery technology, but it is not a solution for every deposit, since characteristics and conditions may change from one to another.

Once the bitumen is recovered from the oilsands deposit, there are two approaches to decrease the viscosity so that the bitumen can be transported by pipeline to market:

- A blend of naphtha, light hydrocarbons or natural gas condensated and bitumen (also known as *dilbit*) can be prepared as a way to transport bitumen, since such diluted bitumen can meet the pipeline specifications. The diluted mixture behaves as a heavy crude oil and hence it will share some of the same characteristics. The ratio between

diluent and bitumen in this mixture will be seasonally dependent. Put differently, on a constant bitumen basis, the amount of the diluent will vary. Table 2.1 [31] shows the typical pipeline specifications for transportation purposes.

**Table 2.1.** Typical Crude Oil pipeline specification [31].

Shipper Must Furnish Assay to Carrier	
S&W	< 1.0 wt%
Pour Point	< 50 °F
Sour Crude	> 0.5 wt% sulfur (ASTM D1552 or D129)
RVP	< 9.5 psia (at 100 °F)
Sweet Crude	< 0.5 wt% sulfur (ASTM D1552 or D129)
RVP	< 8.0 to 10.0 psia (at 100 °F)
Viscosity	< 325 SSU at 60 °F

- Bitumen can also be upgraded to produce a product that will meet pipeline specifications without the need for diluent. After being subjected to the upgrading processes, not only it is going to favour its transportation, but also it will give more valuable products and hence it is going to increase its economic relevance. The development of new technologies or the improvement of the existing ones is a continuous challenge.

Canada has one of the largest oil reserves in the world, oil sands represent 95 % of them. That means oil sands represents an important role in Canadian economy. However, their characteristics make an upgrading process necessary not only for improving bitumen properties e.g. viscosity or boiling point but for transportation purposes because oil sands do not usually meet the pipeline specifications. Visbreaking is a mature upgrading technology that it has not been explored under “soft” conditions. Low temperatures can provide a better understanding of bitumen response to thermal process and it could represent a cost reduction of the bitumen processing.

## Literature cited

- [1] *The Shell Bitumen Industrial Handbook*; Shell Bitumen: Chertsey, 1995, p.53.
- [2] North, F. K. *Petroleum Geology*; Allen & Unwin: Boston, 1985, p.56.
- [3] Tissot, B. P.; Welte, D. H. *Petroleum Formation and Occurrence*; 2nd, rev. and enl.; Springer-Verlag: Berlin, 1984, p.222.
- [4] Flach, P. D. *Oil Sands Geology: Athabasca Deposit North*; Geological Survey Dept., Alberta Research Council: Edmonton, Alta., Canada, 1984.
- [5] Zou, C. Heavy Oil and Bitumen, In *Unconventional Petroleum Geology*; Elsevier: Burlington, Mass., 2013, p. 307-335.
- [6] Hein, F. J.; Berhane, H. *Cold Lake Oil Sands Area Formation Picks and Correlation of Associated Stratigraphy*; Alberta Geological Survey: Edmonton, 2006.
- [7] Strausz, O. P.; Lown, E. M. *The Chemistry of Alberta Oil Sands, Bitumens and Heavy Oils*; Alberta Energy Research Institute: Calgary, 2003.
- [8] McNab, J. G.; Smith, P. V. Jr; Betts, R. L. The evolution of petroleum. *Ind. Eng. Chem.* **1952**, 44, 2556-2563.
- [9] Huc, A. Y. *Heavy crude oils, from geology to upgrading: an overview*; Editions Technip: Paris, 2011.
- [10] Ancheyta Juárez, J.; Rana, M. S.; Trejo, F. Hydrocracking and Kinetics of Asphaltenes. In *Asphaltenes: Chemical Transformation during Hydroprocessing of Heavy Oils*; CRC Press/Taylor & Francis: Boca Raton, FL, 2009.
- [11] ASTM D6560-12: *Standard test method for Determination of Asphaltenes in Crude Petroleum and Petroleum Products*; ASTM: West Conshohocken, PA, 2012.
- [12] Cowan, B. P. *Nuclear Magnetic Resonance and Relaxation*; Cambridge University Press: New York, 1997.

- [13] Ovalles, C.; Rechsteiner, C. J. Application of NMR Technology in Petroleum Exploration and Characterization. In *Analytical methods in petroleum upstream applications*; CRC Press: Boca Raton, 2015
- [14] Borrego, A. G.; Blanco, C. G.; Prado, J. G.; Diaz, C.; Guillen, M. D. <sup>1</sup>H NMR and FTIR Spectroscopic Studies of Bitumen and Shale Oil from Selected Spanish Oil Shales. *Energy Fuels* **1996**, *10* (1), 77–84.
- [15] Gray, M. R. *Upgrading oilsands bitumen and heavy oil*; Pica Pica Press, an imprint of the University of Alberta Press, 2015.
- [16] Karlsson, R.; Isacsson, U. Application of FTIR-ATR to Characterization of Bitumen Rejuvenator Diffusion. *J. Mater. Civ. Eng.* **2003**, *15*(2), 157-165
- [17] Cronauer, D.; Snyder, R.; Painter, P. Characterization of oil shale by FTIR spectroscopy. *Prepr. Pap.-Am. Chem. Soc., Div. Fuel Chemistry* **1982**, *27* (2), 122-131
- [18] Speight, J. G.; Ozum, B. *Petroleum Refining Processes*; Marcel Dekker: New York, 2002, p. 77.
- [19] Masliyah, J. H.; Xu, Z.; Czarnecki, J. A.; Dabros, M. *Handbook on theory and practice of bitumen recovery from Athabasca Oil Sands*; Cochrane, Alta.: Kingsley Knowledge Pub., 2011-2013.
- [20] Bulkowski, P.; Prill, G. *Abridged internal report on bitumen densities as function of temperature*. Internal report, Research Council of Alberta. Edmonton, Alberta. 1978.
- [21] de Klerk, A.; Gray, M. R.; Zerpa, N. Unconventional Oil and Gas: Oilsands, In *Future Energy: improved, sustainable and clean options for our planet*, 2ed; Letcher, T.M. Ed.; Elsevier: London, 2014, p. 95-116.
- [22] Speight, J. G.; Ancheyta Juárez, J. *Hydroprocessing of Heavy Oils and Residua*; CRC Press: Boca Raton, 2007, p. 45.
- [23] Lee, S.; Speight, J. G.; Loyalka, S. K. *Handbook of Alternative Fuel Technologies*; CRC Press: Boca Raton, 2015, p. 222.

- [24] Ancheyta Juárez, J. *Modeling of processes and reactors for upgrading of heavy petroleum*; CRC Press: Boca Raton, 2013, p. 73.
- [25] Wiehe, I. A. *Process chemistry of petroleum macromolecules*; CRC Press: Boca Raton, 2008, p. 369
- [26] Gary, J. H.; Handwerk, G. E. *Petroleum Refining: Technology and Economics*, 5ed; Taylor & Francis Group: Boca Raton, FL, 2007, p. 112.
- [27] Wang, L. Low temperature visbreaking. MSc thesis, University of Alberta, Edmonton, AB, Canada, 2013
- [28] Speight, J. G. Visbreaking: A technology of the past and the future. *Scientia Iranica* **2012**, *19* (3), 569-573.
- [29] Speight, J.G. *The Chemistry and Technology of Petroleum*, 4th ed.; Taylor & Francis Group: Boca Raton, FL, 2007, p. 487-492.
- [30] Speight, J. G. Heavy Feedstock Refining—The Future. In *Heavy And Extra-Heavy Oil Upgrading Technologies*; Gulf Professional Publishing: Oxford, 2013.
- [31] Manning, F. S.; Thompson, R. E. *Oilfield Processing of Petroleum*; PennWell Books: Tulsa, Okla., 1991, p. 19.

### **3. VISBREAKING OF OIL SANDS BITUMEN AT 300 °C**

#### **3.1 INTRODUCTION**

When visbreaking is applied to oil sands bitumen as method to decrease viscosity, lower temperatures have been studied in recent years and provided interesting results [1][2]. By reducing the temperature to 340 °C [1], it was found that temperature was not a limitation to achieve a significant viscosity reduction. Lowering the reaction temperature usually implies that residence time must be increased, but it was reported that two orders of magnitude viscosity reduction could be achieved at much shorter residence times than predicted by standard visbreaking design equations. Lower temperature reduces the number of molecules that will be cracked and the cracking degree. This said, the chemical and structural changes expected are less than the ones expected from the conventional visbreaking.

What if the temperature can be decreased to an even lower temperature? What behaviour can be expected? Is it still possible to reduce bitumen viscosity at 300 °C? These are some of the questions that motivated this work. Little work has previously been published on thermal conversion of oil sands bitumen and heavy oils at low temperature, e.g. [3][4].

Changing visbreaking conditions, extending the residence time to between 1 and 8 hours, and decreasing the temperature to 300 °C yielded very positive results. Compared with a fresh Cold Lake bitumen sample, visbreaking products after conversion at 300 °C showed a decrease in viscosity with little cracking conversion. The initial work was reported [2].

#### **3.2 EXPERIMENTAL**

##### **3.2.1 Materials**

Bitumen from Cold Lake area in Alberta was used for the visbreaking reactions. The sample was provided by the Center for Oil Sands Innovation (COSI) at University of Alberta. Cold Lake bitumen was characterized and the characterization is shown in Table 3.1. The values were similar to that reported before by Wang, et al. [2].

To pressurize the micro-reactor and guarantee an inert atmosphere, nitrogen (99.998%) supplied by Praxair was employed. In order to extract visbreaking products from the micro-reactor,

methylene chloride (99.9%) provided by Fischer Scientific was utilised. Asphaltenes content was determined by precipitation with *n*-pentane (99.7%) obtained from Fischer Scientific.

**Table 3.1.** Characterization of Cold Lake Bitumen.

Description	Cold Lake bitumen	
	x	s
Microcarbon residue (wt %) <sup>a</sup>	11.4	-
Asphaltenes content (wt %)	16.5	0.9
Elemental Analysis (wt %) <sup>b</sup>		
H	10.3	0.1
C	82.6	0.1
N	0.6	0.1
O <sup>c</sup>	2.6	0.1
S	4.7	0.1
Viscosity (Pa.s)		
20 °C	1655	2
30 °C	353	1
40 °C	88	0
60 °C	9	0

<sup>a</sup>Single sample was analyzed.

<sup>b</sup> Mineral matter free; mineral matter content  $0.9 \pm 0.1$  wt % feed

<sup>c</sup> Oxygen was determined by difference

### 3.2.2 Equipment and procedure

Visbreaking reactions were carried out in a batch reaction system. It was built with 316 stainless steel tubing and fittings supplied by Swagelok. A diagram of the reaction system is shown in Figure 3.1.



**Figure 3.1.** Batch reactor system used for visbreaking reactions.

The initial pressure at ambient temperature was 4 MPa N<sub>2</sub> pressure. The reaction temperature for all experiments was 300 °C (internal reactor temperature) and the residence time was varied between one and eight hours. The reaction time starts when the temperature is reached and a typical heat-up time is 6 min.

For every experiment, 8 g of Cold Lake bitumen were required and reactors were purged and pressurized with nitrogen until reaching the reaction pressure. A fluidized sand bath (An Omega Fluidized Bath FSB-3) was utilised to heat and keep the reaction temperature constant.

After reaction, reactors were removed from the sand bath and cooled down until room temperature. Subsequently, reactors were weighed and depressurized. Light products were collected in a gas bag and analyzed afterwards. Reactors were weighed again, the difference between the pressurized and depressurized reactor mass being the mass of the gaseous products. The remaining products in the reactor were dissolved using methylene chloride as solvent and removed from the reaction system. The remaining reaction products was a two phase mixture of liquid and some solids. The solid content was determined by vacuum filtration using a 0.22µm filter. All solids obtained were dried and weighed at room temperature. Liquid products were heated at 45 °C under atmospheric pressure inside a fumehood for one week. A Fischer Scientific Isotemp hot plate was used to evaporate the solvent.

Material balance closure was generally within 98 to 102 wt%. All the experiments were conducted in triplicate and results were reported as an average with one sample standard deviation, this is shown in Table 3.2 and the reaction yield is presented in Table 3.3.

### 3.2.3 Analyses

Viscosity measurements were carried out in an Anton Paar RheolabQC viscometer. A concentric cylinder CC17/QC-LTC measuring cup was used, its internal diameter is 16.664 mm and 24.970 mm length. Around 4 g of sample were required for the analysis. Viscosity measurements were performed at 4 different temperatures: 20, 30, 40 and 60 °C. The temperature was controlled by a Julabo F25-EH circulating heater/chiller whose controller is capable of maintaining the temperature constant to within  $\pm 0.2$  °C. The samples were measured at a constant shear rate of  $10 \text{ s}^{-1}$ .

Refractive index was determined by an Anton Paar Abbemat 200 using the sodium D-line (589 nm). The equipment was factory calibrated with official standards whose results are accurate to 0.0001 nD. The calibration was not experimentally verified. Measurements were performed at 4 different temperatures: 20, 30, 40 and 60 °C and the accuracy of the temperature control was 0.05 °C.

$^1\text{H}$  Nuclear Magnetic Resonance (NMR) spectra were obtained in a Nanalysis 60 MHz NMReady – 60 spectrometer. The equipment was pre-calibrated with deuterated chloroform. For the analysis, 0.15 g of the sample were dissolved in 0.7  $\mu\text{L}$  deuterated chloroform and placed in NMR tubes. The analysis was performed using the following conditions: 0-12 ppm; number of scans for sample: 32; 14.7 seconds was the average scan time and 4096 points were recorded per scan.

Density measurements were performed in an Anton Paar DMA 4500M. The instrument was calibrated with ultra-distilled water and the temperature accuracy was 0.01 °C. Results were accurate to  $0.00002 \text{ g/cm}^3$ . A calibration was carried out with a standard (ultra pure water) provided by Anton Paar at 20 °C.

Fourier transform infrared (FT-IR) spectroscopic analysis were carried out in an ABB MB3000 equipped with a MIRacle TM Reflection Attenuated Total Reflectance (ATR) diamond crystal plate and pressure clamp. The infrared used a deuterated triglycine sulfate (DTGS) detector. The

spectra were obtained at a resolution of  $4\text{ cm}^{-1}$  as the average of 120 scans over the spectral region  $4000\text{-}600\text{ cm}^{-1}$ .

The asphaltenes content was determined using the ASTM D6560-12 [5] standard test method. A low-molecular-weight alkane (*n*-pentane) was used as precipitant. Based on this, 1 g of liquid visbreaking product is mixed with 40 mL of *n*-pentane (*n*-C<sub>5</sub>) in a 250 mL Erlenmeyer and stirred for 1 h. Samples were left inside the fumehood for 24 h and afterwards, they were filtered in a vacuum system using a 0.22µm milipore filter. Solid samples were placed inside the fumehood and stayed there for 2 days when they got dried. Liquid samples were collected and put on a hot plate for evaporating the *n*-pentane.

A Zeiss EVO LS15 EP-SEM was used to obtain the solid products images. The equipment includes a Bruker energy dispersive X-ray spectroscopy (EDS) system with a silicon drift detector with a resolution of 123 eV and a  $10\text{ mm}^2$  window area. It could work at variable pressure and environmental mode. Samples must be coat either gold or carbon for being analyzed.

Light products (gas phase) were analyzed using an Agilent 7890A gas chromatograph outfitted with both flame ionization (FID) and thermal conductivity (TCD) detectors. A HayeSep R column was used to perform the separation. For the analysis, helium was employed as a carrier gas at a constant flow of  $25\text{ mL}\cdot\text{min}^{-1}$ . The injector temperature was set at  $200\text{ }^\circ\text{C}$ . The temperature program started at  $70\text{ }^\circ\text{C}$ , held isothermally for 7 minutes then the temperature was increased up to  $250\text{ }^\circ\text{C}$  with a  $10\text{ }^\circ\text{C}\cdot\text{min}^{-1}$  ramp and then held isothermally at  $250\text{ }^\circ\text{C}$  for 2 min. A ramp of  $30\text{ }^\circ\text{C}\cdot\text{min}^{-1}$  was used to decrease the temperature up to  $70\text{ }^\circ\text{C}$  and this temperature were held for 8 min.

### **3.3 RESULTS**

#### **3.3.1 Material Balance**

Products generated from visbreaking reaction can be considered as a multiphase system, it contains gaseous, liquid and solid products after reaction. The reaction products were obtained under these conditions:  $300\text{ }^\circ\text{C}$ , an initial pressure of 4 MPa N<sub>2</sub> and reaction time varying from 1 to 8 hours. The mass of each phase was determined individually. The overall material balance

(Table 3.2) and the product yields of each phase (Table 3.3) were determined for experiments that were performed in triplicate.

**Table 3.2.** Mass balance (wt %) for visbreaking reactions at 300 °C and initial pressure of 4 MPa for different reaction times.

Reaction time [h]	Balance Material [wt %] <sup>a</sup>	
	x	s
1	100.4	1.6
2	99.0	1.6
3	100.3	1.1
4	103.0	2.1
5	100.4	1.7
6	98.2	0.6
7	102.1	1.3
8	100.3	0.5

<sup>a</sup> Average (x) and sample standard deviation (s) of three experiments are reported.

**Table 3.3.** Product yield (wt%) for visbreaking reactions at 300 °C and initial pressure of 4 MPa for different reaction times.

Time [h]	Material Balance [wt %] <sup>a</sup>					
	Gas		Liquid		Solid	
	x	s	x	s	x	s
1	2.48	1.8	91.58	3.2	6.40	2.3
2	1.44	1.9	91.40	1.7	6.20	2.0
3	2.38	1.7	90.73	1.7	7.22	2.2
4	1.30	1.4	91.24	2.6	10.49	2.9
5	2.01	1.2	89.73	4.0	8.66	4.9
6	1.62	0.9	87.25	4.3	9.30	5.1
7	2.67	0.6	92.63	3.4	6.77	3.8
8	2.05	1.1	90.96	3.3	7.26	3.2

<sup>a</sup> Average (x) and sample standard deviation (s) of three experiments are reported.

In all experiments, except for the ones at 4 h reaction time, the average material balance closed to within 2 %, i.e. material balance was between 98 and 102 %. Products after 4 h reaction showed a material balance closure up to 103 % and this coincides with the highest sample standard deviation. It shows that material balance items are relatively variable compared with the other reaction times.

During the phase separation, some observations were made. Gaseous products contain some H<sub>2</sub>S, which was expected due to the elemental analysis of the feed. Filtration of liquid products took a

long time before solids were obtained and this was found for all experiments. It is likely that the solids were very fine, some pictures were taken using a scanning electron microscope (SEM) to show how solids change from sample to sample. They can be observed in Figure 3.2

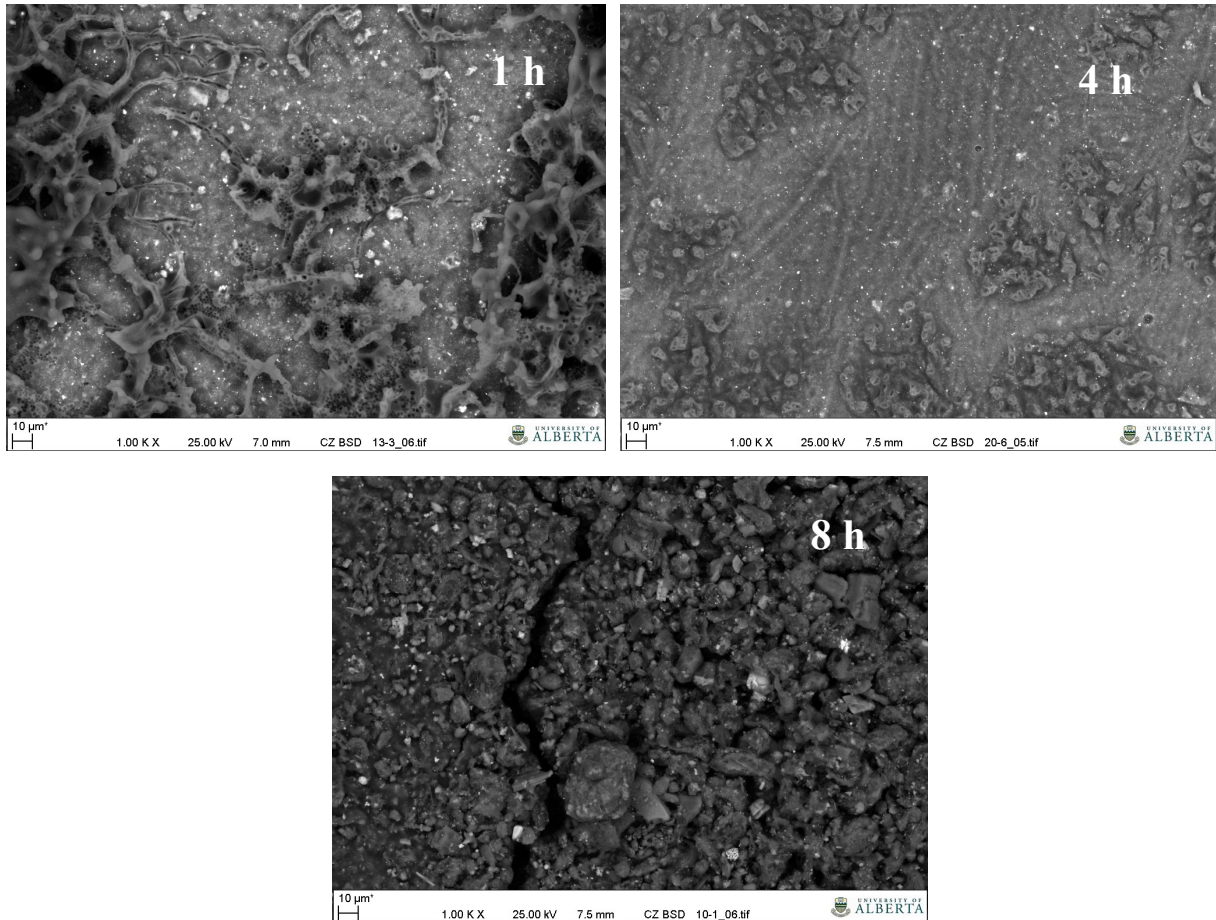


**Figure 3.2.** Images taken of 1h, 4h and 8h reaction solids in SEM. Reaction conditions: 300 °C and 4 MPa.

Figure 3.2 shows the SEM images taken to some of the solid samples collected after reaction. It corresponds to 1, 4 and 8 hours respectively. There is evident that the grain structure of the solids produced will change along residence time. After 8 hours, the shape of the grain is well defined.

### 3.3.2 Products characterization

In order to have a better idea about the changes that took place during this mild thermal treatment. Products were characterized and analysed. The three phases influenced each other; however, this work is mainly focused on those changes related to the liquid phase products.

#### 3.3.2.1 Viscosity

Considering the nature of this research, the first and probably the key product property of this work is the viscosity measurements. Every analysis was performed at 4 different temperatures (20, 30, 40 and 60 °C), but shear rate was kept constant at  $10 \text{ s}^{-1}$ . These results are tabulated in Table 3.4.

**Table 3.4.** Viscosity data performed to Visbreaking products under 300 °C and initial pressure 4 MPa.

Temperature [°C]	Reaction time [h]															
	1		2		3		4		5		6		7		8	
	Viscosity [Pa.s] <sup>a</sup>															
	x	s	x	s	x	s	x	s	x	s	x	s	x	s	x	s
20	60.2	38.7	5.8	5.3	5.6	3.5	0.8	0.7	72.2	104.0	27.6	29.9	11.6	4.3	8.5	4.9
30	19.6	10.4	1.3	1.2	2.4	1.2	0.5	0.3	22.3	30.2	9.3	9.1	4.5	1.4	3.4	1.8
40	7.1	3.4	0.6	0.5	1.1	0.5	0.4	0.3	7.4	9.5	3.3	4.0	1.7	0.4	1.3	0.7
60	1.3	0.5	0.3	0.2	0.3	0.1	0.2	0.2	1.3	1.4	0.6	0.6	0.5	0.1	0.4	0.1

<sup>a</sup> Average (x) and sample standard deviation (s) of three experiments are reported.

After visbreaking at 300 °C, the viscosity of the products decreased by two to three orders of magnitude compared with the raw bitumen. The viscosity of the converted bitumen was orders of magnitude lower (Figure 3.3) to that of the fresh Cold Lake bitumen (Figure 3.4).

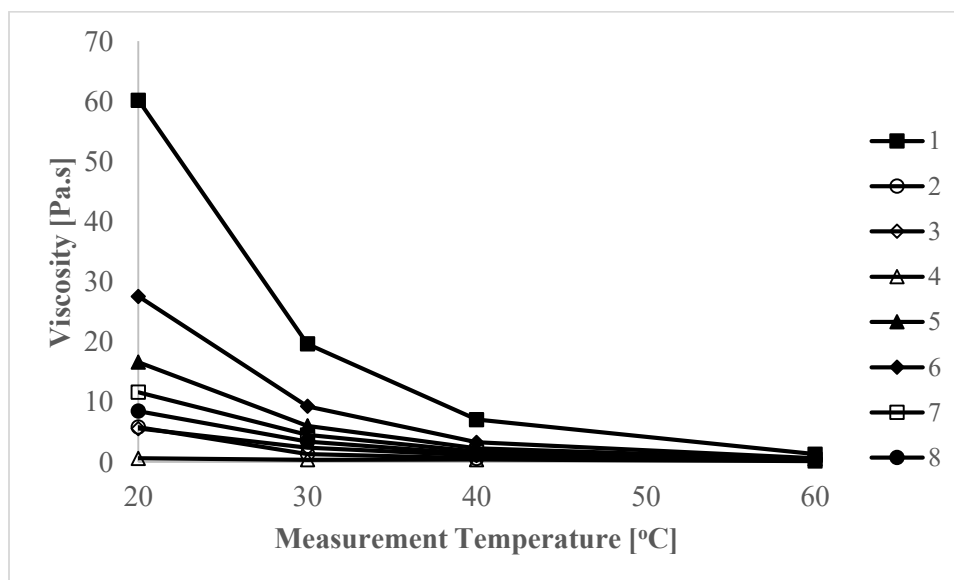


**Figure 3.3.** Viscosity of visbreaking products obtained under 300 °C, initial pressure of 4 MPa and reaction time varying between 1 and 8 hours. Measurements were performed at four different temperatures: 20, 30, 40 and 60 °C.

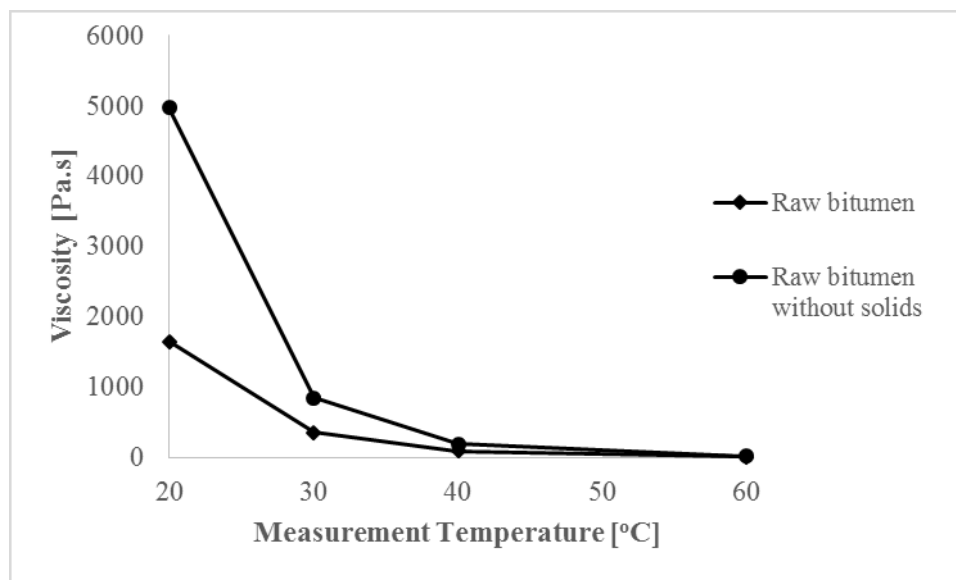


**Figure 3.4.** Viscosity result for raw Cold Lake Bitumen.

It was found that the relative percentage standard deviation decreased as the measurement temperature was increased; the only exceptions were the products after 4 and 6 h reaction time.

### 3.3.2.2 Refractive Index

After the viscosity data was obtained, a small amount of liquid product was used to perform refractive index measurements. Every sample was analyzed at 4 different measurement temperature conditions: 20, 30, 40 and 60 °C, i.e. the same temperatures as for the viscosity data. The results are reported in Table 3.5.

**Table 3.5.** Refractive Index measurements performed on visbreaking products after 300 °C and initial pressure 4 MPa reaction.

Temperature [°C]	Reaction time [h]																	
	0		1		2		3		4		5		6		7		8	
	Refractive Index [nD] <sup>a</sup>																	
	x	s	x	s	x	s	x	s	x	s	x	s	x	s	x	s	x	s
20	1.58437	0.00076	1.58133	0.00226	1.57875	0.00296	1.57990	0.00622	1.58485	0.00622	1.58128	0.00060	1.58440	0.00398	1.58323	0.00270	1.58167	0.00198
30	1.58057	0.00067	1.57827	0.00196	1.57546	0.00292	1.57657	0.00585	1.58138	0.00122	1.57775	0.00045	1.57887	0.00025	1.58090	0.00115	1.57813	0.00186
40	1.57677	0.00067	1.57557	0.00146	1.57279	0.00248	1.57353	0.00587	1.57810	0.00075	1.57455	0.00035	1.57547	0.00040	1.57757	0.00106	1.57497	0.00175
60	1.56917	0.00050	1.56900	0.00078	1.56657	0.00248	1.56780	0.00505	1.57128	0.00029	1.56773	0.00031	1.56897	0.00021	1.56930	0.01509	1.56893	0.00129

<sup>a</sup> Average (x) and sample standard deviation (s) of three experiments are reported.

<sup>b</sup> Raw Cold Lake bitumen

The results are can be visualized in two ways (Figure 3.5a and 3.5b): a) Refractive index versus time in order to emphasize the variation of this property over reaction time, and b) Refractive

index against the measurement temperature (20-60 °C). Although it is not customary to report refractive index at different measurement temperatures, it was hoped that additional information on composition could be extracted from the temperature dependence of the refractive index values. The refractive index value and its temperature dependence contain property information.

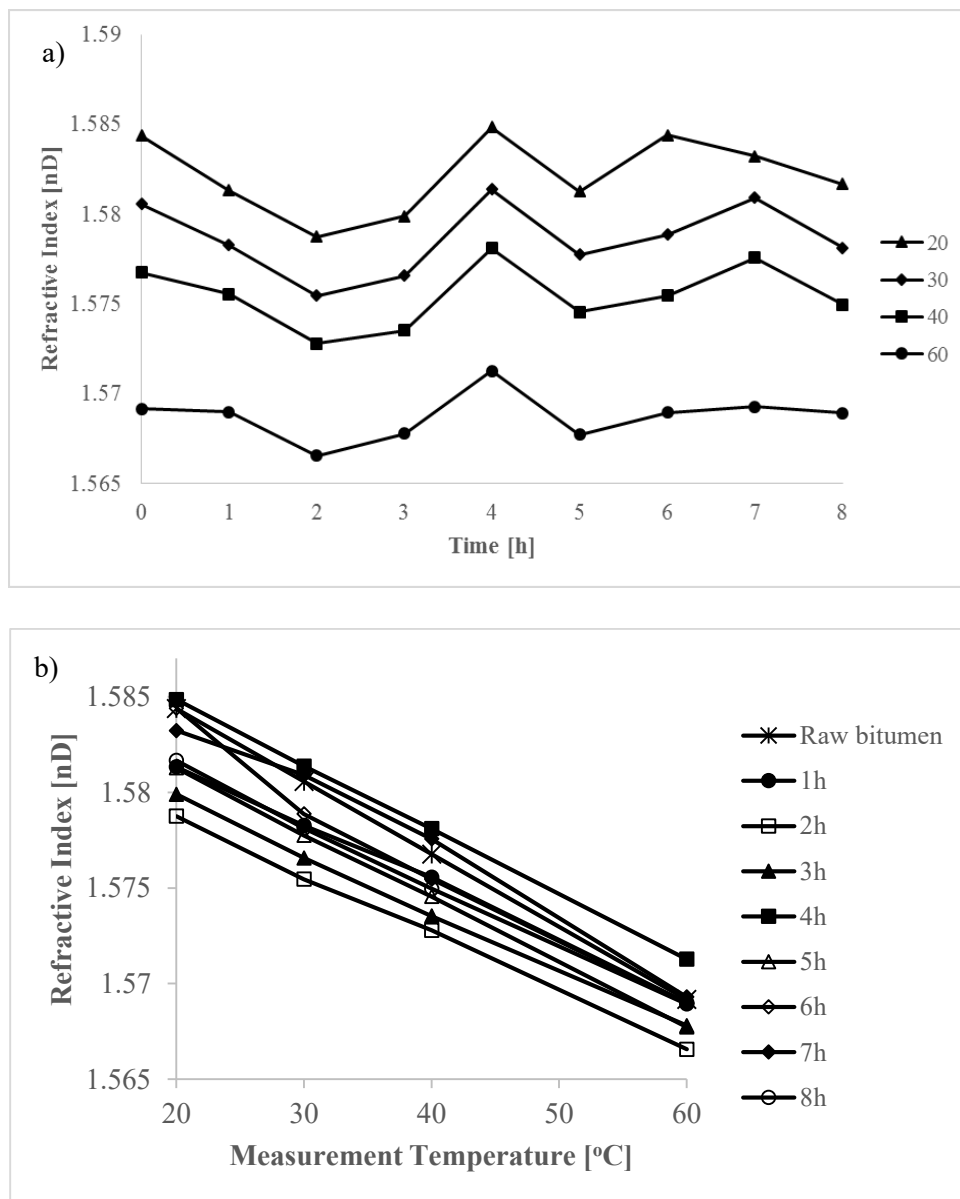


**Figure 3.5.** Refractive Index results for Visbreaking Products at 300 °C, initial pressure of 4 MPa and different reaction times: a) Refractive index vs Time; and b) Refractive index vs Measurement Temperature.

As happened with viscosity results, the standard deviation decreased as temperature of the measurement increased. For Figure 3.5b, most of the plots perfectly agree with a linear equation.

### 3.3.2.3 $^1\text{H}$ NMR

Aliphatic chains have been related with a significant low viscosity. Since bitumen is a mixture of different kind of components, aliphatic chains are part of this system. NMR analysis was used to determine aliphatic and aromatic content and observe how its proportions change under different reaction conditions. Figure 3.6 shows a) the NMR spectra of visbreaking products in order to observe any change related with the aliphatic content, and b) the actual content of aliphatic protons against time for evaluating the impact of the structure change if there is any change. Additional, a peak found around 5 ppm corresponds to the solvent used for the sample preparation.

A big change takes place at the first hour reaction and after that, values keep constant until 5 hours reaction when a light fall in aliphatic hydrogen takes place. Something to remark is the standard deviation places closed to zero except for the 5 hour reaction.

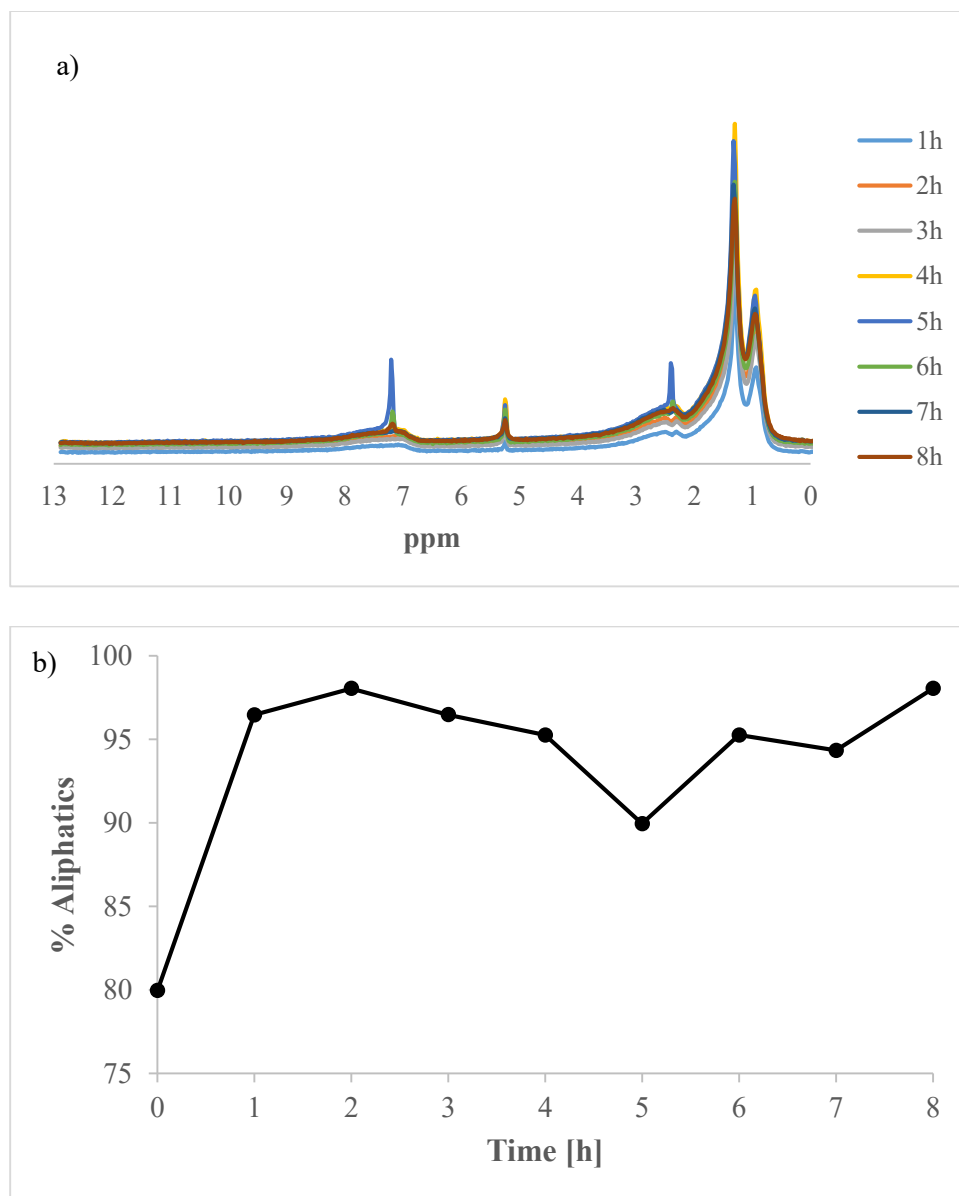


**Figure 3.6.** NMR results of visbroken products after 300 °C, initial pressure of 4 MPa and different times: a) NMR spectra for pyrolysis products; b) % Aliphatic protons vs Time.

### 3.3.2.4 Density

Density measurements were performed to the liquid visbreaking products. Samples must be heated up before being injected in the equipment. Once injected, measurements were done at four different temperatures: 20, 30, 40 and 60 °C. The results of this analysis are presented in Figure 3.7 when they are shown in the following way: a) Density vs Time graph shows how the density products vary over reaction time, and b) Density vs Temperature graph confirms what it

is known about density changes with temperature but it also presents the pattern every product shown under the temperature changes. Density data is presented in Table 3.6.

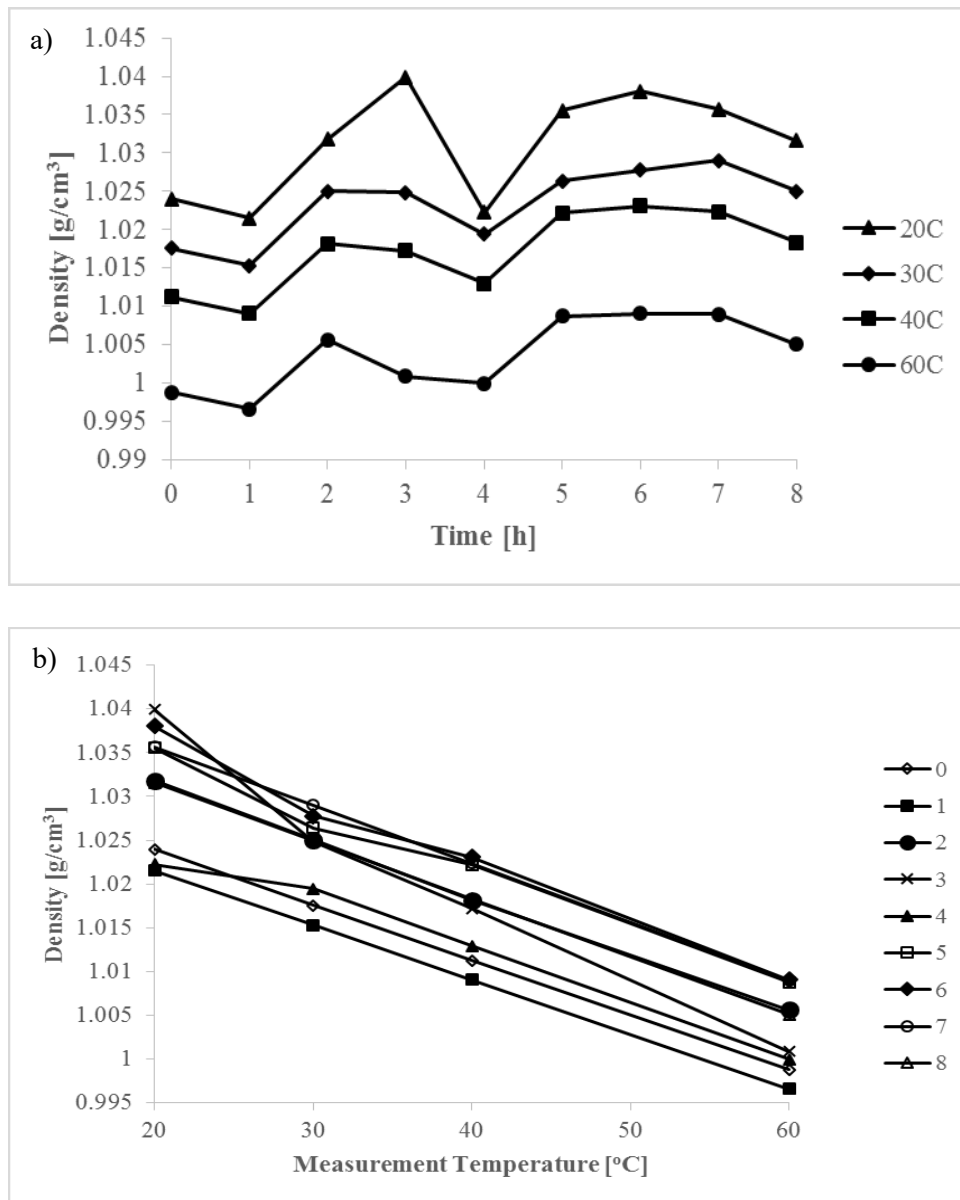


**Figure 3.7.** Density of visbreaking products obtained under 300 °C, initial pressure of 4 MPa and different reaction times: a) Density vs Time; and b) Density vs Measurement Temperature.

Density may be considered slightly constant for most of the products; however, Figure 3.7a shows a maximum density point after 3 hours reaction and a minimum up to 4 hours reaction. Also, at 20 °C, the changes in the density curves are more dramatic changes. Density measurements data is summarized in Table 3.6.

**Table 3.6.** Density measurements performed on visbreaking products after 300 °C and internal pressure 4 MPa reaction and different reaction times.

Temperature [°C]	Density [g/cm <sup>3</sup> ]								
	Time [h]								
	0	1	2	3	4	5	6	7	8
20	1.023993	1.02152	1.03181	1.03992	1.02222	1.03554	1.03804	1.03567	1.03158
30	1.017547	1.01533	1.02504	1.02486	1.01944	1.02638	1.02778	1.02902	1.02499
40	1.011263	1.00907	1.01818	1.01723	1.01295	1.02218	1.02307	1.02235	1.01835
60	0.998813	0.99659	1.00564	1.00088	1.0000	1.00877	1.00906	1.00895	1.00508

### 3.3.2.5 FT-IR

Different chemical groups can be found into bitumen, one of the most useful techniques for identifying them is FT-IR. IR spectra are summarized in Figure 3.8 where the spectrum for every reaction time was plotted.

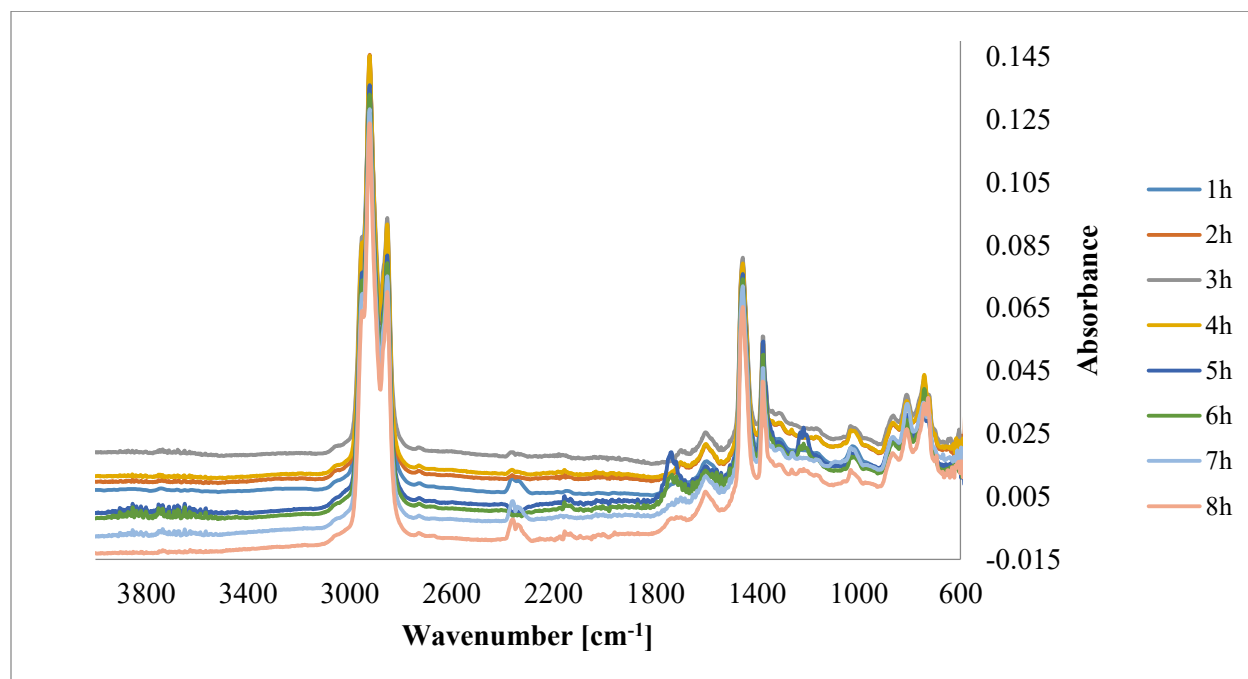


**Figure 3.8.** FTIR spectra for pyrolysis products after 300 °C, initial pressure of 4 MPa and different times reaction.

There is a slightly difference on the absorbance intensity for every reaction time. This could be attributed to its own characteristics properties of the products after reaction at 300 °C.

### 3.3.2.6 Asphaltene content

Asphaltenes are the highest-molecular-weight fraction of petroleum and they can be determined following ASTM D6560-12 [5]. The *n*-pentane precipitated asphaltenes content is shown in Figure 3.9.

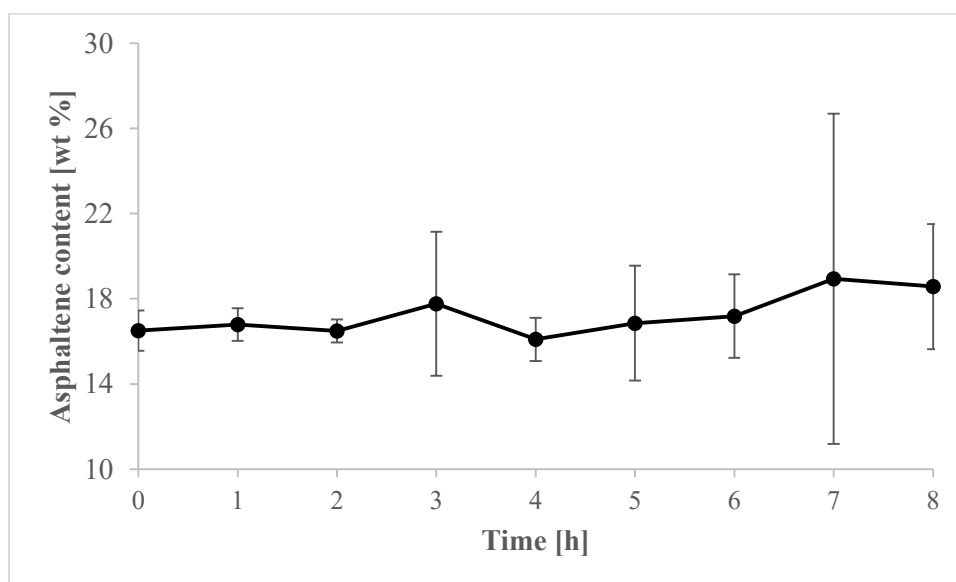


**Figure 3.9.** Asphaltene content for visbreaking products by *n*-pentane precipitation following the ASTM D6560 standard test method. The value at 0 h is for the bitumen feed.

The sample standard deviation was relatively small for most of the reaction times except for the measurement of the asphaltenes content of the product after 7 hours reaction time. When the samples after 7 hours reaction time were placed into the flask, some electrostatic forces between the sample and the glass were evidenced. The electrostatic forces made accurate collection of the asphaltenes more difficult and increased the standard deviation of the analysis of these samples compared to the rest.

### 3.3.2.7 Gas Chromatography

After reaction and once its products reached room temperature, gases were collected in a gas bag and injected in the gas chromatograph to be analyzed. The gaseous product analyses are

summarized in Table 3.7, which lists the concentration obtained for every compound between C<sub>1</sub> to C<sub>6</sub> in the sample.

**Table 3.7.** Gas products associated to pyrolysis of bitumen after reaction at 300 °C and initial pressure 4 MPa.

Compound	Reaction time [h]							
	1	2	3	4	5	6	7	8
	[mole %]							
<b>Methane</b>	0.01	0.02	0.02	2.84	0.09	0.23	0.73	0.66
<b>Ethylene</b>	-	-	-	-	-	0.01	0.01	0.01
<b>Ethane</b>	-	0.01	0.02	0.01	0.02	0.03	0.05	0.08
<b>Propylene</b>	-	-	-	-	0.01	-	-	0.01
<b>Propane</b>	-	-	0.01	0.01	0.02	0.03	0.04	0.07
<b>iso-Butane</b>	-	-	-	-	-	-	0.02	0.01
<b>n-Butane</b>	-	-	-	-	-	-	-	-
<b>cis-2-Butene</b>	-	-	0.01	0.01	0.01	0.02	0.03	0.05
<b>iso-Pentane</b>	-	0.06	0.01	0.01	0.01	0.01	0.03	0.05
<b>n-Pentane</b>	-	0.01	0.02	0.02	0.03	0.04	0.05	0.09
<b>iso-Hexene</b>	-	-	-	-	-	-	-	-
<b>n-Hexene</b>	-	-	-	-	-	-	0.01	0.02
<b>CO<sub>2</sub></b>	0.11	0.11	0.16	0.21	0.24	0.29	0.28	0.37
<b>H<sub>2</sub>S</b>	-	-	-	-	- <sup>a</sup>	- <sup>a</sup>	- <sup>a</sup>	- <sup>a</sup>
<b>H<sub>2</sub></b>	-	-	1.83	1.74	1.73	2.40	1.66	-
<b>Ar</b>	12.94	6.66	11.88	5.88	3.18	2.92	3.09	2.77
<b>N<sub>2</sub></b>	86.90	93.10	85.85	92.03	94.62	93.93	93.90	95.72
<b>CO</b>	0.03	-	0.02	0.02	0.04	0.07	0.09	0.10

<sup>a</sup> H<sub>2</sub>S was observed at very low concentration.

### 3.3.2.8 Solid content

After reactions took place, reactors must be cleaned with a solvent. The mixture obtained contains the solvent, liquid and solid products. Solid are separated from the solvent-liquid product solution through a vacuum filtration system. A milipore filter paper of 0.22 um was used and samples were left inside the fumehood for 2 days to dry. Amount of solids obtained from this process is reflected in Figure 3.10. The numeric values were reported as part of the material balance (Table 3.3).

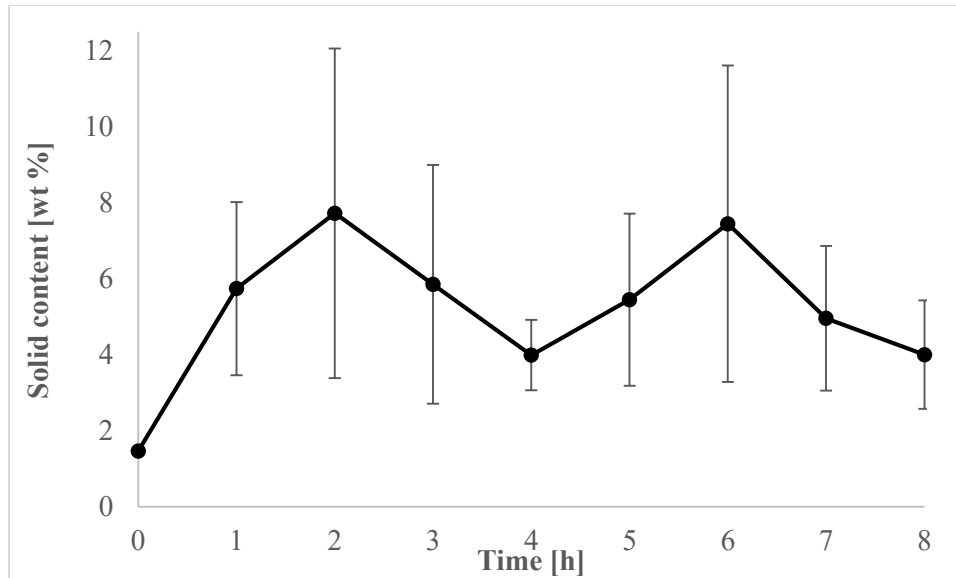


**Figure 3.10.** Solid content in pyrolysis products after reaction at 300 °C. The value at 0 h refers to the feed material.

During filtration, it was found that the separation process was very slow and more than one filter was required. Filtration could take up to 5 hours and require around 12 filter papers.

### 3.4 DISCUSSION

#### 3.4.1 Viscosity-Measurement temperature relationship

Bitumen behaviour challenges all the expectations. Visbreaking is not the exception and its development does not follow the typical relationship between product viscosity and reaction time [1]. Although it is conventional to report the viscosity measurements only at a single measurement temperature, it was of interest to see whether the viscosity versus measurement temperature followed the same relationship with measurement temperature as the bitumen feed. This relationship is based on equation (1) [6]

$$\log_{10}(\mu + 0.8) = \Theta \cdot (\Phi \cdot T)^b \quad (1)$$

For this equation, viscosity ( $\mu$ ) units is mPa.s and the temperature (T) is in K.  $\theta$ ,  $\Phi$  and  $b$  are empirical correlation constants and their values are 160, 0.008 and -4 respectively for Cold Lake Bitumen fractions [6]. ASTM recommends a viscosity-temperature relationship for oils which has the same general format as the previous correlation, as shown in equation 2.

$$\ln[\ln(\mu)] \propto \ln(T) \quad (2)$$

Table 3.8 compares the experimental results with those values calculated by Eq. 1. The error did not surpass 10% which means the empirical correlation expressed by Eq. 1 fits decently with the experimental results. Figure 3.11 shows the  $\ln(\ln(\mu))$  vs.  $\ln(T)$  relationship, where the linear tendency can be seen more clearly. Most of the visbreaking products follow a linear relationship but that was not true for samples after 2, 4 and 7 hours reaction.

**Table 3.8.** Experimental viscosity values for 300 °C visbreaking products at different measurement temperatures calculated by Eq. 1.

Temperature [°C]	Viscosity [mPa.s]		Error [%]
	Experimental	Eq. 1	
20	$2.04 \times 10^5$	$1.94 \times 10^5$	5
30	$4.59 \times 10^4$	$4.22 \times 10^4$	9
40	$1.22 \times 10^4$	$1.15 \times 10^4$	6
60	$1.55 \times 10^3$	$1.48 \times 10^3$	4

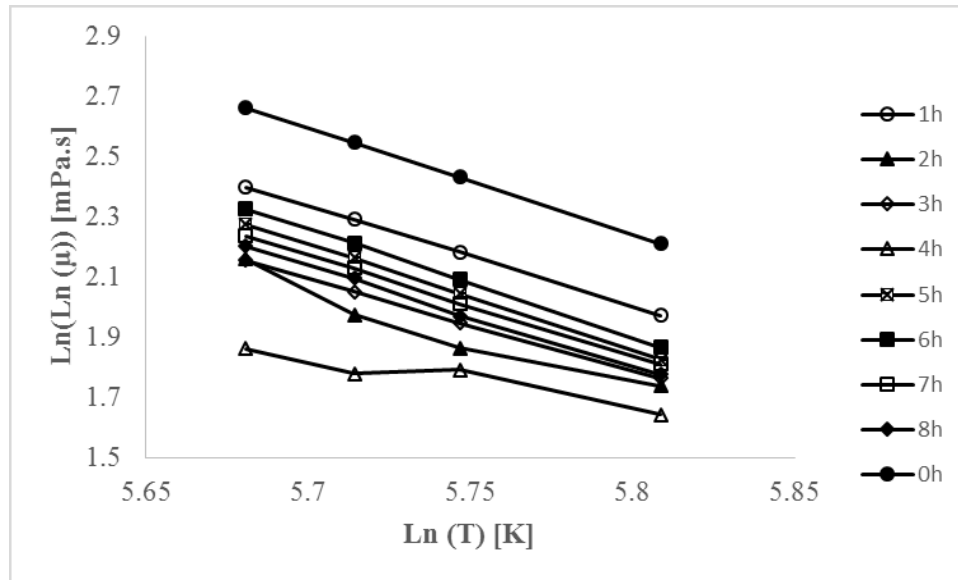


**Figure 3.11.** Viscosity of visbreaking products after 300 °C, internal pressure of 4 MPa along different residence times using Eq (2).

The explanation for this behaviour could be related with the complex nature of bitumen. One of the likely theories about this is related with formation of a second phase (a second liquid phase or a solid phase). Knowing that all visbreaking products were filtered before carrying out all the analysis, the second liquid phase is more likely a structured second liquid phase. In order to show how viscosity varies from sample to sample, Figure 3.3 shows the viscosity for every reaction time performed. To have an idea about the effect of this thermal treatment, Figure 3.4 shows the viscosity data for a fresh Cold Lake bitumen sample.

### 3.4.2 Viscosity-Residence time relationship

Temperature affected bitumen viscosity over time. The viscosity was decreased by orders of magnitude (compare Figure 3.3 with Figure 3.4) and it is likely that most of this decrease in viscosity can be attributed to deaggregation [1].

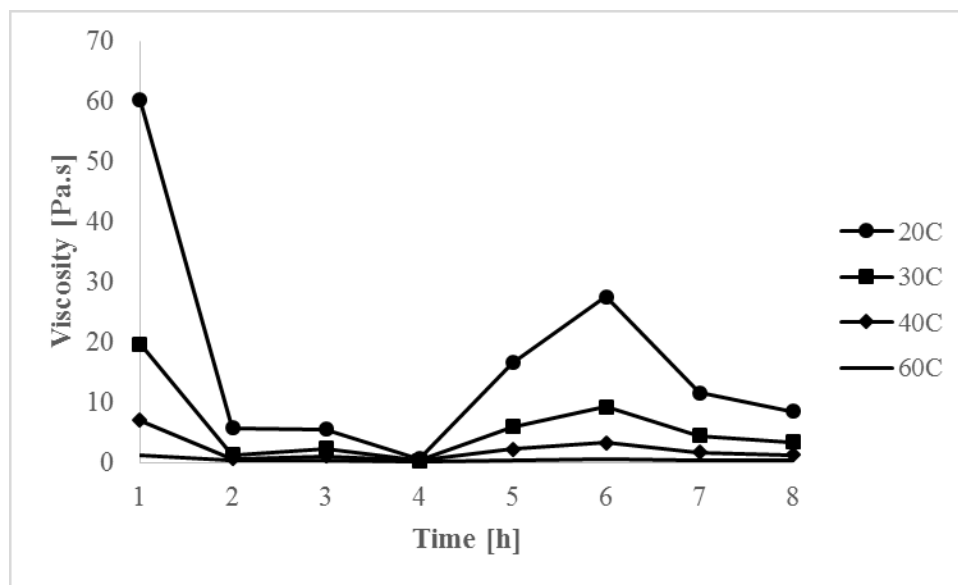


**Figure 3.12.** Viscosity measurements of the pyrolysis products under 300 °C and 4 MPa at different residence time reaction.

Looking Figure 3.12, the 4 hours sample exhibits the maximum viscosity reduction. However, viscosity increases up to 6 hours reaction and then, it decreases again. This shows that viscosity changes are not monotonous and reaction time actually affects products in a more important way, which could be related with the significant influence of the free radical chemistry that takes place during reaction at 300 °C.

Free radical chemistry contains several kind of reactions and some of them may be considered in this work. Addition, fragmentation, termination and rearrangement reactions could explain the changes that bitumen is experiencing after thermal treatment. However, at 300 °C the number of bonds that can be broken is not high and just the weaker ones could be involved. Based on what was said, fragmentation reactions are taking place and it is possible to stimulate the formation of bigger molecules as a consequence of the free radical stability by free radical recombination. In order to reach or maintain that stability, rearrangements could happen just to lower the energy level of the molecules and keep the stability of the product. As it was mention before, the formation of bigger molecules may be a result of some addition reactions, which can increase viscosity and also molecular weight. This would explain the increase in viscosity from 4 to 6 hours. There are different stages of reaction progression and if this interpretation is correct, recombination reactions are dominant only for a limited time period over the range of residence times studied.

### **3.4.3 Effects of hydrogen disproportionation**

The increasing-decreasing viscosity behavior of visbreaking products with increasing reaction time may also be related to hydrogen disproportionation. Regarding Figure 3.5b, it is evident that a big change in the distribution of aliphatic and aromatic hydrogen content is happening, which is an indication of hydrogen disproportionation. Looking back at section 3.4.2, termination reactions after thermal cracking were mentioned as part of the development of visbreaking process. Now, hydrogen disproportionation is included in this type of reactions. This process will be competing with coupling reactions, which is controlled by diffusion [7]. Changes in hydrogen distribution can be seen as a redistribution and re-solubilization process. By analogy from metallurgy: Chromium can redistribute and re-dissolve in stainless steel under certain conditions. One could consider the hydrogen being transferred from some structures (compounds) and due to the increase in reaction times, some unstable products have sufficient time to achieve better stability.

In [8], a reduction in coke formation could be related with a diminishing of the light products generation, in order to equilibrate the H:C ratio. However, hydrogen disproportionation takes place in parallel with thermal cracking and ultimately it will cause coking [9].

Focusing on Figure 3.5a, some regions can be identified based on data showed in [10]. The main regions in  $^1\text{H}$  NMR spectra correspond to 0 to 4.4 ppm refers to the aliphatic protons and between 6 and 8.5 ppm this peak is related with aromatic and phenolic protons. In the aliphatic region of the spectra, there are two main peaks, the first one is associated with methylene hydrogens from straight-chain alkanes and one shoulder right next to them linked with methylene hydrogens in branched chains. The second peak is referred to cyclic methylene, naphthenic hydrogens, aromatic rings and hydrogens in methyl, methylene or methane groups attached to aromatic rings [11].

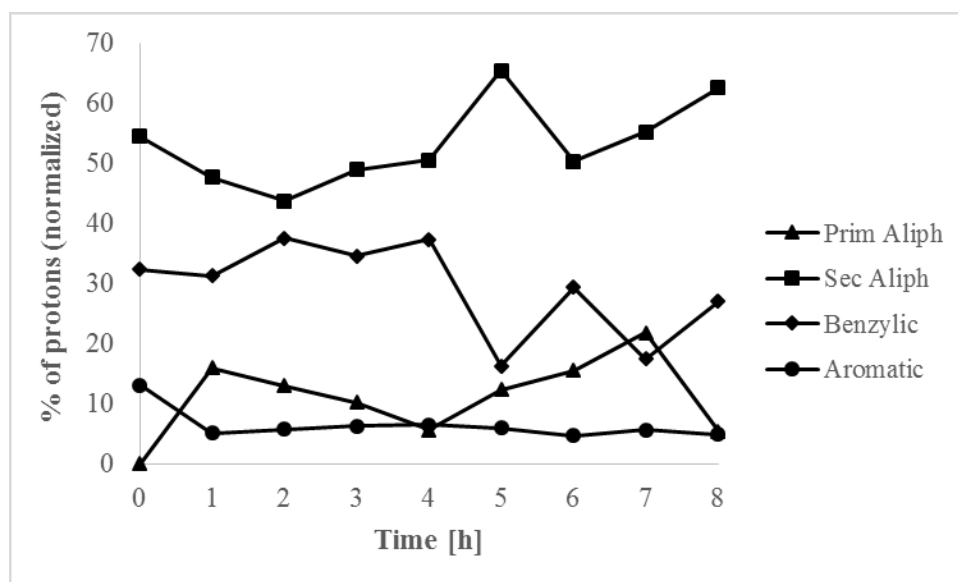


**Figure 3.13.** Area under the curve extracted from the NMR spectra, comparing the amount of the type of proton found in visbroken samples after 300 °C reaction

Based on the results shown in Figure 3.13, primary aliphatic protons were not identified in raw bitumen samples and they started to show up after the first hour reaction. This might be due to a concentration below the detection limit of the instrument used. On the other hand, the amount of secondary aliphatic hydrogen as well as the benzylic hydrogen showed a significant decrease after one hour of reaction but with more time on stream it increased again. Regarding the aromatic hydrogen, it is clear that it decreased and remained at a lower concentration level along time. Since aromaticity could cause an increasing in density, this find may explain a decreasing in density observed in Figure 3.6b. Besides, aromatics can affect viscosity by inducing a thickening effect [12].

### 3.4.4 Refractive Index-Density relationship

Refractive Index (RI) at different measurement temperature is related to measurement temperature in a way that could provide additional information about composition of the products beyond the RI at a single temperature. Based on Figure 3.4b, the relationship between RI and the measurement temperature may be considered linear with a non-constant slope. Such changes could be attributed to compositional changes and hence, molar mass and density variations can be observed. However, at 300 °C, it is not expected to find a significant amount of cracking conversion. It is anticipated that there will be only a small change in molar mass.

Some intermolecular interactions can take place, causing a refractive index variation and, polarizability induced by molecular aggregation [13] that may alter the orientational molecular polarizability, which would have an effect in the electronic molecular polarizability [14]. Another factor that may contribute to RI variations could be related with changes in aromatic content, based on the data presented in [15]. Regarding Figure 3.4a, RI changes behaviour is kind of similar to viscosity and this could be a consequence of the changes in composition caused over time at 300 °C (as discussed in Sections 3.4.2 and 3.4.3).

The RI decreases with an increase in measurement temperature. This is related to the expansion of the products due to the increase in temperature, which also causes a decrease in density. Within the measurement temperature range no big changes in RI are expected. Figure 3.6b, show that relationship between density and measurement temperature is slightly linear for 1, 2, 7, and 8 hour reaction plus the raw bitumen sample. But this is not true for reaction times between 3 and 6 hours. Considering data showed so far, it is clear that biggest changes could take place in this time-period and the non-monotonous change in slope may be indicative of a compositional change.

Now, considering the influence of the reaction time in bitumen density, Figure 3.6a shows how this property changes over time. It is known that temperature may affect density values [16] due to the expansion; nonetheless, measurement temperature does not reach a high value. Density is affected by size and composition of its components and an increasing in boiling point and molar mass also mean an increasing and density values [17]. Density will decrease when the hydrogen content increases. Analyzing all this facts and considering Figure 3.7 that shows the density measurements for pyrolysis products, it was found that with increasing reaction time density

varies in a narrow range. After 4 hours reaction, viscosity and density reach the minimum value which could agree with a compositional change. However, both, viscosity and density increase after that which suggest a “lack” of hydrogen in the whole bitumen structure. Yet, this is not supported by the other experimental data.

### 3.4.5 FT-IR Hints

FT-IR could be considered as one of the most effective techniques for identifying certain groups of compounds. Over the wavelength, peaks could indicate chemical bonds interactions. On the other hand, the intensity of an absorption band will depend on the change in the dipole moment of the bond and the number of specific bonds present [18]. The bond dipole is the result of a) bond length and b) charge difference between the atoms.

Figure 3.8 shows FTIR spectra for the different pyrolysis products. The stretching of methyl groups in aliphatic chains generates a peak around  $2923\text{ cm}^{-1}$ . On the other hand, right next to this peak (approx.  $2853\text{ cm}^{-1}$ ), it is possible to find another peak associated to the stretching of methylene groups in the aliphatic chains. Up to  $2600\text{ cm}^{-1}$ , the stretching of the O-H bond might generate a peak which disappears along reaction time. Around  $1747\text{ cm}^{-1}$ , there is a peak assigned to the stretching of the carbonyl group (C=O) [19][20] which appears after 5 hours reaction. The peak at  $\sim 1600\text{ cm}^{-1}$  it refers to the stretching of C=C bond in a ring structure, likely that of aromatics. To be sure about the aromatic vibrations it should show a peak around  $900\text{ cm}^{-1}$ , which will be the fingerprint of the C-H bond into an aromatic structure. When Figure 8 is checked, a peak close to  $900\text{ cm}^{-1}$  was found. Also, the peaks at  $1375$  and  $1456\text{ cm}^{-1}$  confirm the methyl and methylene groups in aliphatic chains. Sulfur compounds in bitumen can be seen through the peak at  $1040\text{ cm}^{-1}$ , a characteristic peak for the stretching of S=O bond. Finally, there is a group of peaks between  $850$  and  $700\text{ cm}^{-1}$  that are associated with to the out-of-plane deformation vibration of one isolated aromatic C-H bond ( $870\text{ cm}^{-1}$ ), two or three adjacent aromatic C-H bonds ( $814\text{ cm}^{-1}$ ) and four aromatic adjacent aromatic bonds ( $750\text{ cm}^{-1}$ ) [11].

### 3.4.6 Gaseous product contribution

Gaseous products are generated in a very low proportion (Table 3.7). However, it is very important to characterize this phase.

Based on this information, it could be observed that the amount of light products is more significant compared to “heavier” products. The methane ( $C_1$ ) concentration is high. The high methane make could be explained as follows: First, cracking may be considered and that explains a high concentration of  $C_1$ ; or second, the reaction temperature can be considered relatively high to provide enough energy for breaking terminal bonds which may be considered weaker than the other ones. Other lighter products like propane are produce at this temperature and most of the curves are similar except for 4h results, which show a higher production of hexene. It is suspected based on bond dissociation energy that the nature of the bonds that are broken at 300 °C are main aryl–S–alkyl and aryl–O–alkyl in nature, but no direct proof of this is provided.

#### **3.4.7 Solid product contribution**

Looking at the third phase produced in visbreaking, coke and asphaltenes could play an important role. Asphaltenes have been linked with viscosity increments. Following the ASTM D6560-12, the amount of the highest-molecular-weight fraction could be considered stable over time, since the variation of asphaltenes over the whole range fell within a pretty narrow (about 3%) distribution. Figure 8 shows precisely how this variation occurs over time.

Based on this result, it is possible to say that asphaltenes are not solely responsible for the high viscosity of bitumen. It might contribute to its poor fluidity, indeed. These results also give some idea about molecular aggregation in bitumen and how it is changed after thermal cracking. Asphaltenes contain large compounds with alkyl groups [17], which could affect the product viscosity and density according to the branches or structure that they have. Also, asphaltenes are very polar compounds and they could attract or interact with other compounds, thereby forming larger molecules through intermolecular interactions.

A direct result of visbreaking, coking is one of the biggest challenges in industry due to the multiple adverse consequences during process operation. Opposite to the results showed in [21], the solids content which includes coke and mineral matter, increased and then decreased over time. The standard deviation of the solids yield was high (Table 3) and the variation from time to time might not be significant. These results are shown in Figure 3.10.

The nature of bitumen is inherently very complex and that is why it can be considered as a multiphase system with potentially large mesophase and smaller crystalline phases [22]. The solid content that was found includes “coke”, which may come from bitumen mesophase. However, the temperature was low and it is more likely that the carbonaceous deposits represent addition products that became insoluble in the bitumen matrix.

### 3.5 CONCLUSIONS

This work could give a different perspective about what it is really happening during visbreaking reactions and/or re-think about the influence of some factors.

- a) The amount of gaseous products does not exceed 3%. However, results obtained in the gas chromatograph show the presence of C<sub>1</sub>. This may suggest that the energy provided by the reaction temperature was enough to crack at least some bonds in the molecules. It was speculated without proof that the bonds that were broken were aryl-S-alkyl and aryl-O-alkyl.
- b) Viscosity is reduced significantly through visbreaking under these reaction conditions. Deaggregation of aggregated material likely contributed considerably to the observed viscosity decrease. The viscosity changed non-monotonously with increasing reaction time. It is considered that free-radical reaction and mechanisms are responsible for these changes. Arrangement and addition reactions are considered the ones that most contribute in this result. However, some other factors could influence this reduction.
- c) One of the most important factors in this process was the hydrogen disproportionation that was prevalent even at short reaction times. It could favour the rearrangement and addition processes.
- d) It is interesting to see that asphaltenes content is not too high and it stayed in a narrow range. Based on these results, it could be considered that asphaltenes content may affect bitumen viscosity; however, it is just one of the factors that could influence viscosity.

#### Literature cited

[1] Wang, L.; Zachariah, A.; Yang, S.; Prasad, V.; De Klerk, A. Visbreaking oilsands-derived bitumen in the temperature range of 340-400 °C. *Energy Fuels* **2014**, *28*, 5014-5022.

- [2] Yanez, L.; De Klerk, A. Visbreaking of Oil Sands bitumen at 300 °C. *Prepr. Pap.-Am. Chem. Soc., Div. Energy Fuels* **2015**, *60*(1), 31-34.
- [3] Jha, K. N.; Montgomery, D. S.; Strausz, O. P. Chemical composition of gases in Alberta bitumens and in low-temperature thermolysis of oil sand asphaltenes and maltenes. In *Oil sand and oil shale chemistry*; Strausz, O. P., Lown, E. M. Eds.; Verlag Chemie: New York, **1978**, p.33-54.
- [4] Stangeby, P. C.; Sears, P. L. Yield of heated oil sand. In *Oil sand and oil shale chemistry*; Strausz, O. P., Lown, E. M. Eds.; Verlag Chemie: New York, **1978**, p.101-118.
- [5] ASTM D6560-12: *Standard test method for Determination of Asphaltenes in Crude Petroleum and Petroleum Products*; ASTM: West Conshohocken, PA, **2012**.
- [6] Mehrotra, A. K. A generalized viscosity equation for liquid hydrocarbons: Application to oil-sand bitumens. *Fluid Phase Equil.* **1992**, *75*, 257-268.
- [7] Parsons, A. F. *An introduction to free radical chemistry*; Blackwell: Oxford, **2000**.
- [8] Wang, L. Low temperature visbreaking. MSc thesis, University of Alberta, Edmonton, AB, Canada, 2013
- [9] Zachariah, A. Low temperature pyrolysis and its application in bitumen processing. MSc thesis, University of Alberta, Edmonton, AB, Canada, 2014.
- [10] Majid, A.; Pihillagawa, I. Potential of NMR Spectroscopy in the Characterization of Nonconventional Oils; *Journal of Fuels* **2014**, *1*, 1–7.
- [11] Borrego, A. G.; Blanco, C. G.; Prado, J. G.; Diaz, C.; Guillen, M. D. <sup>1</sup>H NMR and FTIR Spectroscopic Studies of Bitumen and Shale Oil from Selected Spanish Oil Shales. *Energy Fuels* **1996**, *10* (1), 77–84.
- [12] Abou El Naga, H. H.; Abd El Aziem, M. W.; Mazin, A. S. The effect of the aromaticity of base stocks on the viscometric properties of multigrade oils. *Lubrication Sci.* **1998**, *10*, 343–363.
- [13] Goual, L.; Firoozabadi A. Measuring Asphaltenes and Resins, and Dipole Moment in Petroleum Fluids. *AIChE J.* **2002**, *48*, 2646-2663.

- [14] Evdokimov, I. N.; Losev, A. P. Effects of molecular de-aggregation on refractive indices of petroleum-based fluids. *Fuel* **2007**, *86*, 2439-2445.
- [15] Sachanen, A. N.; Tilicheev, M. D. *Chemistry and Technology of Cracking*; Chemical Catalog Co.: New York, 1932.
- [16] Chopra, S. *Heavy Oils: Reservoir Characterization and Production Monitoring*; Society of Exploration Geophysicists: Tulsa, OK, 2010.
- [17] Gray, M. R. *Upgrading oilsands bitumen and heavy oil*; Pica Pica Press, an imprint of the University of Alberta Press, 2015.
- [18] Hardinger, S. "Infrared Spectroscopy". *Department of Chemistry and Biochemistry at University of California*, Los Angeles. 29 August **2006**. Visited 29 October 2015 <[http://www.chem.ucla.edu/harding/notes/notes\\_14C\\_IR.pdf](http://www.chem.ucla.edu/harding/notes/notes_14C_IR.pdf)>
- [19] Karlsson, R.; Isacson, U. Application of FTIR-ATR to Characterization of Bitumen Rejuvenator Diffusion. *J. Mater. Civ. Eng.* **2003**, *15*(2), 157-165
- [20] Bunghez, I-R.; Ion, R-M.; Fierascu, R. C.; Radu, C.; Dumitriu, I.; Ion, M-L.; Neata, M.; Doncea, S-M. GC-MS and FTIR Analysis of Bitum/Kerogen as Organic Geochemistry Index. *Petroleum - Gas University of Ploiesti Bulletin, Technical Series* **2010**, *62* (3A), 163-168
- [21] Wiehe, I. A. *Process chemistry of petroleum macromolecules*; CRC Press: Boca Raton, 2008, p. 42
- [22] Masson, J.-F.; Polomark, G. Bitumen Microstructure by Modulated Differential Scanning Calorimetry. *Thermochimica Acta* **2011**, *374* 105–114.

## 4. VISBREAKING OF OIL SANDS BITUMEN AT 250 °C

### 4.1 INTRODUCTION

In Chapter 3, visbreaking was performed at a low temperature (300 °C). Results were very interesting due to the reaction conditions. At this temperature, it is not expected to crack many molecules. That is why results in previous chapter were “peculiar”. It was found that viscosity could be reduced two orders of magnitude under these conditions. Some compositional changes were evidenced and probed through refractive index and density results. Also, <sup>1</sup>H NMR results showed a redistribution of the type of hydrogen that could be related with the changes observed in fluidity.

Viscosity could be decreased during visbreaking at 300 °C and although this was a lower temperature than typically employed in visbreaking, the role of thermal cracking still has to be taken into account. What would be the result if temperature were lowered up to 250 °C? Why 250 °C? This temperature is close to the maximum temperature that can be practically be reached by steam heating. Besides, the difference between this temperature and the one used in the previous chapter could be considered not wide based on the overall temperature range (150 – 300 °C) that was utilised for this work

Cold Lake bitumen was thermally treated at 250°C, 4 MPa and reaction times from 1 to 8 hours. After reaction, bitumen showed lower viscosity than raw bitumen and little cracking conversion was observed; the decrease in viscosity was not monotonous with reaction time.

### 4.2 EXPERIMENTAL

#### 4.2.1 Materials

Bitumen from Cold Lake area in Alberta was used for visbreaking reactions, which was provided by the Center for Oil Sands Innovation (COSI) at University of Alberta. Bitumen used in these experiments belongs to the same barrel as the bitumen samples utilised on the previous experiments in Chapter 3. Cold Lake bitumen characterization is shown in Table 3.1.

The origin and purity of nitrogen and methylene chloride were described in Chapter 3. These materials were also used in this Chapter’s experiments.

#### 4.2.2 Equipment and procedure

The same experimental set-up used in Chapter 3 was also employed in this chapter's investigations. All visbreaking experiments were carried out in batch reactors in batch mode, i.e. closed system. The main difference with respect to the description in Chapter 3 was that the reactions were performed at an internal reactor temperature of 250 °C.

### 4.2.3 Analyses

Analyses performed in Chapter 3 were also performed on the products in this chapter and the description of the instruments and analysis procedures is the same.

## 4.3 RESULTS

### 4.3.1 Material Balance

Visbreaking reaction products contained three phases: gaseous, liquid and solid. They were obtained from a reaction carried out at conditions of 250 °C, an initial pressure of 4 MPa and a reaction time varying from 1 to 8 hours. The experimental section in Chapter 3, Section 2 described the procedure for determining each phase's mass in detail.

Every experiment was performed in triplicate and the overall material balance is shown in Table 4.1 and a detailed material balance is presented in Table 4.2

**Table 4.1.** Mass balance (wt %) for visbreaking reactions at 250 °C and initial pressure of 4 MPa for different reaction times.

Reaction time [h]	Balance Material [wt %] <sup>a</sup>	
	x	s
1	99.9	1.4
2	100	0.0
3	101.2	2.0
4	102.6	1.2
5	99.0	2.9
6	99.6	1.3
7	100.8	0.3
8	99.9	0.4

<sup>a</sup> Average (x) and sample standard deviation (s) of three experiments are reported

**Table 4.2.** Product yield (wt%) for visbreaking reactions at 250 °C and initial pressure of 4 MPa for different reaction times.

Time [h]	Material Balance [wt %] <sup>a</sup>					
	Gas		Liquid		Solid	
	x	s	x	s	x	s
1	0.46	0.16	94.12	1.57	5.30	2.18
2	0.46	0.16	94.70	0.71	4.84	2.92
3	0.49	0.18	97.56	0.71	3.18	1.63
4	0.50	0.18	99.49	0.85	2.63	0.88
5	0.53	0.20	95.49	2.40	2.99	0.25
6	0.49	0.17	96.02	2.12	3.10	0.17
7	0.67	0.10	96.76	2.67	3.34	0.46
8	0.86	0.28	96.05	0.66	2.99	0.95

<sup>a</sup> Average (x) and sample standard deviation (s) of three experiments are reported

Experiments performed under these conditions showed an average material balance that closed within 1 %, i.e. material balance was between 99 and 101 %. This was not true for the results after 4 h reaction where the material balance was 103 %.

After gaseous products were collected and reactor was opened, some observations were made. Some H<sub>2</sub>S was produced during reactions, which could be smelled despite care being taken in the depressurization of the reactors after experiments. This was foreseen due to the bitumen composition that is sulfur-rich (Table 3.1). Nevertheless, it will later be shown that the concentration of H<sub>2</sub>S was very low and near the detection limit of the gaseous product analysis. Filtration time was very long. Also, some bubbles were visible in visbreaking products right after the reactor was opened. Light gases were therefore dissolved in the product.

### 4.3.2 Products characterization

Each phase produced during visbreaking reaction was characterized in order to identify critical conditions and identify changes produced. This work is focused mainly in liquid products; however, gaseous and solid products were also analysed.

### 4.3.2.1 Viscosity

Visbreaking objective is to reduce viscosity of the bitumen without causing instability. Based on that definition, viscosity results are central to this work. In order to determine the relationship between temperature and viscosity, measurements were performed at 4 different temperatures: 20, 30, 40, and 60 °C. Shear rate was held constant at 10 s<sup>-1</sup>. Figure 4.1 shows the results obtained from these experiments. Table 4.3 reports the numeric viscosity results with standard deviations.

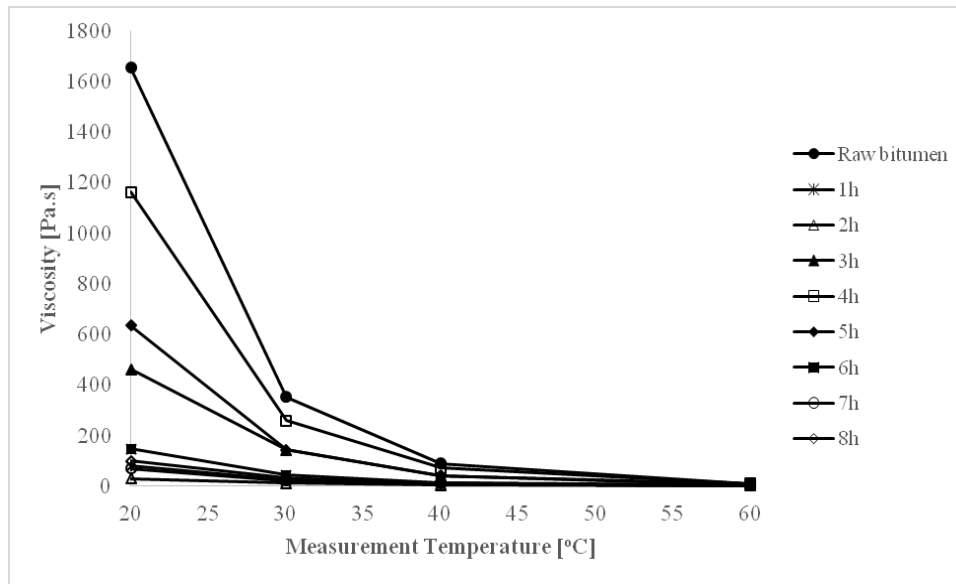


**Figure 4.1.** Viscosity of visbreaking products obtained under 250 °C, initial pressure of 4 MPa and reaction time varying between 1 and 8 hours.

**Table 4.3.** Viscosity of visbreaking products after reaction at 250 °C and initial pressure of 4 MPa.

Temperature [°C]	Reaction time [h]															
	1		2		3		4		5		6		7		8	
	Viscosity [Pa.s] <sup>a</sup>															
	x	s	x	s	x	s	x	s	x	s	x	s	x	s	x	s
20	78.6	67.3	30.3	11.0	460.9	152.1	1163.0	335.6	634.9	572.7	146.4	126.9	70.1	72.9	98.9	77.4
30	23.7	19.6	11.5	2.5	143.2	36.3	258.5	65.6	143.1	118.1	42.4	35.2	21.0	23.6	31.0	21.9
40	8.1	6.5	4.4	0.8	38.6	4.5	71.7	14.1	40.4	32.2	13.4	10.5	10.6	5.6	10.3	6.4
60	1.4	1.0	0.9	0.2	6.8	3.5	8.5	1.1	5.4	3.3	2.2	1.3	2.9	1.9	1.8	0.9

<sup>a</sup> Average (x) and sample standard deviation (s) of three experiments are reported

Viscosity can be decreased one order of magnitude. The most decrease in viscosity was observed after 2 hours reaction time, with the viscosity measured at 20 °C being decreased from 1650 Pa·s in the raw bitumen to 30 Pa·s in the visbroken product. At reaction times longer than 2 hours the viscosity increased again, reaching a maximum viscosity after 4 hours reaction time, this sample was performed 6 times in order to be sure about this behaviour. However, after 4 hours, viscosity decreases one order of magnitude reaching a minimum of 70 Pa·s (viscosity measured at 20 °C) after 7 hours of reaction.

From Figure 4.1, the relation between measurement temperature and viscosity seems to be exponential for every sample.

#### **4.3.2.2 Refractive Index**

Once viscosity was analyzed, refractive index measurements were performed. These measurements were also executed at four different temperatures: 20, 30, 40, and 60 °C. A small amount of visbreaking products was taken from every sample and subsequently analyzed. All the results are reported in Figure 4.2 which shows: a) Refractive index vs time for revealing how refractive index changes according to the reaction time; and b) Refractive index vs measurement temperature which could give an insight about visbreaking products changes. Refractive index results have been summarized in Table 4.4.

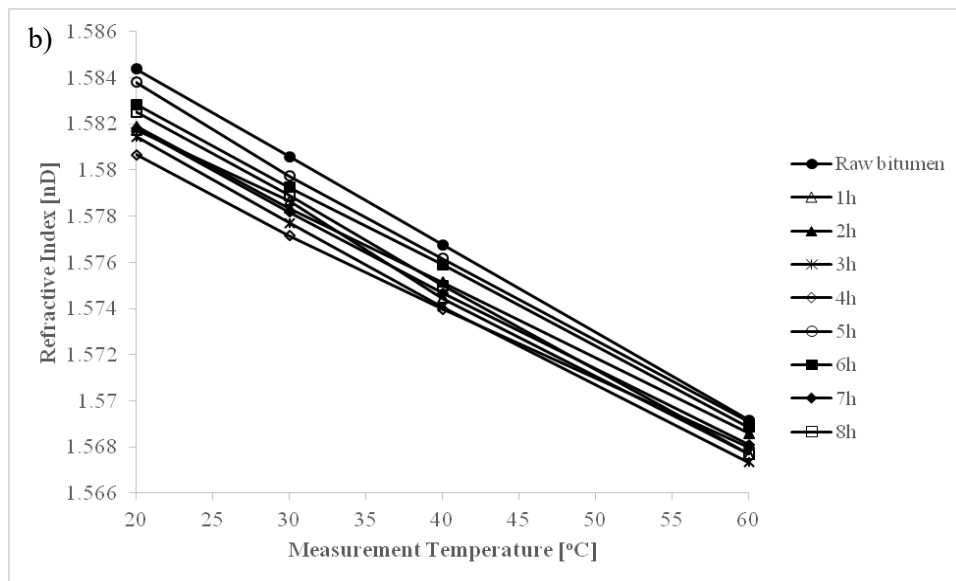
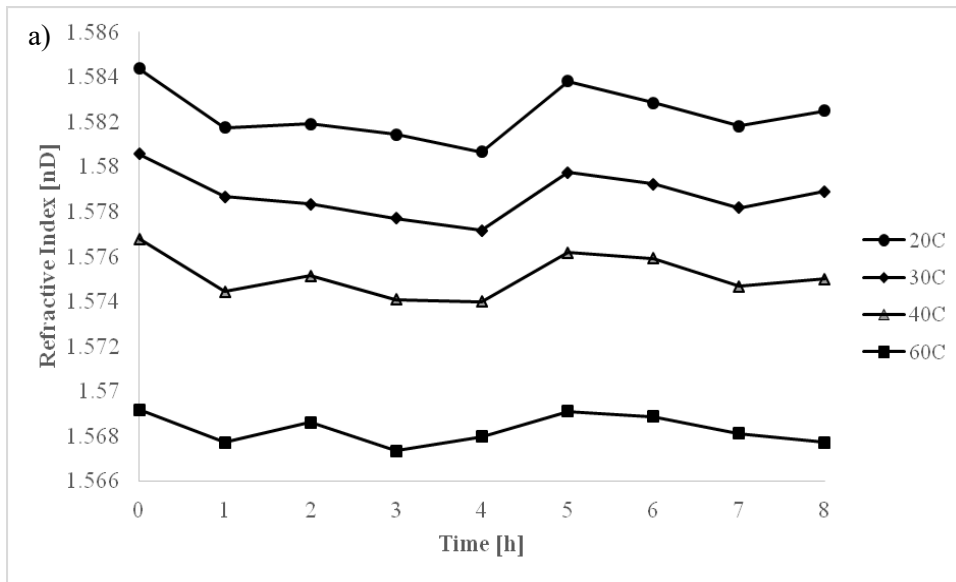


**Figure 4.2.** Refractive Index results for Visbreaking Products at 250 °C, initial pressure of 4 MPa and different reaction times: a) Refractive index vs Time; and b) Refractive index vs Measurement Temperature.

**Table 4.4.** Refractive Index measurements performed on visbreaking products after 250 °C and internal pressure 4 MPa reaction.

Temperature [°C]	Reaction time [h]																	
	0		1		2		3		4		5		6		7		8	
	Refractive Index [nD] <sup>a</sup>																	
	x	s	x	s	x	s	x	s	x	s	x	s	x	s	x	s	x	s
20	1.58437	0.00076	1.58173	0.00191	1.58190	0.00207	1.58144	0.00264	1.58065	0.00762	1.58380	0.00147	1.58283	0.00103	1.58180	0.00276	1.58250	0.00275
30	1.58057	0.00067	1.57867	0.00072	1.57833	0.00186	1.57770	0.00226	1.57715	0.00761	1.57973	0.00116	1.57923	0.00083	1.57817	0.00256	1.57890	0.00265
40	1.57677	0.00067	1.57443	0.00130	1.57443	0.00155	1.57408	0.00209	1.57398	0.00640	1.57617	0.00101	1.57590	0.00062	1.57467	0.00236	1.57500	0.00304
60	1.56917	0.00050	1.56770	0.00095	1.56770	0.00092	1.56734	0.00160	1.56798	0.00340	1.56910	0.00070	1.56887	0.00032	1.56810	0.00140	1.56770	0.00336

<sup>a</sup> Average (x) and sample standard deviation (s) of three experiments are reported.

The standard deviation is very low. It was well known that standard deviation decreases as the measurement temperature increases. Results obtained in Figure 4.2b fits in a linear equation. The slopes of the RI vs temperature varied between 0.00032 and 0.00038 K<sup>-1</sup>. Most of the products are found above 0.00035 K<sup>-1</sup>, samples after 2, 4 and 7 hour reaction are below that value which the slopes are 0.00033, 0.00032 and 0.00034 K<sup>-1</sup> respectively. These differences can be clearly observed in Figure 4.2b.

#### 4.3.2.3 <sup>1</sup>H NMR

The concentration of aromatic compounds could affect the products viscosity. NMR analysis was performed in order to determine the proportion of aromatic and aliphatic components in visbreaking products. Figure 4.3a will show the NMR spectra for every reaction time. The peak at around 5 ppm is due to the solvent.

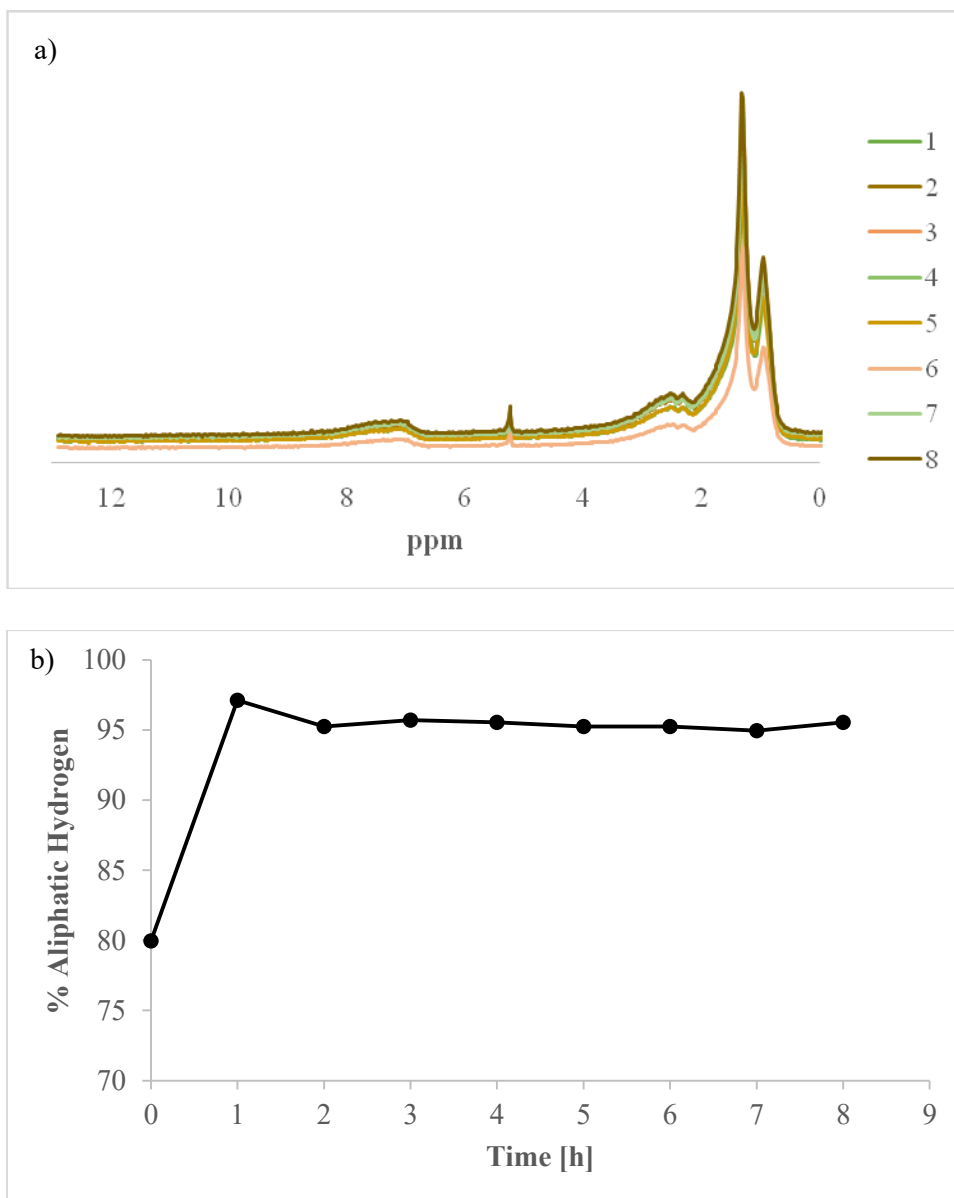


**Figure 4.3.** NMR results of visbroken products after 250 °C, initial pressure of 4 MPa and different times: a) NMR spectra for pyrolysis products; b) % Aliphatic protons vs Time.

On the other hand, Figure 4.3b will exhibit the curve produced for the aliphatic chains concentration along time. It is clear that a big change takes place after the first hour reaction. After two hours reaction, the aliphatic fraction of hydrogen will remain approximately constant around 95 %.

#### 4.3.2.4 Density

Density changes could represent a hint about some compositional changes. These measurements were also carried out at four different temperatures: 20, 30, 40, and 60 °C. In order to analyze the samples, they must be warm up right before being injected. Figure 4.4a shows a plot of density vs reaction time to reveal visbreaking products changes after reaction. In its part, Figure 4.4b will display Density vs measurement temperature, which will give a pattern, or at least an indication about the density behaviour under such conditions. The numeric values for density determination are listed in Table 4.5.

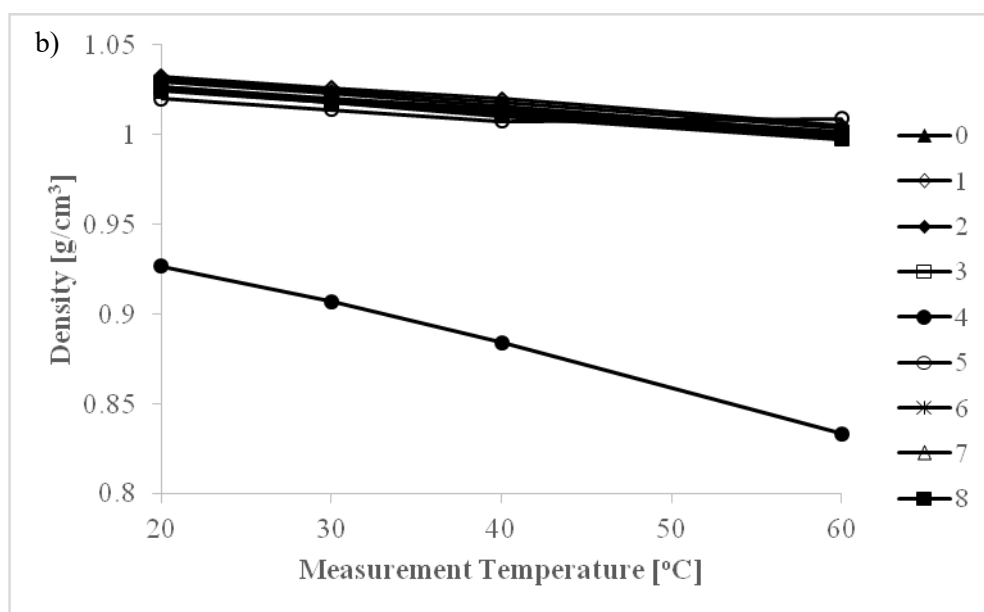
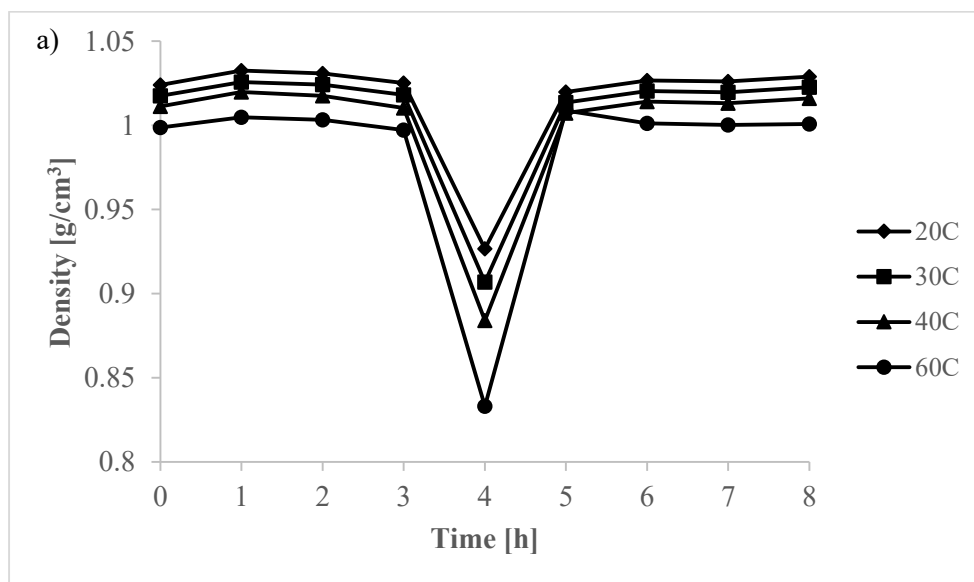


**Figure 4.4.** Density of visbreaking products obtained under 250 °C, initial pressure of 4 MPa and different reaction times: a) Density vs Time; and b) Density vs Measurement Temperature.

**Table 4.5.** Density measurements performed at four different temperatures: 20, 30, 40 and 60 °C to visbreaking products after reaction at 250 °C.

Temperature [°C]	Density [g/cm <sup>3</sup> ]								
	Time [h]								
	0	1	2	3	4	5	6	7	8
20	1.023993	1.03251	1.03087	1.02514	0.92664	1.01982	1.02674	1.02619	1.02906
30	1.017547	1.0258	1.02429	1.018245	0.906955	1.01365	1.02034	1.01966	1.02263
40	1.011263	1.01977	1.01766	1.010295	0.88407	1.00733	1.01424	1.0132	1.01601
60	0.998813	1.00491	1.00324	0.997205	0.833105	1.00877	1.00124	1.00031	1.00084

It could be considered for these samples that density does not experienced significant variations. However, the 4 hour reaction sample shows a different behaviour in respect of the other products analyzed. To make sure about this result, six experiments were performed giving the same results. Also, 5 hour products shows a deviation of the linear relationship, increasing density when it is measured at 60 °C. The samples do not show any difference in appearance. The only observable difference was that the product after 4 hours of reaction does not flow, which is different from the other products.

#### 4.3.2.5 FT-IR

This technique could be a useful way to determine some compositional changes since it could show different chemical groups. The spectrum for every reaction time was plotted and the spectra are shown in Figure 4.5.

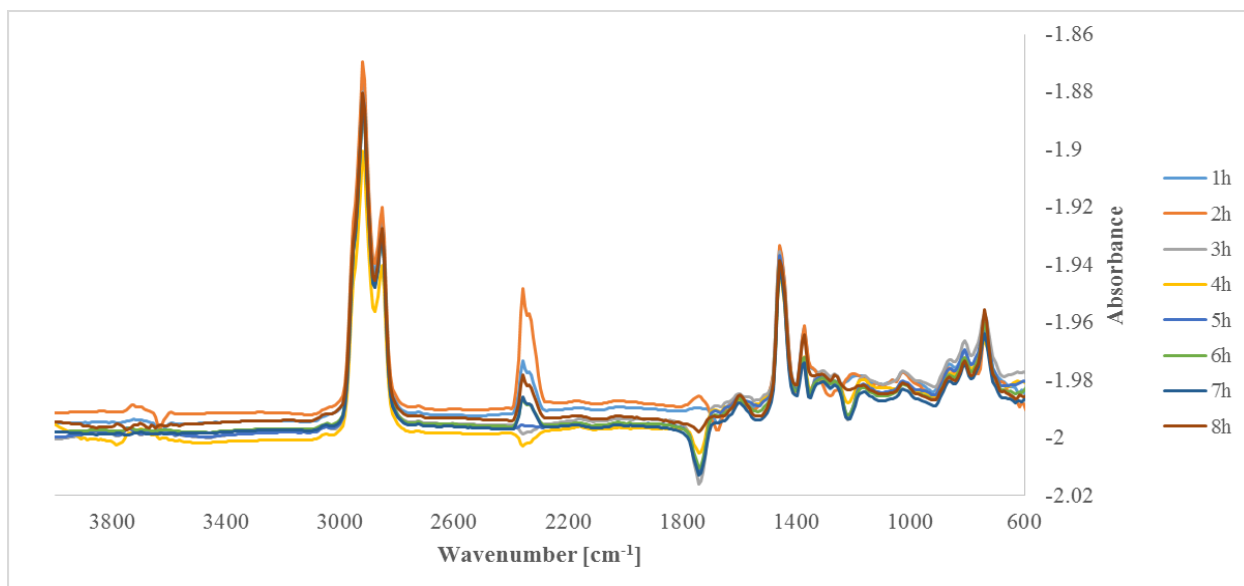


**Figure 4.5.** FTIR spectra for pyrolysis products after 250 °C, initial pressure of 4 MPa and different times reaction.

This analysis was performed in the wavenumber range of 600 – 4000  $\text{cm}^{-1}$ . Based on the spectra, IR curves seem to show a similar behaviour, composition and absorbance. The 2 hour sample show a different peak from the other products at  $\sim 1730 \text{ cm}^{-1}$ . A background spectrum was recorded roughly every hour. It appears that there was a definite difference in the carbonyl region. The size of the peaks could be a direct indication about the amount of the compound in the sample [4].

#### 4.3.2.6 Asphaltene content

“Asphaltenes could be defined as the fraction of bitumen or petroleum that is soluble in toluene, but which precipitates when a large excess of *n*-alkane is added” [5]. *n*-Pentane (*n*-C<sub>5</sub>) or *n*-heptane (*n*-C<sub>7</sub>) are usually utilised for this purposes. In this work, *n*-pentane was employed to precipitate the asphaltenes; the ratio products-solvent was 1:40. The result is compiled in Figure 4.6.

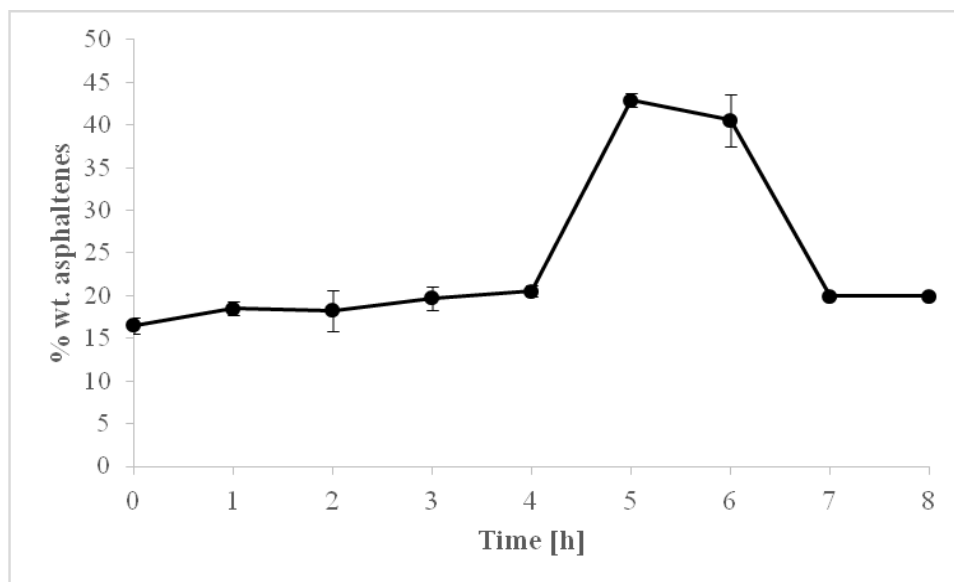


**Figure 4.6.** Asphaltene content for visbreaking products by ASTM D6560. 0 h refers to Raw Cold Lake bitumen

#### 4.3.2.7 Gas Chromatography

Once visbreaking reaction was finished, the gaseous products were collected and analyzed by gas chromatography. The analysis conditions were previously mentioned in Chapter 3. These results are reported in Table 4.6.

**Table 4.6.** Gaseous products generated during visbreaking under 250 °C and an initial pressure of 4 MPa.

Compound	Reaction time [h]							
	1	2	3	4	5	6	7	8
	[mole %]							
<b>Methane</b>	0.01	0.01	-	0.01	-	-	6.03	0.01
<b>Ethylene</b>	-	-	-	-	-	-	0.41	-
<b>Ethane</b>	-	-	-	-	-	-	1.18	-
<b>Propylene</b>	-	-	-	-	-	-	0.55	-
<b>Propane</b>	-	-	-	-	-	-	0.97	-
<b>i-Butane</b>	-	-	-	-	-	-	-	-
<b>n-Butane</b>	-	-	-	-	-	-	0.59	-
<b>cis 2-Butene</b>	-	-	-	-	-	-	-	-
<b>i-Pentane</b>	-	-	-	0.01	-	-	14.06	-
<b>n-Pentane</b>	0.04	0.01	0.01	0.01	0.01	-	9.38	0.01
<b>i-Hexene</b>	-	-	-	-	-	-	0.17	-
<b>n-Hexene</b>	-	-	-	-	-	-	-	-
<b>CO<sub>2</sub></b>	0.10	0.08	0.08	0.09	0.07	0.08	0.06	0.10
<b>H<sub>2</sub></b>	-	-	1.92	-	-	-	-	-
<b>Ar</b>	2.05	2.30	3.47	4.01	9.26	12.51	11.20	5.69
<b>N<sub>2</sub></b>	97.78	97.59	96.43	95.87	90.65	87.40	55.39	94.19
<b>CO</b>	0.01	-	-	-	-	0.01	-	-

#### 4.3.2.8 Solid content

It was expected that some solids were going to be produced during visbreaking reaction. In order to obtain the amount of solids generated during this process, products were filtered and weighed to determine the actual amount of this phase. Methylene chloride was the solvent utilised for diluting visbreaking products. Figure 4.7 presents the solid content results; it is expressed as the division of the consolidated material over the initial amount of bitumen.

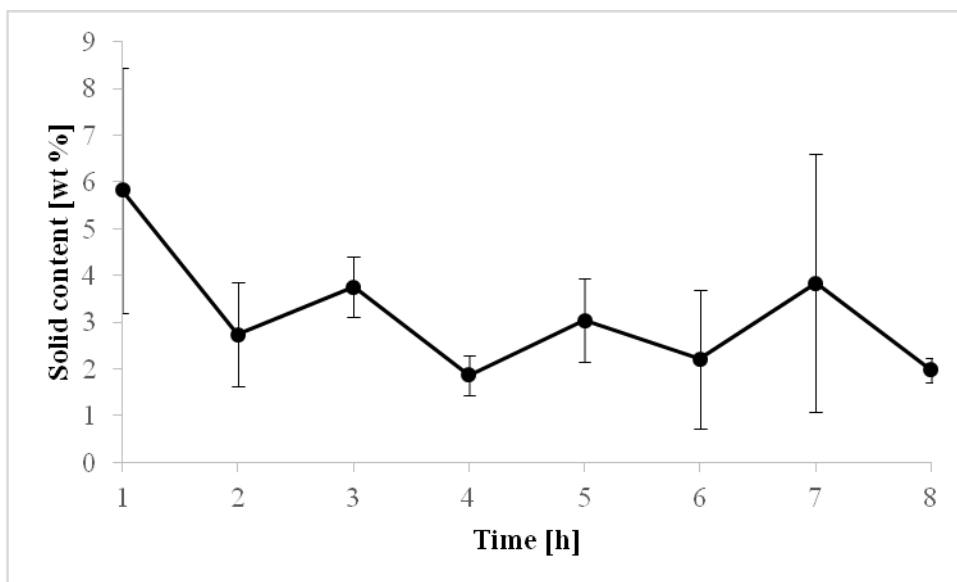


**Figure 4.7.** Solid content in pyrolysis products after reaction at 250 °C.

## 4.4 DISCUSSION

### 4.4.1 Temperature effects

Temperature can be a determining factor for bitumen viscosity. Its effects can be observed in those properties measured at different temperatures. The relation between viscosity and measurement temperature was previously discussed in Chapter 3, it is given by

$$\ln[\ln(\mu)] \propto \ln(T) \quad (1)$$

Experimental data was plotted using the relationship described by Eq. 1 and these results are shown in Figure 4.8. According to them, most of the products follow a linear behaviour, but this is not true for products after 7 hours reaction. Formation of a second phase may explain the variation in the sample after 7 hours reaction. The 7 hour reaction samples was at a local viscosity minimum (Table 4.3) and the onset of the formation of a second phase to increase the viscosity at longer reaction time may just be starting. A minor change in measurement temperature may affect the extent of expression of the second phase, thereby affecting the relationship between viscosity and measurement temperature.

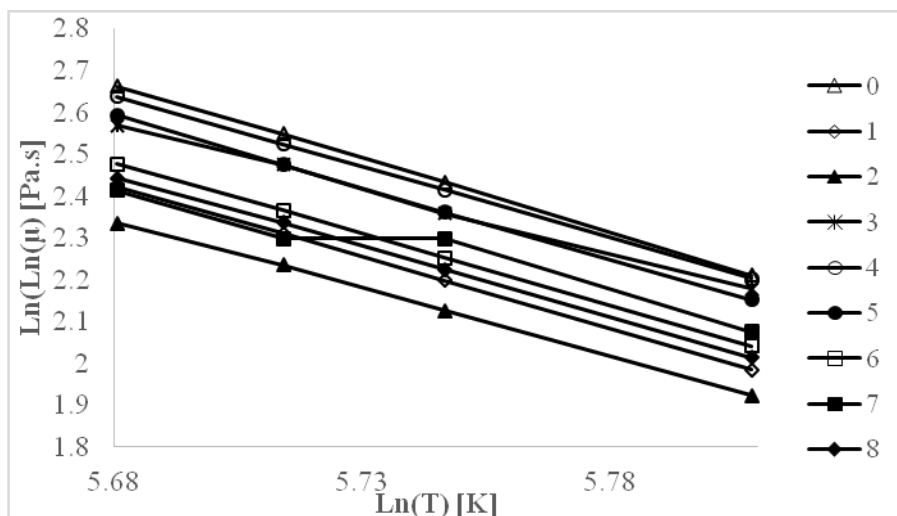


**Figure 4.8.** Viscosity of visbreaking products after 250 °C and 4 MPa along different residence times based on Eq. 1.

Considering what was said previously, at a lower reaction temperature the development of a second phase is reduced, but still observed (at least in the 7 hour sample). Compared with results in Chapter 3, the amount of samples that showed a deviation of the linear behaviour are less. A low temperature will not promote the free radical cracking as at a higher typical visbreaking temperatures. Instead, some addition reactions can take place, which would increase higher molecular mass species that could affect solubility and promote the formation of a second phase.

Regarding Table 4.3, it is clear that viscosity can be reduced through visbreaking at 250 °C. However, the impact of this temperature is less than visbreaking at 300 °C, which corresponds to those experiments performed in Chapter 3. Based on the results obtained, the effect of reaction temperature on viscosity is diminishing as it is decreased.

#### 4.4.2 Consequences of residence time

The influence of the reaction time is getting stronger along with decreasing reaction temperature. Figure 4.1 shows a maximum in viscosity at 4 hours reaction. The hypothesis for this behaviour is based on the preference of the free radical mechanisms at lower temperatures. At 250 °C, the addition and/or redistribution reactions are favoured thermodynamically. They could be achieved through a hydrogen disproportionation observed in Figure 4.3b where an increase in the aliphatic hydrogen content is significant after one hour reaction and this may promote the further development of these processes.

Looking at Figure 4.2a and Figure 4.4a, it is evident that residence time has a strong effect on the visbreaking. An example of this can be seen in refractive index and density results. While RI does not present “significant” changes, density exhibits a big drop up to four hours reaction. The maximum value for viscosity coincides with this drop. However, the density increases after this event, which could be considered a transition point or process that may change in order to achieve a better stability along the four hours. Looking at RI results, changes are not that obvious. However, the slopes can show better the variations. It was found that products after four hour reaction exhibits the lowest slope and considering the density results, Figure 4.6a reveals a significant drop in density plus Figure 4.6b allows one to appreciate how this product is out of the trend. Based on these observations, a compositional change could be considered and an increasing in the paraffinic content may be contemplated as possible explanation. However, both RI and density values return to the general trend, which could mean that the restructuring reactions that took place were transient in some way.

Based on [9], the size of the aromatic compounds may affect refractive index. An increasing in aromatic component size will reflect in smaller changes in RI. This could be explained by the increasing of the dipole moment along the aromatic molecule when it is bigger. Also, molecular structure may affect the dipole moment.

#### **4.4.3 Spectroscopy hints**

Some changes can be found. Useful techniques like  $^1\text{H}$  NMR and FT-IR can give an idea about what is happening and could help explain the results of the visbreaking at 250 °C. It was not expected to observe many changes at this reaction condition. Perhaps, this thermal cracking could contribute to a minor extent to the observed variations.

An increase in aliphatic hydrogen content is observed after one hour reaction. In Figure 4.3b, it is possible to see that the amount of this kind of protons remains approximately constant with further increase in reaction time. Due to the abrupt increase in aliphatic hydrogen content, hydrogen disproportionation could be considered. It may be seen as the most important step in thermal cracking reactions since it may lead several kind of free radical reactions.

Regarding Figure 4.3a, it is possible to identify 5 peaks which can divided in three sections: the first two peaks (around 0.9 and 1.3 ppm) are related with the aliphatic protons, the third peak is

linked with benzylic protons (approximately 2.3 ppm). On the other hand, peak number four corresponds to the solvent employed for diluting the sample. Lastly, a peak for aromatic and/or phenolic protons (about 7.3 ppm) was found. Making a distinction on the aliphatic peaks is necessary. The first peak (~0.9 ppm) corresponds to a primary aliphatic protons which can be linked with straight-chain alkanes, likely alkyl chains. The second peak (~ 1.3 ppm) is associated with a secondary aliphatic proton as well as methylene groups in branches and chains.

Based on the results presented in Figure 4.3a, the protons distribution was found and it is shown in Figure 4.9. At first, the amount of primary aliphatic hydrogen could not be determined for Cold Lake bitumen feed. It could be due to an overlapping or a low concentration in this sample. After one hour reaction, it is possible to see the peak linked to the primary aliphatic hydrogen. The amount of secondary aliphatic and benzylic protons did not experienced much variation with reaction time. However, the main “redistribution” is related with the primary aliphatic and aromatic protons.

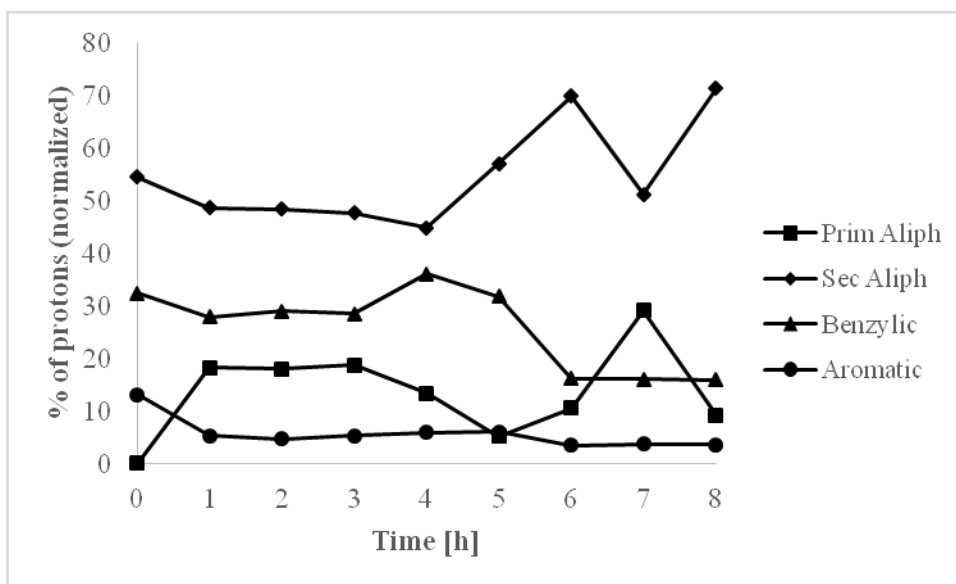


**Figure 4.9.** Area under the curve extracted from the NMR spectra, comparing the different type of proton found for visbreaking products obtained at 250 °C reaction.

To determine changes that bitumen had experienced after a thermal cracking procedure could be hard. However, some of them can be identified through the right tools. As it was mentioned before, dipole moment could affect some of the analysis performed. In the case of FT-IR, it will determine the intensity of the absorption peaks.

Figure 4.5 shows the FT-IR spectra for visbreaking products. A small peak around  $3700\text{ cm}^{-1}$  was identified, it could be related with the stretching of O-H bond for an intermolecularly bonded hydrogen. The stretching of methyl groups in aliphatic chains presents a peak at  $2923\text{ cm}^{-1}$  and it is followed by a peak around  $2853\text{ cm}^{-1}$ , which is related with the stretching of the methylene groups in an aliphatic chain. A carbonyl group (C=O) stretching appear around  $1743\text{ cm}^{-1}$  accompanied by a peak at  $1600\text{ cm}^{-1}$  that is linked to the stretching of C=C bond into a ring structure. This last peak should have a “confirmation” peak around  $900\text{ cm}^{-1}$ , which is related with the C-H bond in an aromatic structure and it did. Two peaks appear around  $1456\text{ cm}^{-1}$  and  $1375\text{ cm}^{-1}$ , respectively; they corroborate the presence of methyl and methylene groups in the sample associated with peaks at  $2923$  and  $2853\text{ cm}^{-1}$ . Sulfur compounds also can be observed in FT-IR spectra, the stretching of the S=O bond shows a peak around  $1030\text{ cm}^{-1}$ . A group of peaks observed in Chapter 3 is observed too. This group is related with the out-of-plane deformation vibration of one isolated aromatic C-H bond, two or three adjacent aromatic C-H bonds and four aromatic adjacent aromatic bond at  $870$ ,  $814$  and  $750\text{ cm}^{-1}$  respectively [10].

#### 4.4.4 Gas products

Table 4.6 summarized the gases produced during visbreaking reactions under the experimental conditions used in this Chapter. Gas chromatography was used to characterize this phase.

Based on the results obtained, the amount of gas produced under these conditions is lower than the amount obtained in the previous Chapter. Most of the products generated correspond to  $C_5$  products. This is not true for the products at 7 hours reaction where almost all of the gaseous hydrocarbon products were generated. However this particular event, it does not seem related with any other result. To produce a significant amount of  $CH_4$  implies that the amount of energy provided should be important. That could be the explanation for the lack of lighter products, the energy supplied is not enough to break the terminal bonds and generate a  $CH_3$  radical that will ultimately lead to the formation of methane.

#### 4.4.5 Solid products

Through visbreaking a solid phase could be produced: Asphaltenes and coke. Chapter 3 explained how asphaltenes and solids were obtained, that procedure was also followed in this chapter. Figure 4.7 shows the amount of asphaltenes produced along reaction time. The amount of asphaltenes may be considered constant except for the reaction product after five and six

hours of reaction where it reached 45 wt %. Interestingly the maximum asphaltenes content was found in the reaction period that preceded the local viscosity minimum, yet, there was no meaningful increase in solids yield.

These events could be explained through the development of some addition and/or aggregation reactions that appeared to lead to products that were not persistent. These results may affect the data obtained from RI since asphaltenes are considered compounds with higher RI. Besides, the possible stronger polar character of these molecules and some intermolecular interactions can be created which could “increase” the size of some molecules.

The production of coke may be part of the nature of bitumen. Higher temperatures could promote the formation of this solid phase. Based on that, the amount of coke expected is small. However, having a multiphase system could make up that changes happen at different periods. Considering a large mesophase with small crystalline phases [11], a stark difference in physical and chemical properties could avoid the proper peptization of asphaltenes making the entire system unstable [12]. Compared with the initial amount, solid content is higher but the general tendency shows a decrease in the formation of solids along the residence time.

#### **4.5 CONCLUSIONS**

This work presented some similarities with Chapter 3. However, some responses to the thermal cracking process differ of it.

- a) There is not expected to have a significant conversion. Perhaps, the production of lighter products suggest some changes associated with it. Regarding the gaseous phase, compounds developed during these experiments suggest that the energy supplied by the temperature condition, it is not enough to overcrack the bitumen.
- b) Viscosity can be reduced by thermal cracking and this was possible through some redistribution mechanisms explained by the free-radical chemistry. Based on the results of the gaseous phase characterization, it is clear that the amount of bonds broken during these experiments is smaller compared with results obtained in Chapter 3 and just the weaker bonds were broken.

- c) The influence of residence time is having more impact on the visbreaking reaction. Longer residence times could promote the stabilization of larger molecules. This means that the structures may vary until a lower energy conformation is achieved.
- d) Variations in refractive index (RI) and density could confirm a decrease in the aromaticity. Both properties can give information about compositional changes. A diminishing in both values may be related with an increase of the naphthenic (cycloparaffinic) molecules.

### Literature cited

[1] de Klerk, A.; Gray, M. R.; Zerpa, N. Unconventional Oil and Gas: Oilsands, In *Future Energy: improved, sustainable and clean options for our planet*, 2ed; Letcher, T.M. Ed.; Elsevier: London, 2014, p. 95-116.

[2] Joshi, J. B.; Pandit, A. B.; Kataria, A. B.; Kulkarni, R. P.; Sawarkar, A. N.; Tandon, D.; Yad, R.; Mohan, K. M. Petroleum Residue Upgradation via Visbreaking: A Review. *Ind. Eng. Chem. Res.* **2008**, *47*(23), 8960-8988.

[3] Gary, J. H.; Handwerk, G. E. *Petroleum Refining: Technology and Economics*, 5ed; Taylor & Francis Group: Boca Raton, FL, 2007.

[4] ThermoScientific. Introduction to Fourier Transform Infrared Spectroscopy. *Molecular Materials Research Centre, Beckman Institute, California Institute Technology*. Visited November 6, 2015. <http://mmrc.caltech.edu/FTIR>

[5] Gray, M. R. *Upgrading oilsands bitumen and heavy oil*; Pica Pica Press, an imprint of the University of Alberta Press, 2015.

[6] Carrillo, J. A.; Pantoja E.; Garz6n, G.; Barrios, H.; Fernandez, J.; Carmona, E.; Saavedra, J. Control of severity in visbreaking. *Prepr. Pap.-Am. Chem. Soc., Div. Energy Fuels* **2000**, *45*(3), 617-621.

[7] Speight, J. G., Ozum, B. *Petroleum Refining Processes*; Marcel Dekker: New York, 2002, p. 385.

- [8] Strausz, O. P.; Lown, E. M. *The Chemistry of Alberta Oil Sands, Bitumens and Heavy Oils*; Alberta Energy Research Institute: Calgary, 2003, p. 119.
- [9] Sachanen, A. N.; Tilicheev, M. D. *Chemistry and Technology of Cracking*; Chemical Catalog Co.: New York, 1932, p. 155.
- [10] Borrego, A. G.; Blanco, C. G.; Prado, J. G.; Diaz, C.; Guillen, M. D. <sup>1</sup>H NMR and FTIR Spectroscopic Studies of Bitumen and Shale Oil from Selected Spanish Oil Shales. *Energy Fuels* **1996**, *10* (1), 77–84.
- [11] Masson, J.-F.; Polomark, G. Bitumen Microstructure by Modulated Differential Scanning Calorimetry. *Thermochimica Acta*. **2011**, *374* 105–114.
- [12] Zong-xian Wang; Ai-Jun Guo; Guo-he Que. Coke formation and characterization during thermal treatment and hydrocracking of Liaohe vacuum residuum. *Prepr. Pap.-Am. Chem. Soc., Div. Energy Fuels* **1998**, *43*(3), 758-764.

## **5. VISBREAKING OF OIL SANDS BITUMEN AT 200 °C**

### **5.1 INTRODUCTION**

In previous chapters, visbreaking was performed at two different temperatures, 300 and 250 °C. The results that were obtained could be considered promising. Compared with typical visbreaking temperatures (430-490 °C), the temperatures studied were significantly lower, but it has been shown that viscosity can be decreased one or two orders of magnitude under these lower temperatures.

The energy provided at these lower temperatures was not high enough to break many molecular bonds and hence, apart from the significant decrease in viscosity and the impact of hydrogen disproportionation, there were no severe changes. In order to determine if viscosity could be reduced at an even lower temperature, the effect of this thermal process was evaluated at 200 °C. Compositional changes were monitored through several techniques, such as refractive index, density, <sup>1</sup>H NMR and FT-IR.

200 °C is not considered a high temperature and the results obtained from this set of experiments will represent a better understanding of bitumen behaviour at a temperature condition seldom studied and reported in literature.

Visbreaking reactions were carried out at 200 °C, 4 MPa and reaction times were varied between 1 and 8 hours. Cold Lake bitumen was used for these experiments and results were compared with the raw bitumen characterization. These experiments showed a little cracking conversion and some interesting changes along reaction time.

### **5.2 EXPERIMENTAL**

#### **5.2.1 Materials**

Bitumen employed in these experiments belongs to the Cold Lake area in Alberta. It was supplied by the Center for Oil Sands Innovation (COSI) at University of Alberta. The same barrel was used for the entire set the experiments. Cold Lake bitumen characterization is shown in Table 3.1.

In addition to Cold Lake bitumen, nitrogen and methylene chloride utilised in this chapter were the same as described in Chapter 3.

### **5.2.2 Equipment and procedure**

This set of experiments was performed in batch mode. Equipment and procedures were not changed from the previous chapters. All the details are provided in Chapter 3. Reaction conditions were 200 °C, 4 MPa and residence time from 1 to 8 hours. For the first two sets of experiment, Fisherbrand™ Class B Clear Glass Threaded vials of 23 x 85 mm (22 mL) were used. For this chapter, Fisherbrand™ Clear Straight-Sided Jars of 60 mL were used.

### **5.2.3 Analyses**

Analyses performed in this set of experiments were described in Chapter 3. However, the conditions for viscosity analysis were changed and it will be presented below.

Viscosity measurements were performed in an Anton Paar RheolabQC viscosimeter. The measuring cup utilised was CC17/QC-LTC with an internal diameter of 16.664 mm and 24.970 mm length. For carrying out this analysis, 4 g of sample was required. Measurements were performed at four different temperatures (20, 30, 40 and 60 °C). A Julabo F25-EH circulating heater/chiller was employed to control the temperature. Its controller is capable of maintaining the temperature constant within  $\pm 0.2$  °C. A constant shear rate of  $1.2 \text{ s}^{-1}$  was used. It is a different value compared with the previous chapters. Shear rate had to be changed due to an equipment limitation. Samples obtained from these experiments were significantly more viscous and  $1.2 \text{ s}^{-1}$  was the maximum value of shear rate at which measurements could be performed.

## **5.3 RESULTS**

### **5.3.1 Material Balance**

A multiphase system (gaseous, liquid and solid phases) was produced after visbreaking took place. These products were the result of the following reaction conditions: 200 °C, an initial pressure of 4 MPa and a reaction time varying from 1 to 8 hours. Material balance closure was generally within 100 to 103 wt%. All the experiments were conducted in triplicate and results were reported as an average with one sample standard deviation, this is shown in Table 5.1. Additionally, the reaction yield data is presented in Table 5.2.

**Table 5.1.** Overall Mass Balance (wt %) for Visbreaking Reactions at 200 °C and Constant Pressure (4 MPa) for different reaction times.

Reaction time [h]	Material balance [wt %] <sup>a</sup>	
	x	s
1	100.9	0.7
2	100.2	2.0
3	100.0	0.3
4	102.1	0.5
5	103.4	0.8
6	101.9	2.7
7	102.8	0.9
8	101.6	0.6

<sup>a</sup> Average (x) and sample standard deviation (s) of three experiments are reported

**Table 5.2.** Product yield (wt%) for visbreaking reactions at 200 °C and initial pressure of 4 MPa for different reaction times

Time [h]	Material Balance [wt %] <sup>a</sup>					
	Gas		Liquid		Solid	
	x	s	x	s	x	s
1	0.83	1.53	98.32	1.24	1.80	0.33
2	1.07	1.57	97.90	1.11	1.97	0.31
3	1.03	1.41	97.79	0.66	2.12	0.47
4	1.41	0.70	97.34	0.29	2.21	0.36
5	1.32	0.76	97.74	0.74	1.92	0.58
6	1.19	0.38	98.28	0.78	1.49	0.25
7	1.50	1.57	98.02	0.28	1.45	0.21
8	1.61	1.14	96.77	0.20	2.58	1.57

<sup>a</sup> Average (x) and sample standard deviation (s) of three experiments are reported

Highest standard deviations were observed for the products after 2 and 6 hour reaction. When reactors were opened, some bubbles were observed. Filtration time had reduced significantly compared to reactions performed at 300 and 250 °C. Also, as mentioned in the experimental section, the storage containers were changed in order to speed up the solvent evaporation from the liquid products.

### 5.3.2 Product characterization

It was required to characterize every phase for studying the changes that occurred during the visbreaking reactions. Even though this work was focused on liquid products characterization, gaseous and solid products were analyzed as well.

#### 5.3.2.1 Viscosity

Viscosity was of primary interest, measurements were performed at four different temperatures: 20, 30, 40, and 60 °C. Measurement shear rate was constant at 1.2 s<sup>-1</sup> for all the experiments. Results obtained have been summarized in Figure 5.1 and Table 5.3.

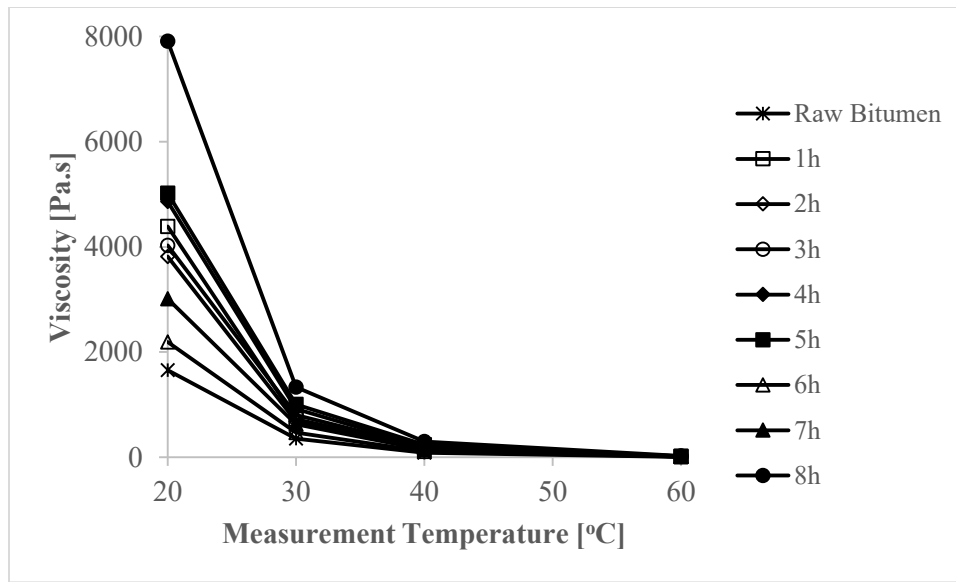


**Figure 5.1.** Viscosity of visbreaking products obtained under 200 °C, initial pressure of 4 MPa and reaction time varying between 1 and 8 hours.

**Table 5.3.** Viscosity data from measurements performed to Visbreaking products under 200 °C and initial pressure 4 MPa.

Temperature [°C]	Reaction time [h]															
	1		2		3		4		5		6		7		8	
	Viscosity [Pa.s] <sup>a</sup>															
	x	s	x	s	x	s	x	s	x	s	x	s	x	s	x	s
20	4,389.2	523.7	3,817.1	1,373.7	4,028.2	303.1	4,862.0	3,757.2	5,018.8	888.4	2,188.4	534.4	3,014.4	566.8	7,907.5	2,913.6
30	724.3	170.4	685.4	239.0	803.6	3.4	918.6	637.7	1,006.4	213.1	467.6	81.7	629.6	98.2	1,336.3	428.9
40	175.2	25.9	161.0	46.8	187.3	3.3	204.8	131.7	239.8	65.6	112.8	19.6	148.4	21.5	300.7	96.9
60	16.3	1.8	14.1	2.6	12.9	2.9	16.7	8.8	19.8	5.1	11.1	1.6	10.4	4.6	23.6	6.7

<sup>a</sup> Average (x) and sample standard deviation (s) of three experiments are reported

Viscosity results show a significant increasing compare with visbroken products obtained in the previous chapters. Also, viscosity of Cold Lake bitumen feed is lower than the products generated from this set of experiments at 200 °C. Raw bitumen has a viscosity of  $1.7 \times 10^3$  Pa·s but the highest value for this samples corresponds to 8 hour reaction which viscosity is  $7.9 \times 10^3$  Pa·s.

The difference with Chapter 3 and 4 is visible. These products do not move, they look like a solid. And it was hard to take the sample out for performing the analyses showed in this chapter

#### **5.3.2.2 Refractive Index**

A small amount of sample was taken to perform the measurements. The analysis was carried out at four different temperatures like viscosity: 20, 30, 40 and 60 °C. Results are reported in Figure 5.2 showing a) Refractive index vs time in order to show variations along reaction time; and b) Refractive index vs measurement temperature for getting information about the changes produced.

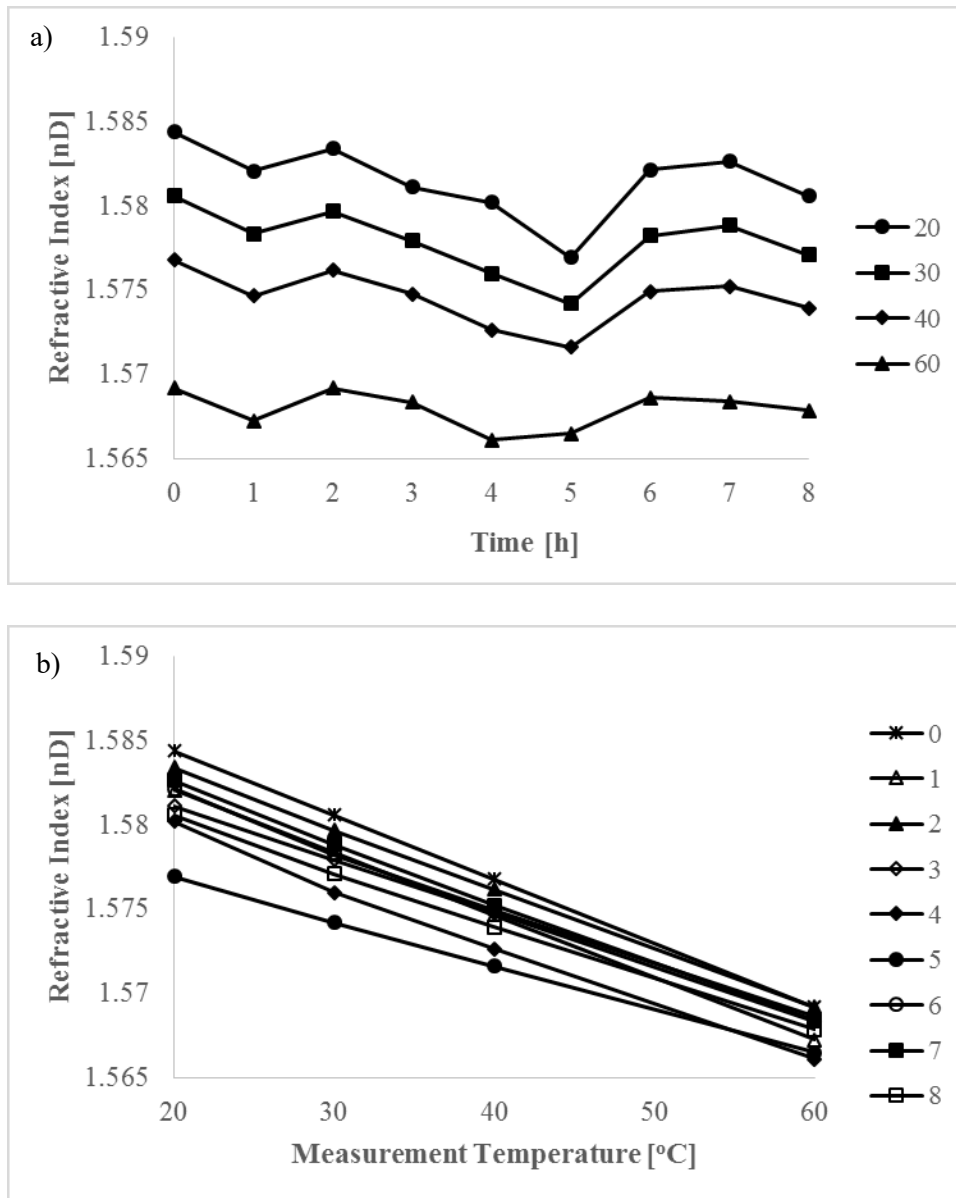


**Figure 5.2.** Refractive Index results for Visbreaking Products at 200 °C, initial pressure of 4 MPa and different reaction times: a) Refractive index vs Time; and b) Refractive index vs Measurement Temperature.

Measurement results are presented in Table 5.4. Standard deviation is decreased along measurement temperature. However, this is not true for samples after 1 and 8 hour reaction. Figure 5.2b shows how results obtained almost fit perfectly a linear equation. The slope of refractive index vs measurement temperature is not constant for visbroken products, it varies between  $-0.00026$  to  $-0.00038 \text{ K}^{-1}$ . The lowest value corresponds to 5 hour reaction sample.

**Table 5.4.** Refractive Index measurements performed on visbreaking products after 200 °C and initial pressure 4 MPa reaction.

Temperature [°C]	Reaction time [h]																	
	0 <sup>a</sup>		1		2		3		4		5		6		7		8	
	Refractive Index [nD] <sup>a</sup>																	
	x	s	x	s	x	s	x	s	x	s	x	s	x	s	x	s	x	s
20	1.58437	0.00076	1.58207	0.00340	1.58340	0.00340	1.58110	0.00078	1.58020	0.00594	1.57693	0.00775	1.58213	0.00138	1.58263	0.00147	1.58057	0.00083
30	1.58057	0.00067	1.57833	0.00345	1.57967	0.00345	1.57793	0.00064	1.57597	0.00721	1.57420	0.00635	1.57823	0.00146	1.57883	0.00121	1.57709	0.00125
40	1.57677	0.00067	1.57467	0.00347	1.57617	0.00347	1.57477	0.00057	1.57263	0.00629	1.57163	0.00463	1.57493	0.00129	1.57523	0.00114	1.57393	0.00105
60	1.56917	0.00050	1.56727	0.00336	1.56917	0.00336	1.56833	0.00071	1.56610	0.00318	1.56650	0.00190	1.56863	0.00042	1.56840	0.00098	1.56784	0.00079

<sup>a</sup> Average (x) and sample standard deviation (s) of three experiments are reported

<sup>b</sup> 0 h is referring to the Cold Lake bitumen feed.

### 5.3.2.3 <sup>1</sup>H NMR

This technique could give information about the changes occurred after visbreaking at 200 °C, based on the distribution of the type of hydrogen observed in these products. Figure 5.3a shows the spectra for those products. It allows to observe the peaks that will be include in the analysis of this chapter. This figure can be considered crucial in order to determine the specific kind of hydrogen in each sample.

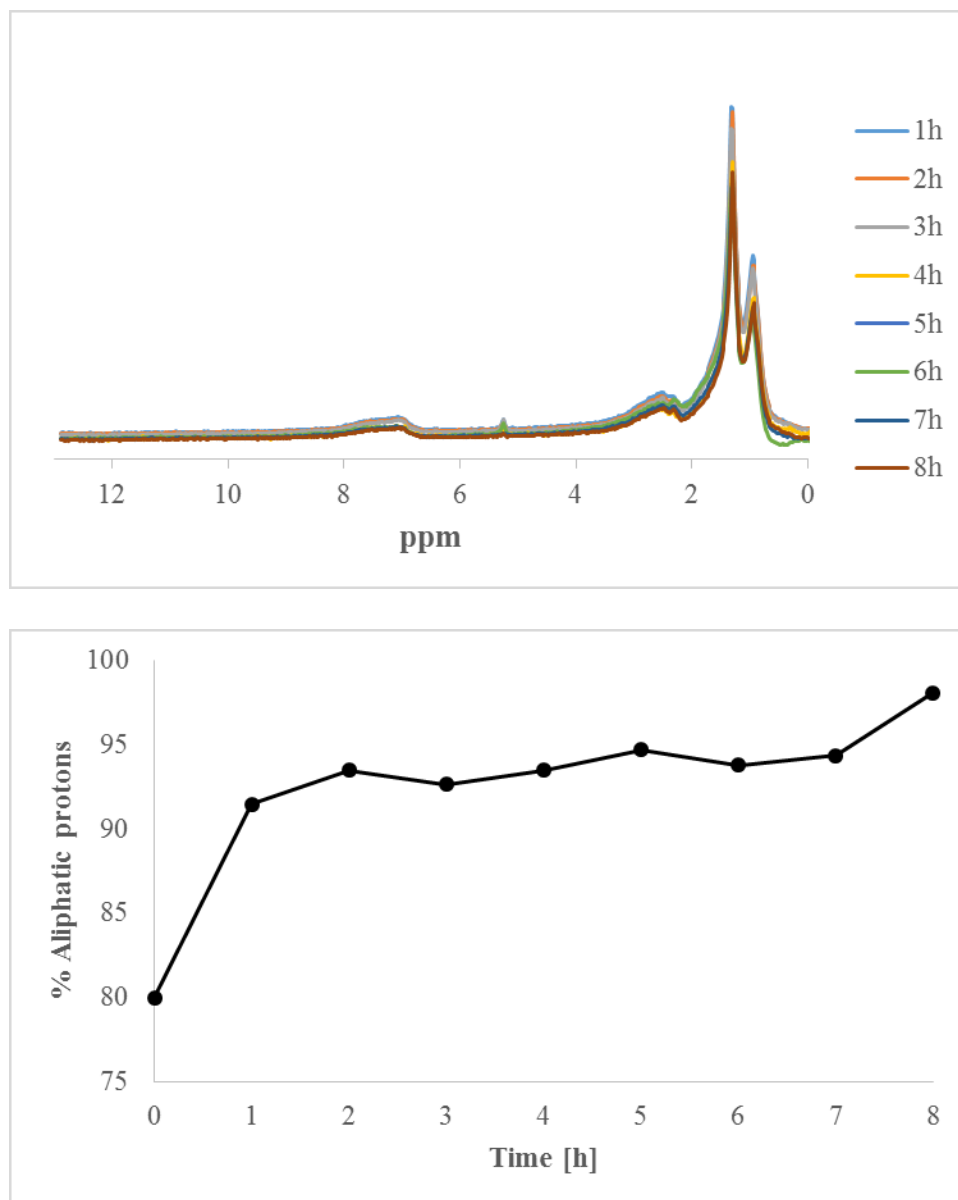


**Figure 5.3.** NMR results of visbroken products after 200 °C, initial pressure of 4 MPa and different times:  
 a) NMR spectra for pyrolysis products; b) % Aliphatic protons vs Time.

On the other hand, Figure 5.3b shows the relative amount of aliphatic hydrogen observed in visbroke products. A big change was evidenced after one hour of reaction and the amount of aliphatic hydrogen kept increasing up to 98%, this point was reached at 8 hours reaction time.

#### 5.3.2.4 Density

Having variations in density could be a sign for changes in composition. Samples were analyzed at four different temperatures: 20, 30, 40, and 60 °C. To perform these measurements, samples

must be warmed up first so that the samples can be injected into the equipment. Figure 5.4a shows density vs reaction time to show changes produced during visbreaking along the residence time. Density behaviour as function of measurement temperature is shown in Figure 5.4b.

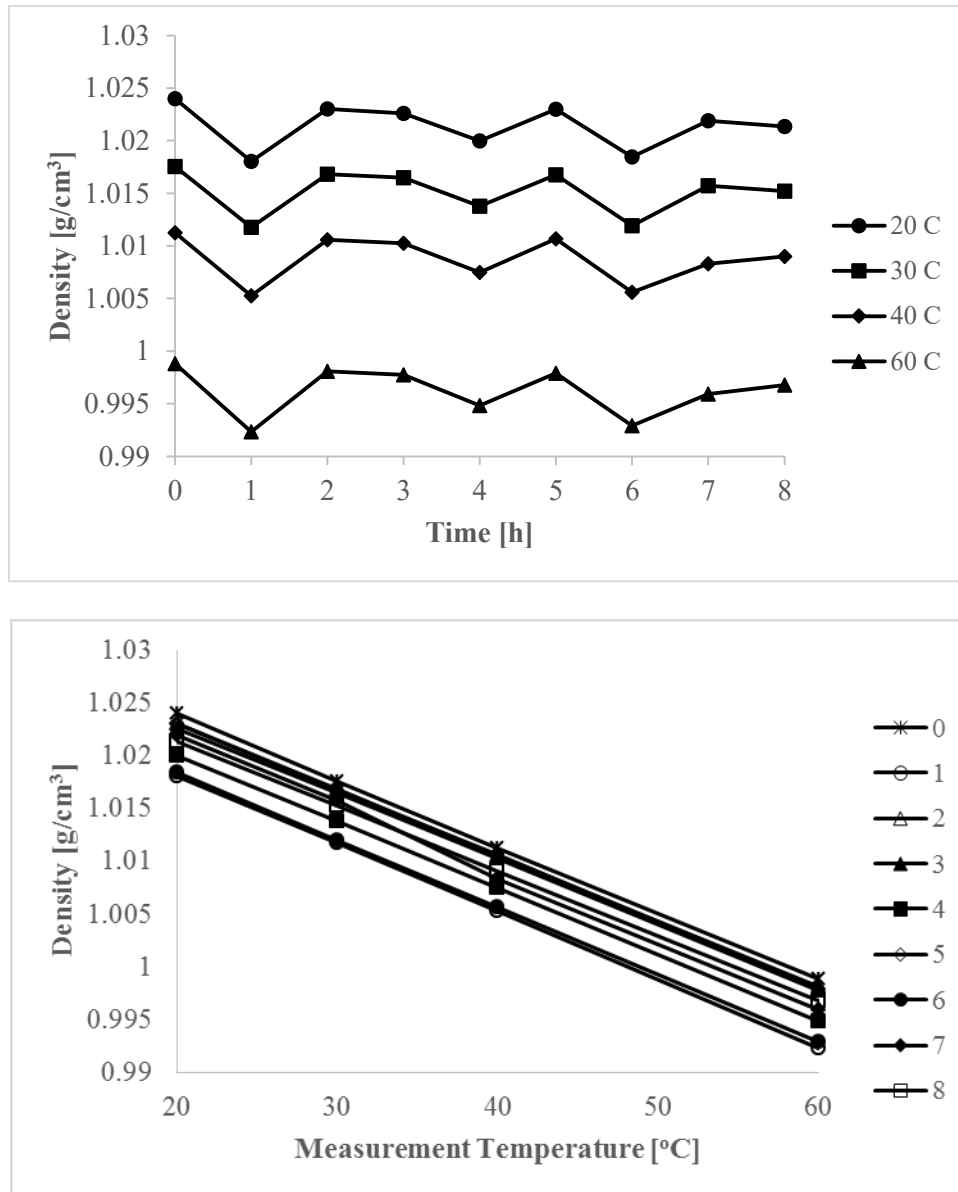


**Figure 5.4.** Density of visbreaking products obtained under 200 °C, initial pressure of 4 MPa and different reaction times: a) Density vs Time; and b) Density vs Measurement Temperature..

**Table 5.5** Density measurements performed at four different temperatures: 20, 30, 40 and 60 °C to visbreaking products after reaction at 200 °C.

Temperature [°C]	Reaction time [h]								
	0 <sup>a</sup>	1	2	3	4	5	6	7	8
	Density [g/cm <sup>3</sup> ]								
<b>20</b>	1.02399	1.01802	1.02302	1.02259	1.01998	1.02298	1.01846	1.02189	1.02136
<b>30</b>	1.01755	1.01178	1.01683	1.01647	1.01377	1.01676	1.01192	1.01571	1.0152
<b>40</b>	1.01126	1.00525	1.01057	1.01023	1.00748	1.01068	1.0056	1.00831	1.00901
<b>60</b>	0.99881	0.99233	0.99807	0.99774	0.99482	0.99788	0.99291	0.99591	0.99676

<sup>a</sup> 0 h is referring to the Cold Lake bitumen feed

Table 5.5 compiles density data results. A linear behaviour is observed in Figure 5.4b. Most of them shows the same slope except for the sample after 7 hour reaction which value is -0.0007 cm<sup>3</sup>.°C/g. For these products, density results are lower than the ones obtained in Chapter 3 and 4, they vary between 1.018 and 1.024 g/cm<sup>3</sup>.

### 5.3.2.5 FT-IR

FT-IR spectra can provide information about the composition in a sample and all samples were analysed (Figure 5.5). The infrared absorptions agreed with all of those found in previous chapters. There are slight differences in absorbance and one of the peaks related with the 4 hour reaction samples exhibited a higher intensity than the other products. In general, the infrared spectra have been consistent throughout this study.

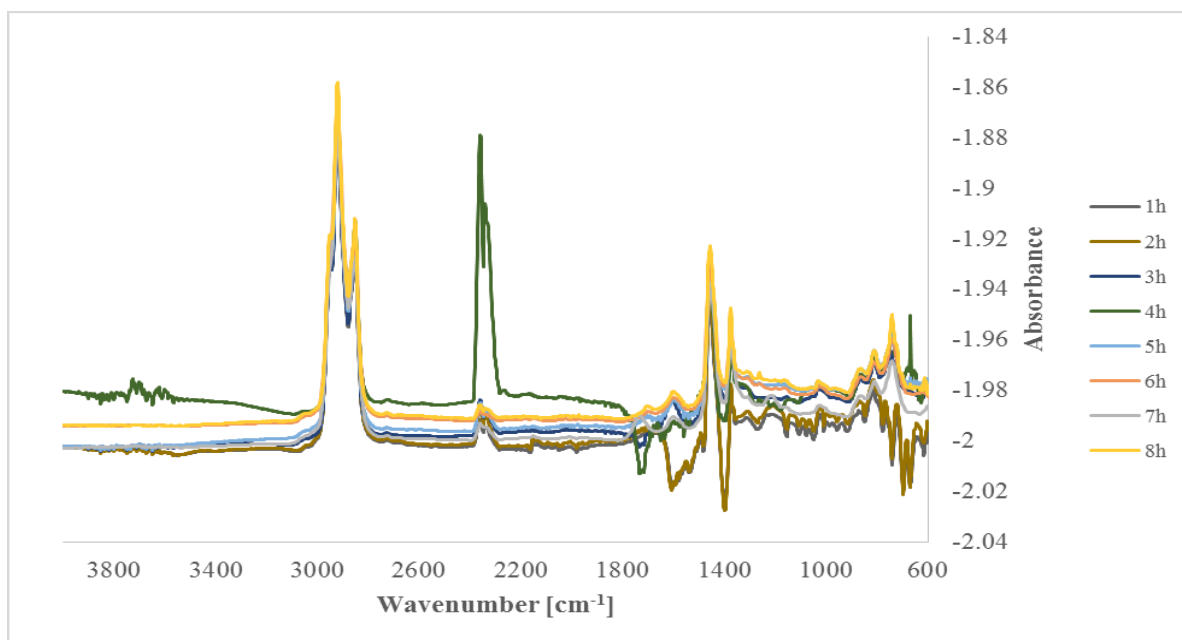


**Figure 5.5.** FTIR spectra for pyrolysis products after 200 °C, initial pressure of 4 MPa and different times reaction.

### 5.3.2.6 Asphaltene content

The asphaltenes fraction of bitumen can be determined by the ASTM D6560-12 using *n*-pentane as solvent, since an excess of *n*-alkanes promotes the precipitation of this solubility fraction. The product-solvent ratio utilised was 1:40.

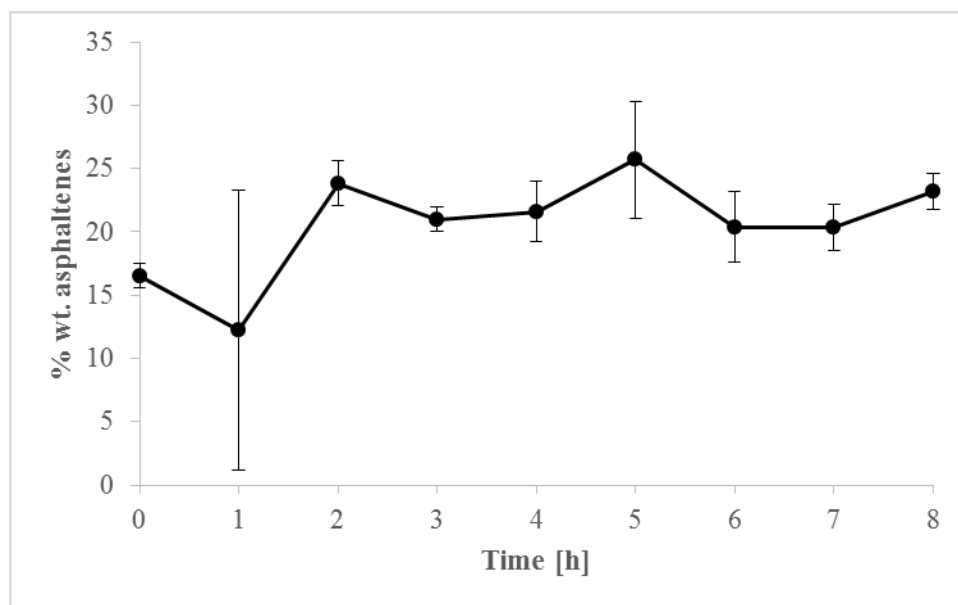


**Figure 5.6.** Asphaltene content for visbreaking products by ASTM D6560.

The results obtained were presented in Figure 5.6. Standard deviations for the samples after 1 and 5 hours reaction were abnormally high due to the nature of the samples.

### 5.3.2.7 Gas Chromatography

As part of the products characterization, the gas phase was analyzed in a Gas Chromatograph, which was described in Chapter 3. The analysis conditions were the same. The results obtained from this technique is summarized in Table 5.6.

**Table 5.6.** Gas products associated to pyrolysis of bitumen at 200 °C.

Compound	Reaction time [h]							
	1	2	3	4	5	6	7	8
	[mole %]							
<b>Methane</b>	-	-	-	-	-	-	-	-
<b>Ethylene</b>	-	-	-	-	-	-	-	-
<b>Ethane</b>	-	-	-	-	-	-	-	-
<b>Propylene</b>	-	-	-	-	-	-	-	-
<b>Propane</b>	-	-	-	-	-	-	-	-
<b>i-Butane</b>	-	-	-	-	-	-	-	-
<b>n-Butane</b>	-	-	-	-	-	-	-	-
<b>cis 2-Butene</b>	-	-	-	-	-	-	-	-
<b>i-Pentane</b>	0.03	0.03	-	0.14	0.10	-	0.01	0.10
<b>n-Pentane</b>	-	-	-	-	-	-	-	-
<b>i-Hexene</b>	-	-	-	-	-	-	-	-
<b>n-Hexene</b>	-	-	-	-	-	-	-	0.01
<b>CO<sub>2</sub></b>	0.03	0.04	0.04	0.04	0.07	0.03	0.08	0.07
<b>H<sub>2</sub></b>	-	2.34	-	-	-	-	-	1.45
<b>Ar</b>	4.04	3.38	7.29	3.91	7.61	2.96	15.57	9.32
<b>N<sub>2</sub></b>	95.66	93.42	92.67	95.91	92.22	97.01	84.33	89.04
<b>CO</b>	-	-	-	-	-	-	0.01	-

### 5.3.2.8 Solid content

Due to the low temperature utilised for these experiments, the amount of solids expected is small. This phase was obtained by the filtration of liquid products. These results are compiled in Figure 5.7 where the standard deviations are also shown. Less solids were obtained at 200 °C than at higher temperatures.

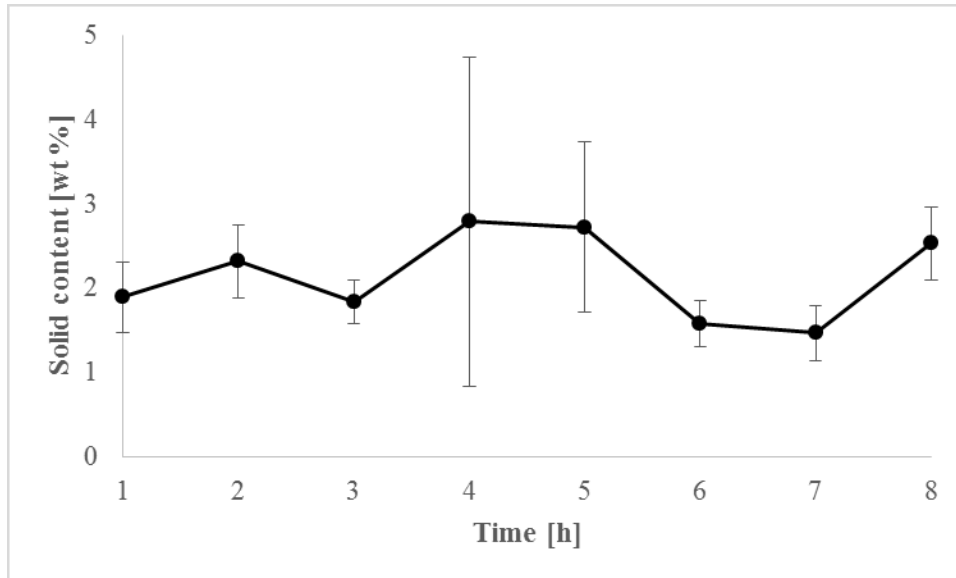


**Figure 5.7.** Solid content in pyrolysis products after reaction at 200 °C.

## 5.4 DISCUSSION

### 5.4.1 Viscosity – Temperature relationship

At 200 °C, it is not expected to have much changes due to chemical reactions and cracking reactions in particular. However, temperature can always affect bitumen behaviour and cause some small changes. Viscosity is explained by the relationship between shear rate and shear stress, Equation (1) shows it.

$$\mu = \frac{\sigma}{\gamma} \quad (1)$$

Where  $\mu$  is viscosity [Pa.s],  $\sigma$  is shear stress [Pa] and  $\gamma$  is shear rate [ $s^{-1}$ ]. The variation on shear rate will be reflected on the changes in shear stress and hence, viscosity will vary as well.

Results obtained in Chapters 3 and 4 were satisfactory because a viscosity reduction was accomplished. From Figure 5.1, these results show an enormous viscosity increase compared with the Cold Lake bitumen feed and the products obtained in the first two set of experiments. All visbroken products possessed higher viscosity than the raw bitumen. Such dramatic increase can potentially be explained by the presence of addition reactions. Free radical addition

reactions are favour at lower temperatures like this one (200 °C). As a consequence, viscosity has reached huge values.

It would be of value to know more about the addition reactions that take place, but this was outside of the scope of this study.

Since these changes were observed, a viscosity-temperature relationship for oils recommended by ASTM (Eq. 2) was utilised to see whether the products followed a similar behaviour.

$$\ln[\ln(\mu)] \propto \ln(T) \quad (2)$$

It is expected a linear relationship when Equation (2) is plotted. Figure 5.8 shows these results. Most of the samples behave in the way that it was expected. However, the sample after 7 hours of reaction presents a different performance. Such deviation could be seen when temperature is lowered and bitumen started to congeal [1]. Measurement temperatures were the same for all the experiments, which may indicate the onset of the formation of a second phase in the bitumen after 7 hours reaction. Long reaction times could favour aggregation reactions or promote certain changes that may develop some intermolecular interactions. Analogous findings were reported in Chapter 4.

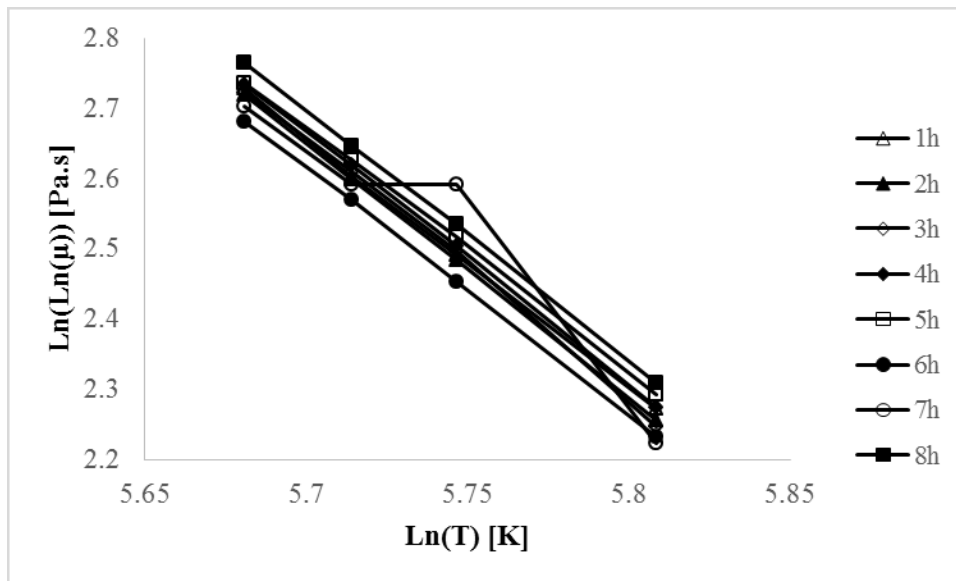


**Figure 5.8.** Viscosity of visbreaking products after 200 °C and 4 MPa along different residence times based on the ASTM relationship.

#### 5.4.2 Influence of reaction time

Reaction time is one of key design parameters for visbreaking technology. Reaction time in combination with temperature determines the severity of this process. At the temperature that these experiments were performed, it is not expected to have big changes.

Reaction time had a major influence in this work. Regarding Figure 5.9, visbreaking products showed big changes along reaction time; it is particularly obvious for those measurements performed at 20 °C. Figure 5.2a and 5.4a show the refractive index and density measurements, respectively, along time. For RI, it seems that changes can be observed easily at low measurement temperatures. On the other hand, density experiments do not exhibit a significant difference as an effect of the measurement temperature.

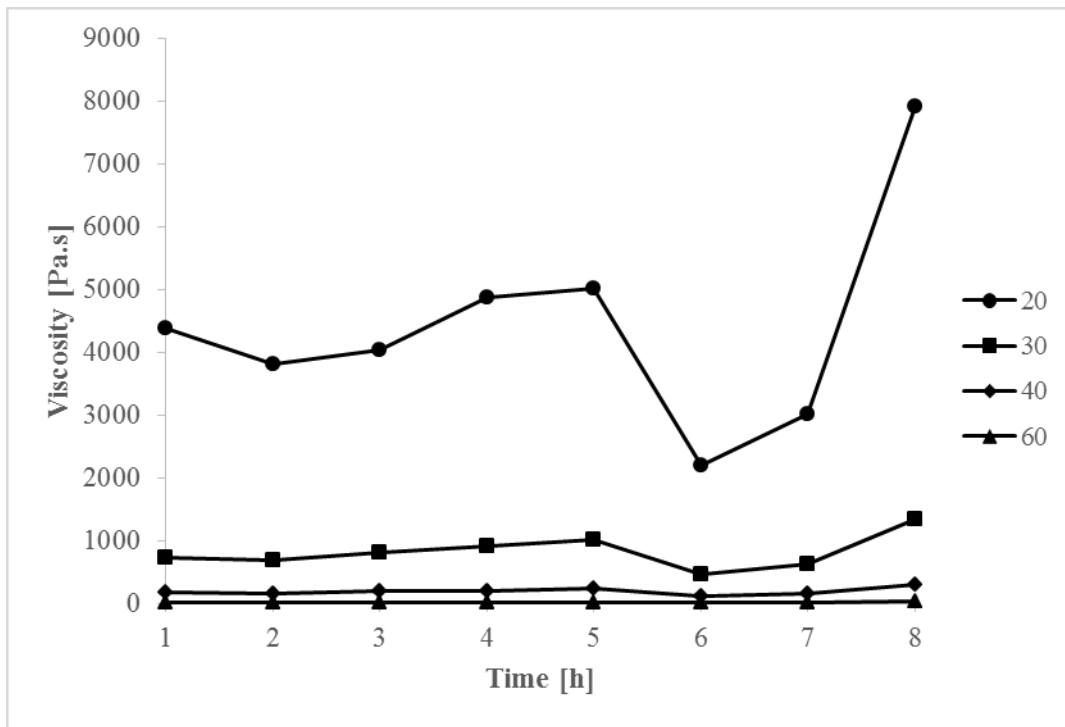


**Figure 5.9.** Viscosity measurements performed at  $1.2 \text{ s}^{-1}$  to visbreaking products under  $200 \text{ }^\circ\text{C}$  and initial pressure of  $4 \text{ MPa}$ .

When reaction temperature is lowered, the amount of energy provided to the reaction will decrease. As a consequence, the development of free-radical reactions will be slower. It is here where the reaction time gains importance, because introducing bitumen feed under the reaction temperature for a significant period could favour the evolution of products from some slower

processes. Having long reaction times could give enough time for some reactions to take place, which will be reflected in the final product.

### 5.4.3 NMR results

A significant change took place after one hour reaction, it can be observed in Figure 5.3b. It also shows that the percentage of aliphatic protons in visbreaking products at 200 °C and 4 MPa, increases along reaction time, reaching approximately 98%. In Chapter 3, it was mentioned that such changes could be explained by hydrogen disproportionation. This could be considered the main step in the processes that could take place at 200 °C in order to promote rearrangement, addition reactions and all other free-radical reactions taking place.

In Figure 5.3a, five peaks can be distinguished. The first peak will be related with primary aliphatic protons that may be linked with straight-chain alkanes. It usually appears around 0.9 ppm. The second peak is associated with the secondary aliphatic protons, these protons may correspond to branched chains and it shows up approximately at 1.3 ppm. Around 2.3 ppm, a peak related with benzylic hydrogen of aromatics will be seen. A small peak close to 5 ppm corresponds to the solvent utilised in the sample preparation. The last peak is associated with aromatic and/or phenolic protons, it will appear around 7.3 ppm.

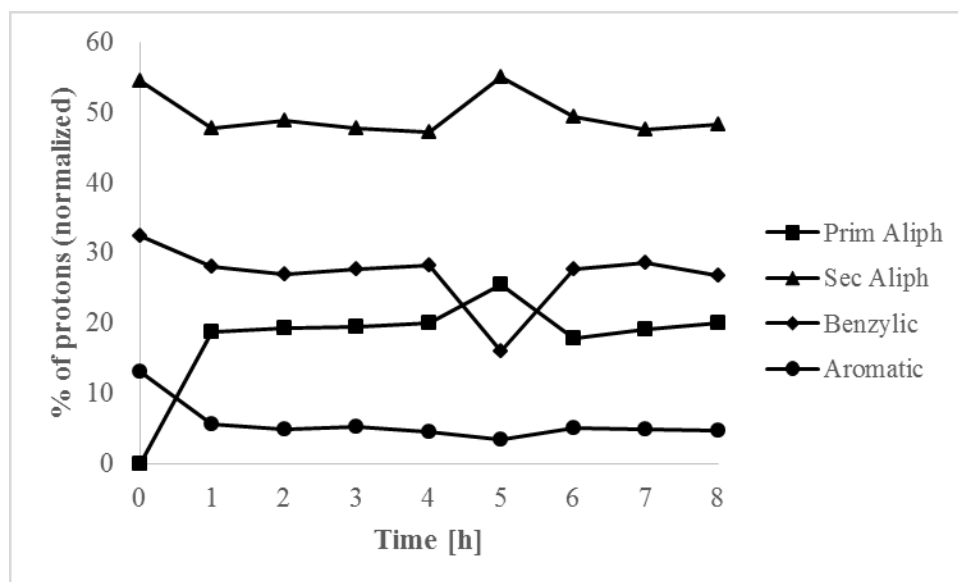


**Figure 5.10.** Area under the curve extracted from the NMR spectra, comparing the amount of the type of proton found in visbroken samples after 200 °C reaction.

Based on Figure 5.3a, the distribution of hydrogen on the different products can be established. This is shown in Figure 5.10. As it was mentioned previously, raw bitumen does not exhibit the peak associated to primary aliphatic hydrogen. It could be due to overlapping by the wide peak related with the secondary aliphatic hydrogen. The most visible change in this distribution took place up to 5 hour reaction when the secondary and aliphatic protons increased but benzylic and aromatic protons decreased. Unlike previous chapters, the amount of aromatic hydrogen shows a sharp decrease after one hour reaction and it could be considered constant along with reaction time after it.

#### **5.4.4 The relationship between Density and Refractive Index**

Refractive index and density can tell more about the changes that occurred during this thermal cracking process. Both are indicators of compositional changes as well as they can give information about the degree of upgrading [2]. Besides that, aromaticity can be found in higher values of RI [3]. This is also true for density analyses.

Refractive index seems to be constant in these products. However, the slopes obtained from Figure 5.2b show that there are some subtle changes. The most significant variation is found in the 5 hours reaction. Compared with Cold Lake bitumen feed, all these products experienced some changes except for the first hour reaction. In Figure 5.2a, it is possible to see that the lowest value corresponds to the product after 5 hours of reaction. This agree with the observation made about the slopes regarding Figure 5.2b.

Also, a comparison between the results in the first three experimental chapters indicate that products obtained from visbreaking at 300 °C had lower refractive indices than the samples obtained from visbreaking at 250 and 200 °C. This could suggest an increasing in the aromatic content in the products, or that the products became heavier (higher molecular mass).

Regarding density figures, Figure 5.4a show the oscillation of density along with reaction time. The lowest value was obtained after one hour reaction and the highest after two hours reaction. However, the difference is not huge. These results are significantly lower compared to the densities found in Chapter 3 and 4 for the visbroken products.

Figure 5.4b shows the linear relationship between density and measurement temperature. From this plot, it is possible to determine some changes based on the slope of each curve. It was found

that just the 7 hour reaction sample has a different slope ( $-0.007 \text{ cm}^3 \cdot \text{°C/g}$ ). This difference can be an indication about a compositional change. However, it is particularly interesting that the variation in refractive index and density do not correspond to each other. Since refractive index is affected by density, the magnitude of the compositional change must be even more than suggested by the change in the refractive index on its own.

#### **5.4.5 FT-IR**

As mentioned before, the spectra have been similar in all these chapters. No additional observations could be highlighted for discussion, apart from the apparent increase in C=C content.

#### **5.4.6 Gaseous products**

The compounds found in this analysis correspond to C<sub>5</sub> and C<sub>6</sub>. C<sub>1</sub> to C<sub>4</sub> were not observed. This supports the assertion that the energy provided at this temperature is relatively low for breaking terminal bonds and that could be the explanation of the C<sub>1</sub> absence in the gaseous products. As it was expected, the amount of nitrogen after reaction is higher than what it was found in the other set of experiments. It could be related with the solubility at these conditions.

#### **5.4.7 Solid products**

A third phase can be identified in visbreaking products. It is interesting that the amount of asphaltenes reaches 25 wt %. Comparing this with results obtained in Chapter 4, these amounts may be the result of aggregation mechanisms that were not clearly observed in those reactions performed at 300 °C. Asphaltenes are described as a high molecular weight fraction with polar aromatic character. They are partially dissolved into nonpolar resins that prevent the aggregation and are partially dispersed in crude oil [5]. Knowing that, it is possible to contemplate that visbreaking is actually causing compositional changes, since the initial amount of asphaltenes is lower than the one obtained from these experiments.

On the other hand, the amount of solids (coke and mineral matter) produced from these experiments is relatively low compared with the previous chapters. This could be explained by the low temperature, since the formation of a solid phase is attributed to high temperatures. A general tendency that has been observed from the experiments performed up to this chapter (Chapters 3 to 5) is that the quantity of solids determined shows a decreasing trend along

reaction time. The opposite has been said in [6], where it suggests an increasing of this phase along reaction time. This discrepancy could give a hint about the bitumen behaviour after being subjected to a thermal cracking process at higher compared to lower temperatures.

## 5.5 CONCLUSIONS

This work has showed some important differences compared with Chapter 3 and 4. Maintaining bitumen at a low temperature can generate more changes than what was expected.

- a) A reduction in viscosity was not observed. In fact, the viscosity of the visbroken products was higher than that of the Cold Lake bitumen feed. The highest value corresponded to the 8 hour sample and it is 5 times the viscosity of the feed. At this temperature, free radical addition is thermodynamically favoured and the impact of the addition reactions could be seen on these experiments.
- b) As expected, there are not many changes in the products regarding refractive index and density results. However, it seems they are enough to increase visbroken products viscosity. A high asphaltenes content can also suggest a compositional change, since the precipitation of them are usually a consequence of the change in resins composition.
- c) Energy provided by temperature is low, which avoided the formation of C<sub>1</sub> – C<sub>4</sub> products and at the same time, the amount of solids was low compared with the previous results obtained after thermal treatment at 250 and 300 °C. It could be related with the generation and distribution of gaseous products.
- d) FT-IR results showed a high influence of the double bond presence. It could be possible that this thermal cracking reaction promotes the formation of double bond structures.

### Literature cited

- [1] Schmidt, P. F. *Fuel Oil Manual. Volume 10*; Industrial Press, Inc.: New York, 1985, p.72.
- [2] Strausz, O. P.; Lown, E. M. *The Chemistry of Alberta Oil Sands, Bitumens and Heavy Oils*; Alberta Energy Research Institute: Calgary, 2003, p.119.

- [3] Speight, J.G. *The Chemistry and Technology of Petroleum*, 4th ed.; Taylor & Francis Group: Boca Raton, FL, 2007, p. 266.
- [4] Borrego, A. G.; Blanco, C. G.; Prado, J. G.; Diaz, C.; Guillen, M. D. <sup>1</sup>H NMR and FTIR Spectroscopic Studies of Bitumen and Shale Oil from Selected Spanish Oil Shales. *Energy Fuels* **1996**, *10* (1), 77–84.
- [5] Ghanavati, M.; Shojaei, M.-J.; Ahmad Ramazani, S. A. Effects of Asphaltene Content and Temperature on Viscosity of Iranian Heavy Crude Oil: Experimental and Modeling Study. *Energy & Fuels* **2013**, *27*(1) 7217–7232.
- [6] Wiehe, I. A. *Process chemistry of petroleum macromolecules*; CRC Press: Boca Raton, FL, 2008, p. 142

## **6. VISBREAKING OF OIL SAND BITUMEN AT 150 °C**

### **6.1 INTRODUCTION**

Visbreaking at 300, 250 and 200 °C have been presented in the previous chapters. For the first two, results can be considered successful from an application point of view, since it has been possible to decrease bitumen viscosity. On the other hand, it was found that performing visbreaking at 200 °C could promote some addition reactions and aggregation resulting in significantly higher viscosity for those products. Although the exact cause of the increased viscosity of the products after thermal treatment at 200 °C was not proven, this explanation became the working hypothesis for investigating conversion at an even lower temperature.

Conversion at 150 °C is a very low temperature and not normally associated with thermal conversion. It is possible that the effect of temperature in these experiments would be small, or that the addition reactions and aggregation will be exacerbated. Based on the results obtained in the previous chapter, there is a possibility that these products would have similar characteristics as the visbroken products obtained in Chapter 5. The reaction time will determine the extent of changes occurring during this process. It is expected to see some changes; however, it is not expected to observe much reaction that involves cleavage of bonds.

In this chapter the experiments performed at 150 °C, 4 MPa and reaction time between 1 and 8 hours will be discussed.

### **6.2 EXPERIMENTAL**

#### **6.2.1 Materials**

Bitumen from the Cold Lake area in Alberta was utilised for this set of experiments. It was provided by the Center for Oil Sands Innovation (COSI) at University of Alberta. All the experiments used bitumen from the same barrel. The characterization of this feed (Cold Lake bitumen) was presented previously in Table 3.1.

As part of the experiments, nitrogen and methylene chloride were used. They are described properly in Chapter 3.

#### **6.2.2 Equipment and procedure**

These experiments were performed in batch mode. All the equipment utilised for these reactions were described in detail in Chapter 3. Regarding the procedures and conditions, most of them were shown in Chapter 3. However, Chapter 5 contains the description for the modified viscosity measurements. In addition, Fisherbrand™ Clear Straight-Sided Jars of 60 mL were used to store the visbroken products from the experiments performed in this chapter, i.e. similar to Chapter 5.

### 6.2.3 Analyses

Analyses performed to this set of experiments were described formerly in Chapter 3. The procedure and analysis conditions were provided previously in Chapter 3. However, conditions for viscosity analysis were changed and they were shown in Chapter 5.

## 6.3 RESULTS

### 6.3.1 Material Balance

As before, visbreaking produced three different phases: solid, liquid and gaseous. Reaction conditions utilised for this set of experiments were 150 °C, an initial pressure of 4 MPa and residence time varying between 1 and 8 hours. Material balance closure was around 100 wt %. All the experiments were conducted in triplicate. Table 6.1 reports these results as an average with one sample standard deviation. A second table, Table 6.2, presents the reaction yield data for these experiments.

**Table 6.1.** Mass Balance (wt %) for Visbreaking Reactions at 150 °C and Constant Pressure (4 MPa) for different reaction times.

Reaction time [h]	Material Balance [wt %] <sup>a</sup>	
	x	s
1	100.4	1.6
2	100.2	0.3
3	100.1	0.3
4	100.1	0.1
5	100.1	0.2
6	100.6	0.5
7	100.2	0.3
8	100.3	0.3

<sup>a</sup> Average (x) and sample standard deviation (s) of three experiments are reported

The highest standard deviation was found in the samples after one hour reaction. Reactors were depressurized and opened. It was found that liquid products showed a concave shape. This is

different compared with the previous experiments where liquid products inside the reactor showed a convex shape.

**Table 6.2.** Product yield (wt%) for visbreaking reactions at 150 °C and initial pressure of 4 MPa for different reaction times.

Time [h]	Material Balance [wt %] <sup>a</sup>					
	Gas		Liquid		Solid	
	x	s	x	s	x	s
1	4.91	1.53	93.90	1.24	1.61	0.33
2	4.55	1.57	94.15	1.11	1.47	0.31
3	2.01	1.41	96.62	0.66	1.51	0.47
4	1.52	0.70	97.14	0.29	1.47	0.36
5	1.62	0.76	97.00	0.74	1.47	0.58
6	2.60	0.38	96.50	0.78	1.48	0.25
7	2.65	1.57	96.02	0.28	1.48	0.21
8	2.88	1.14	95.89	0.20	1.49	1.57

<sup>a</sup> Average (x) and sample standard deviation (s) of three experiments are reported

The contact angle of the material after treatment at 150 °C is therefore different to the contact angle of material after treatment at 200 to 300 °C.

Filtration times were significant diminished compared to 300 and 250 °C samples. As mentioned in the experimental section, the vials were changed to speed up the solvent evaporation.

### 6.3.2 Product characterization

The main objective of visbreaking is to reduce the viscosity of the fossil fuel as much as possible. This work is focused on liquid products. However, the solid and gaseous fractions were analyzed and reported.

#### 6.3.2.1 Viscosity

The shear rate for viscosity measurements employed was 1.2 s<sup>-1</sup> due to the high apparent viscosity of the products after treatment. The viscosity measurements were performed at four different temperatures: 20, 30, 40 and 60 °C and the results are presented in Figure 6.1. Also, the numeric viscosity data is summarized in Table 6.3 where the averages and standard deviations are reported.

As expected, viscosity increased significantly compared to visbroken products obtained in Chapter 3 and 4 plus the Cold Lake bitumen feed. The behaviour is similar to the results presented in Chapter 5. Viscosity tends to increase along reaction time. The highest value was found in the 7 hour reaction sample which was  $5.6 \times 10^3$  Pa.s. This value is 3 times the viscosity of the raw bitumen approximately.

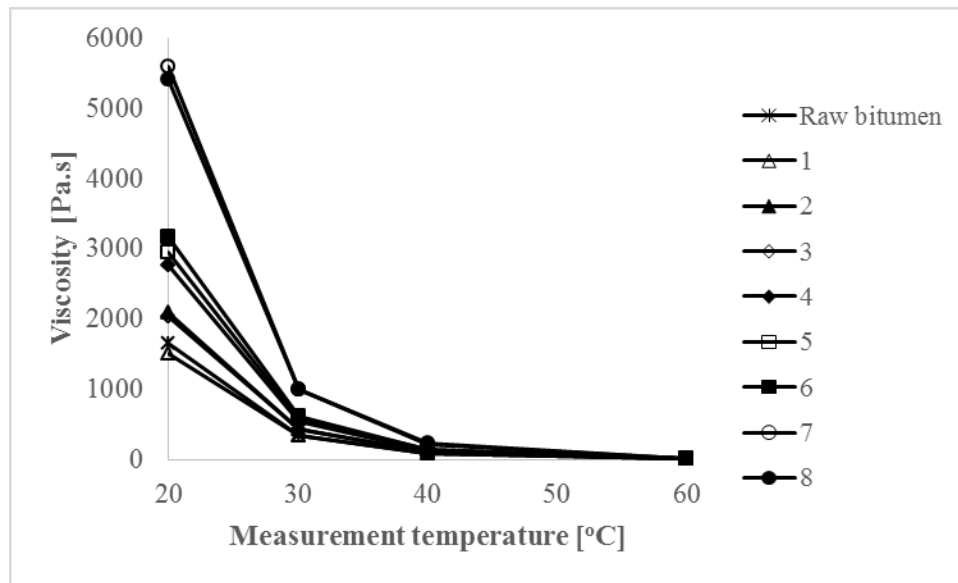


**Figure 6.1.** Viscosity of visbreaking products obtained under 150 °C, initial pressure of 4 MPa and reaction time varying between 1 and 8 hours. Measurements were performed at four different temperatures: 20, 30, 40 and 60 °C.

**Table 6.3.** Viscosity data from measurements performed to Visbreaking products under 150 °C and initial pressure 4 MPa.

Temperature [°C]	Reaction time [h]															
	1		2		3		4		5		6		7		8	
	x	s	x	s	x	s	x	s	x	s	x	s	x	s	x	s
20	1,511.4	648.7	2,087.1	679.0	2,045.6	367.4	2,766.3	1,178.8	2,951.6	133.3	3,166.0	866.8	5,594.2	783.7	5,407.8	1,432.0
30	351.9	152.9	436.6	132.7	428.3	56.5	552.8	215.4	587.8	28.1	621.7	142.2	1,002.3	97.0	1,005.7	185.8
40	85.7	32.3	106.9	30.0	103.5	12.3	131.8	46.8	140.3	4.6	147.4	30.4	225.1	21.3	230.3	48.7
60	7.3	1.9	10.5	2.2	10.2	0.8	12.1	3.5	13.2	0.3	13.7	2.3	18.8	1.5	19.0	2.6

<sup>a</sup> Average (x) and sample standard deviation (s) of three experiments are reported

These samples are similar to the ones obtained in Chapter 5. At room temperature, they do not flow. It seems to be a semi-solid product.

### 6.3.2.2 Refractive Index

This analysis was performed at four different temperatures: 20, 30, 40 and 60 °C. A small amount of sample was required to carry out these measurements. As a result, Figure 6.2 shows a) Refractive index vs time to observe the variations that visbroken products experienced along with reaction time; b) Refractive index vs measurement temperature for extracting more information about the possible changes.

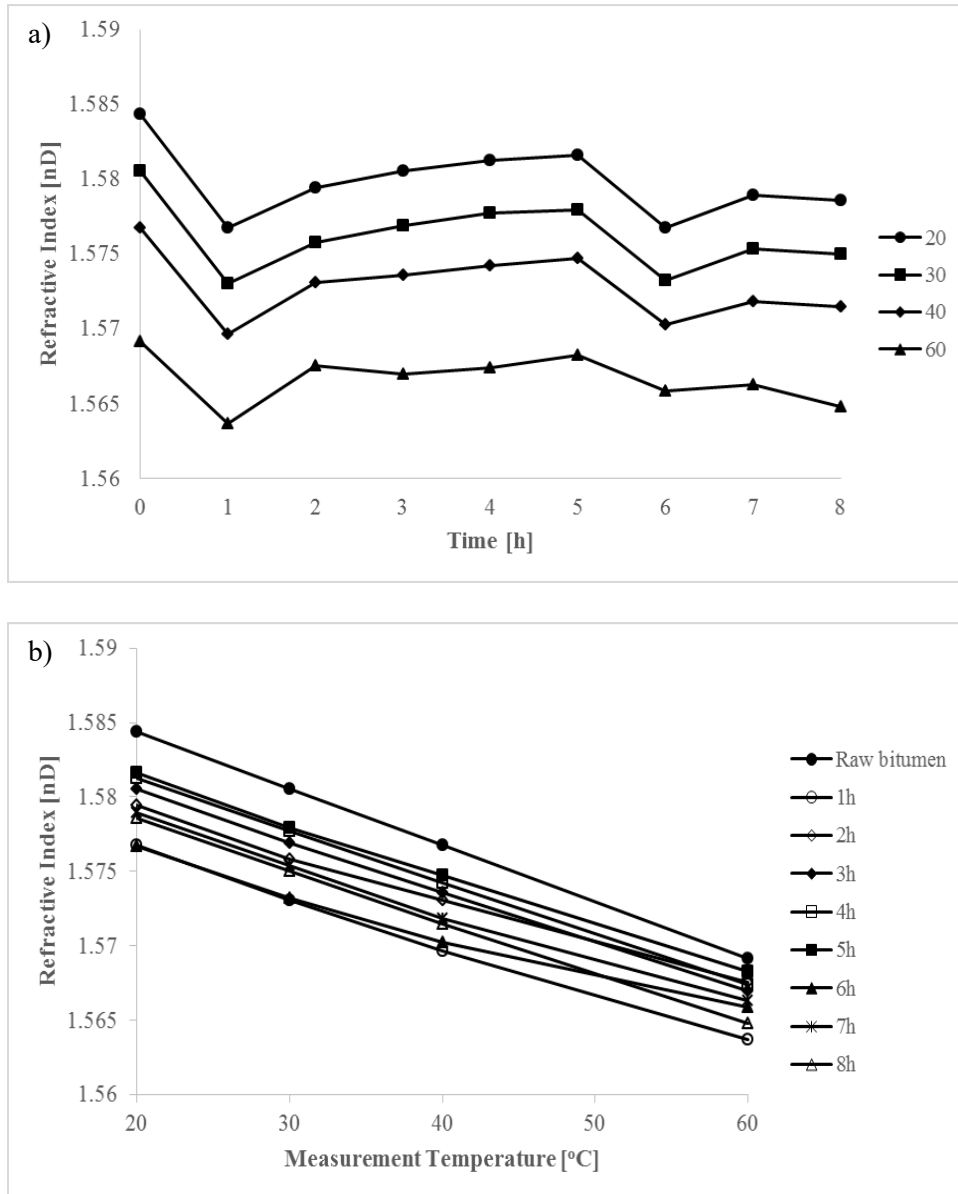


**Figure 6.2.** Refractive Index of visbreaking products obtained under 150 °C, initial pressure of 4 MPa and reaction time varying between 1 and 8 hours. Measurements were performed at four different temperatures: 20, 30, 40 and 60 °C.

Refractive index data is compiled in Table 6.4. Most of the standard deviations decrease along with measurement temperature but this is not true for samples after 4 and 7 hours of reaction when it increases for the last temperature value.

**Table 6.4.** Refractive Index measurements performed on visbreaking products after 150 °C and internal pressure 4 MPa reaction

Temperature [°C]	Reaction time [h]																	
	0		1		2		3		4		5		6		7		8	
	Refractive Index [nD] <sup>a</sup>																	
	x	s	x	s	x	s	x	s	x	s	x	s	x	s	x	s	x	s
20	1.58437	0.00076	1.576767	0.00525	1.57943	0.00771	1.58053	0.00361	1.58127	0.00049	1.58160	0.00130	1.57673	0.01059	1.57893	0.00234	1.57857	0.00598
30	1.58057	0.00067	1.573067	0.00531	1.57580	0.00758	1.57693	0.00325	1.57773	0.00057	1.57797	0.00131	1.57323	0.01016	1.57537	0.00228	1.57503	0.00578
40	1.57677	0.00067	1.569667	0.00535	1.57310	0.00611	1.57357	0.00339	1.57420	0.00071	1.57473	0.00071	1.57027	0.00915	1.57183	0.00217	1.57147	0.00572
60	1.56917	0.00050	1.5637	0.00497	1.56757	0.00339	1.56697	0.00247	1.56743	0.00120	1.56827	0.00059	1.56590	0.00450	1.56630	0.00235	1.56483	0.00515

<sup>a</sup> Average (x) and sample standard deviation (s) of three experiments are reported

Figure 6.2b shows the linear tendency of refractive index with measurement temperature. The slopes could be found from these lines and they are between  $-0.00027$  and  $-0.00038 \text{ K}^{-1}$ . The lowest value correspond to 6 hour reaction sample. Most of the samples have a slope of over  $-0.00030 \text{ K}^{-1}$  except for samples after 2 and 6 hours.

### 6.3.2.3 <sup>1</sup>H NMR

Initially, NMR was used just to differentiate aliphatic and aromatic protons. However, this technique has been very useful for identifying different kind of protons. Figure 6.3a shows the spectra of the visbroken products after reaction at 150 °C. It is possible to determine the presence of several types of protons and based on these curves, Figure 6.3 was made to present the distribution of the different kind of hydrogen in these products.

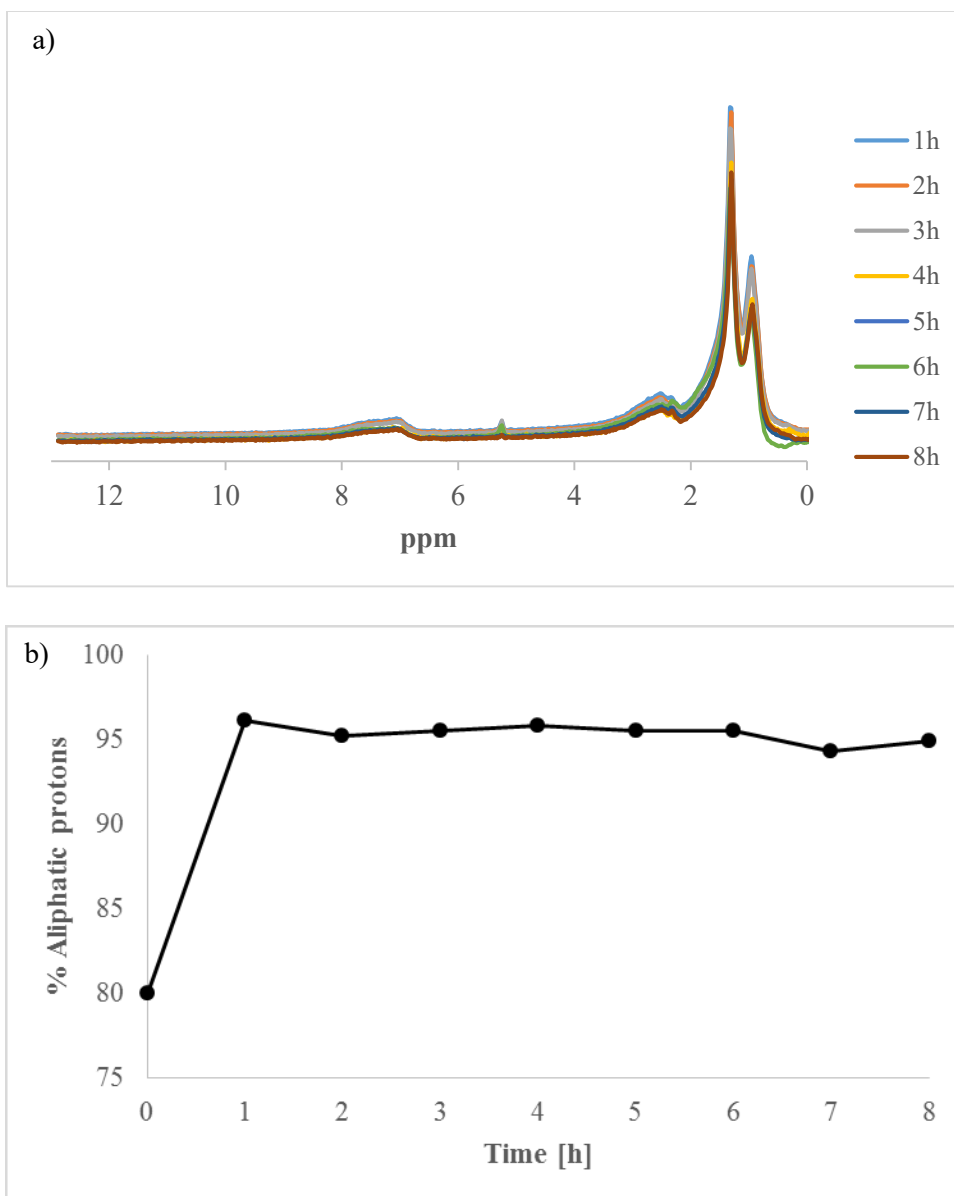


**Figure 6.3.** NMR results of visbreaking products obtained under 150 °C, initial pressure of 4 MPa and reaction time varying between 1 and 8 hours.

On the other hand, Figure 6.3b shows the relative amount of the aliphatic protons along with reaction time. As it was observed before, after the first hour reaction a maximum of aliphatic hydrogen was reached and the quantity of these protons kept approximately constant around 95 %.

#### 6.3.2.4 Density

Due to the semi-solid nature of the products, the samples had to be heated until they could flow freely before they could be injected into the equipment. Figure 6.4 shows a) Density vs reaction time to present the variation of this property along with time; and b) Density vs measurement temperature where these compositional changes can be observed.

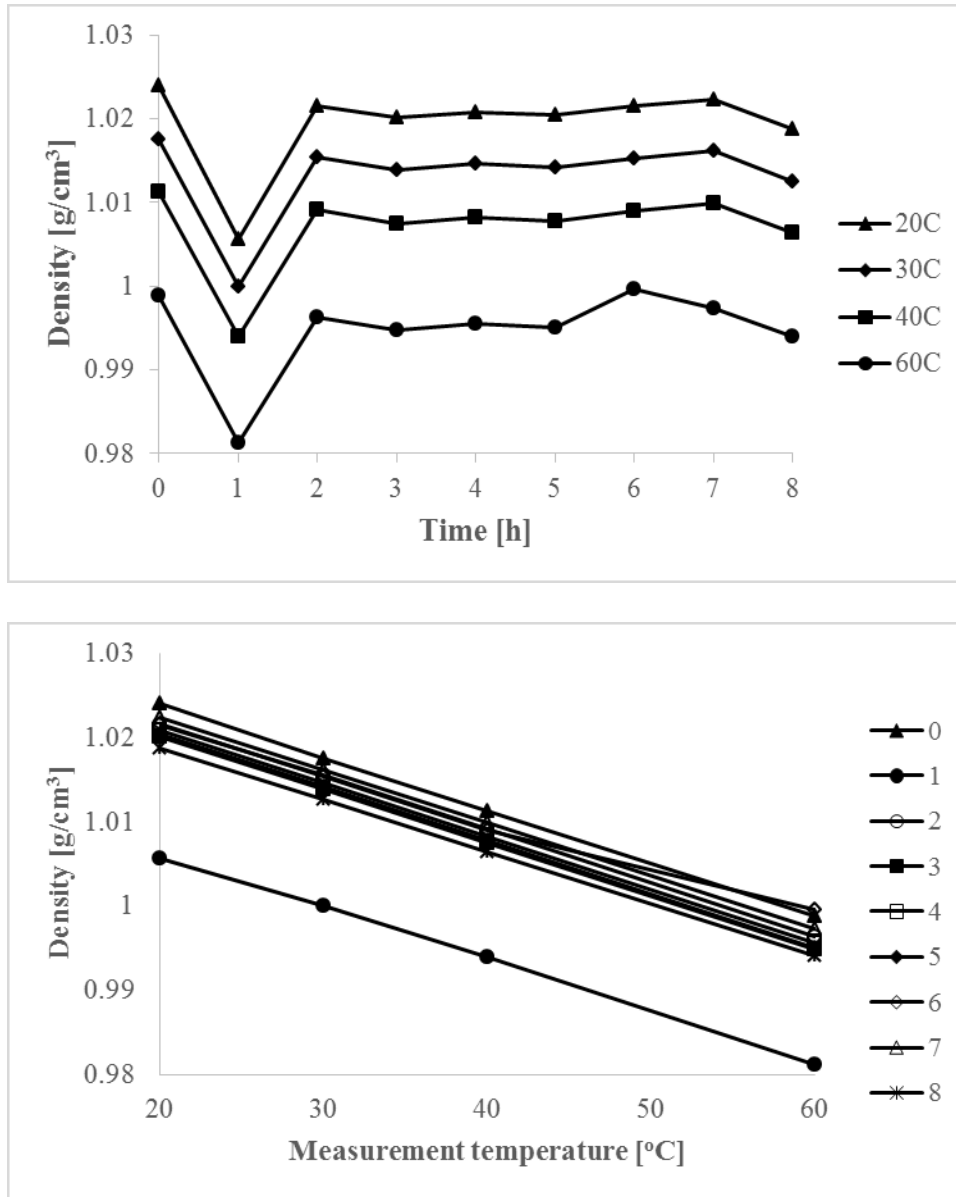


**Figure 6.4.** Density of visbreaking products obtained under 150 °C, initial pressure of 4 MPa and reaction time varying between 1 and 8 hours. Measurements were performed at four different temperatures: 20, 30, 40 and 60 °C.

From Figure 6.4b, it is possible to see that most of the curves follow a linear tendency and the slopes are the same. However, this is not true for samples after 2 and 6 hour reaction where the slopes are smaller than  $-0.00063 \text{ cm}^3 \cdot \text{°C/g}$ . Density values are reported in Table 6.5.

**Table 6.5.** Density measurements performed at four different temperatures: 20, 30, 40 and 60 °C to visbreaking products after reaction at 150 °C.

Temperature [°C]	Reaction time [h]								
	0 <sup>a</sup>	1	2	3	4	5	6	7	8
	Density [g/cm <sup>3</sup> ]								
20	1.023993333	1.00564	1.02146	1.02013	1.02083	1.02042	1.02152	1.02232	1.01873
30	1.017546667	0.99999	1.01547	1.01384	1.01457	1.01417	1.01531	1.01615	1.01257
40	1.011263333	0.99393	1.00918	1.00748	1.00824	1.00781	1.009	1.00988	1.0064
60	0.998813333	0.98125	0.99634	0.99479	0.99559	0.99506	0.99964	0.99733	0.99405

<sup>a</sup> Raw bitumen sample

### 6.3.2.5 FT-IR

Through FT-IR is possible to determine some changes due to the variation of the functional groups by evaluating the infrared absorptions associated with different kinds of bonds. These results are presented in Figure 6.5 where every reaction time has been plotted.

As in the previous chapters, most of the infrared spectra were quite similar. The absorbance of the absorption spectra of the different samples was almost the same, except for the sample after 8 hours of reaction time that showed a higher absorbance. Also, the peaks found were the same as found in Chapter 3, 4 and 5. However, the 4 hour product exhibited a couple of peaks that differed from the other products, with a very strong carbonyl absorption being apparent.

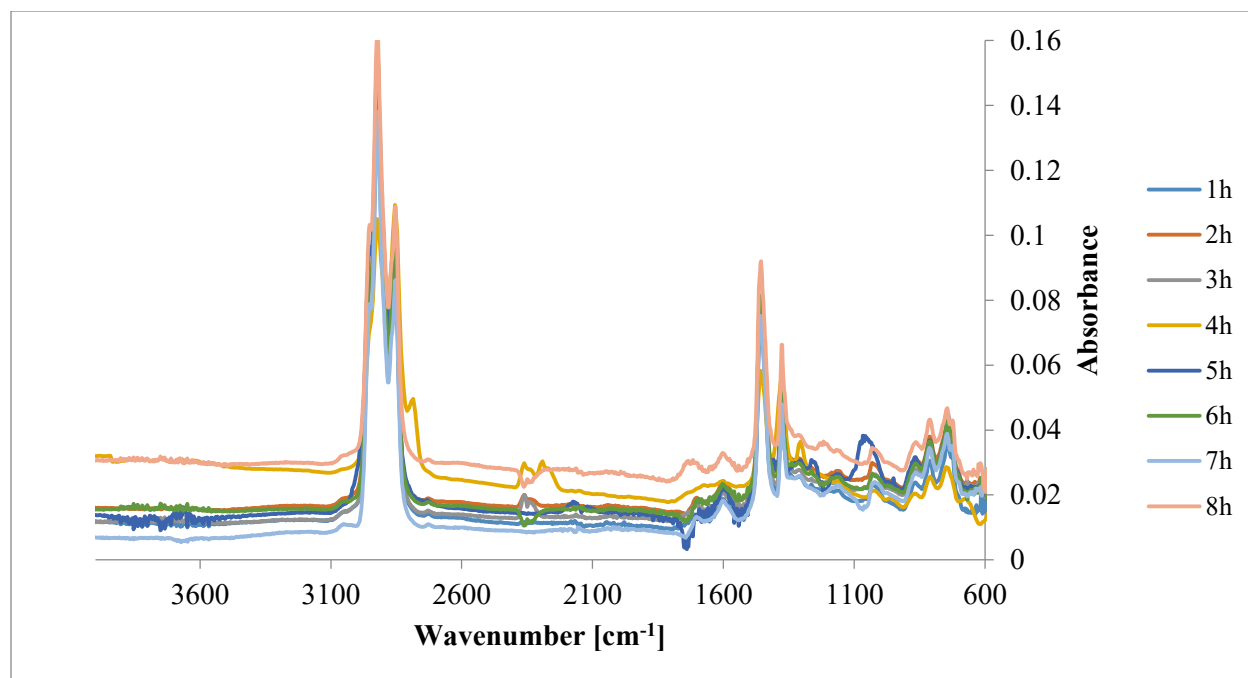


**Figure 6.5.** FT-IR results of visbreaking products obtained under 150 °C, initial pressure of 4 MPa and reaction time varying between 1 and 8 hours.

### 6.3.2.6 Asphaltene content

The asphaltenes content was determined by n-pentane precipitation (Figure 6.7). It was found that the asphaltenes content was very variable. This can be seen from the standard deviations for these samples that were high. This was not true for all of the samples, the exceptions were the raw material feed and the samples after heating at 150 °C for 3, 4 and 8 hours. It is important to mention that 0 h sample corresponds to the Cold Lake bitumen feed without any treatment.

Something to highlight about these samples was the tendency of the dry asphaltenes to cling to the walls of the container and to the spatula. This behavior was not due to stickiness, the asphaltenes were not sticky to the touch, but clung to different surfaces possibly due to static charges that were not dissipated. This made it very difficult to collect and transfer the samples. It seems that these molecules were particularly attracted to the spatula's material (Stainless Steel - Fisherbrand™ Spoonulet™ Lab Spoon by Fisher Scientific).

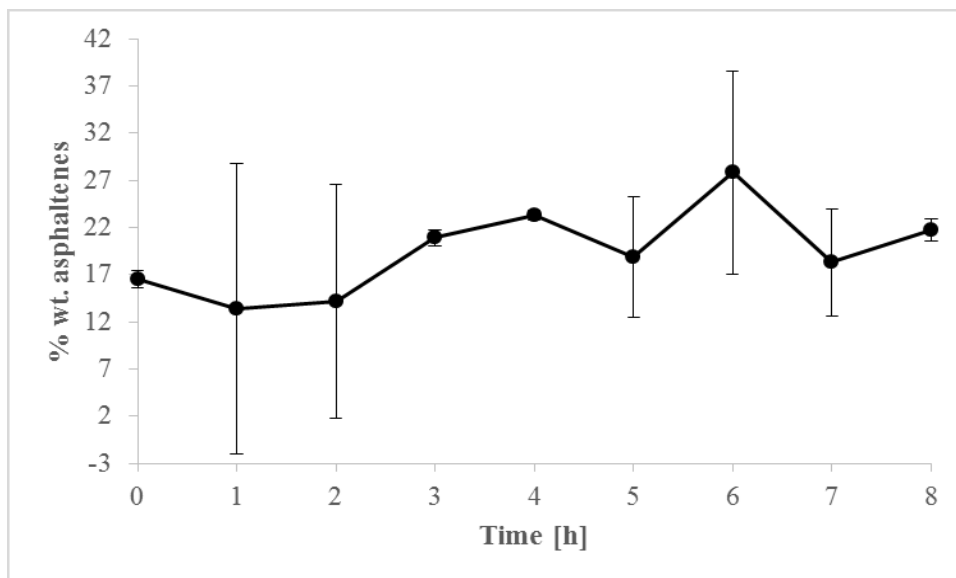


**Figure 6.6.** Asphaltene content of visbreaking products obtained under 150 °C, initial pressure of 4 MPa and reaction time varying between 1 and 8 hours.

### 6.3.2.7 Gas Chromatography

The gaseous products from the reactions were analyzed by Gas Chromatography (Table 6.7). Just C<sub>4</sub> and C<sub>5</sub> hydrocarbons were found, there was no evidence of lighter gaseous products. Also the amount of nitrogen in these samples was higher than the amount found on the previous chapters. This suggested that less light hydrocarbons were formed during conversion than found at higher temperatures.

**Table 6.6.** Gas products associated to pyrolysis of bitumen at 150 °C.

Compound	Reaction time [h]							
	1	2	3	4	5	6	7	8
	[mole %]							
Methane	-	-	-	-	-	0.03	-	0.24
Ethylene	-	-	-	-	-	-	-	-
Ethane	-	-	-	-	-	-	-	-
Propylene	-	-	-	-	-	-	-	0.13
Propane	-	-	-	-	-	-	-	-
i-Butane	-	-	-	-	-	-	-	-
n-Butane	-	-	-	-	-	-	-	-
cis 2-Butene	-	-	0.01	-	-	0.24	-	0.07
i-Pentane	0.03	0.06	-	-	0.02	0.01	0.16	0.03
n-Pentane	-	-	-	-	-	-	-	-
i-Hexene	-	-	-	-	-	-	-	-
n-Hexene	-	-	-	-	-	-	-	-
CO <sub>2</sub>	0.07	0.03	0.06	0.04	0.04	0.08	0.07	0.06
H <sub>2</sub>	7.56	-	-	-	0.14	-	-	-
Ar	14.71	7.27	12.94	8.87	8.36	18.11	15.42	13.54
N <sub>2</sub>	77.63	92.63	86.98	91.08	91.43	81.46	84.35	85.92
CO	-	-	-	-	-	0.01	-	-

### 6.3.2.8 Solid content

Previously, it was mentioned that high temperatures will promote the coke formation. Based on that, it is not expected to see a significant amount of solids, since these experiments were performed at a very low temperature.

Solid samples were collected from the filtration of liquid products. These results are compiled in Figure 6.8 where the standard deviations are shown as well. Compared to previous chapters, the solid content found in these samples was low.

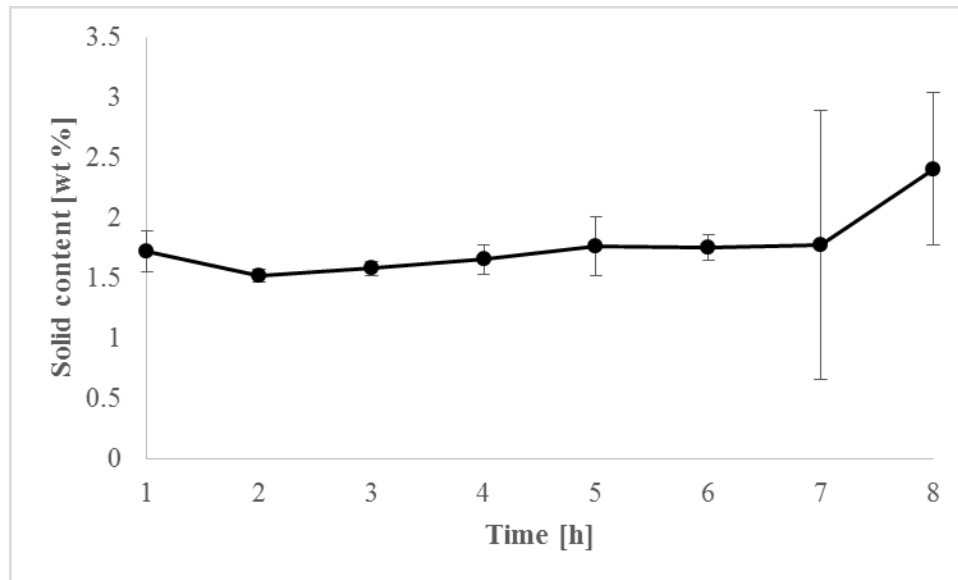


**Figure 6.7.** Solid content of visbreaking products obtained under 150 °C, initial pressure of 4 MPa and reaction time varying between 1 and 8 hours.

## 6.4 DISCUSSION

### 6.4.1 Viscosity changes

As was seen in Chapter 5, lower temperature favoured addition and aggregation, which adversely affected visbroken product viscosity. With the additional data for conversion at 150 °C that exhibited similar behaviour as conversion at 200 °C, a more general observation can be made. There seems to be a transition point between 250 and 200 °C where there is a change in the response of viscosity to the thermal process. It is clear to see that bitumen viscosity increases after being subjected to visbreaking.

The viscosity of the visbroken products is definitively higher than the Cold Lake bitumen feed for all but the product after 1 hour of reaction time. The results indicate that even at a low temperature such as 150 °C, it is possible to promote changes in bitumen composition.

As said, it was postulated that addition reactions are taking place at this temperature that could increase the formation of larger compounds. The increase in heavier compounds may in turn have an impact on bitumen properties and a consequence of this can be the results obtained for visbroken products viscosity.

A viscosity-temperature relationship for oils is recommended by ASTM, it was used to determine the formation of a second phase. It is given by Equation (1), shown in Chapter 4.

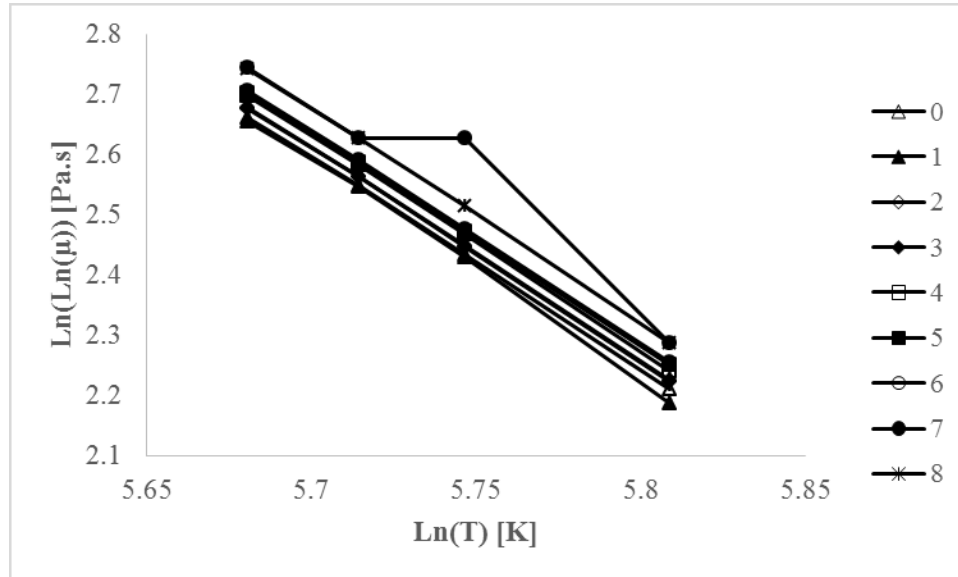


**Figure 6.8.** Viscosity of visbreaking products after 150 °C and 4 MPa along different residence times calculated through the ASTM relationship.

Figure 6.8 shows the results obtained after replacing experimental values into Eq. (1). A linear response is expected, but the 7 hour reaction sample deviated from such behaviour. Small deviations can be observed, they could be the result of high-boiling point materials or the presence of non-hydrocarbon compounds [1] that do not follow a linear relationship. Besides, at low temperatures, bitumen will start to congeal [2] and it could be another explanation for the deviated response of the 7 hour reaction sample.

#### 6.4.2 Impact of reaction time

This is one of the determining factors in visbreaking as well as temperature. Short residence times are usually preferred to avoid polymerization and coking reactions [3]. In contrast, thermal reactions can proceed to completion, i.e. coking, when residence times are high [4][5].

At low temperature it was anticipated that reaction time would be important, since little thermal energy was available to accelerate conversion.

The product after 1 hour at 150 °C was different to all subsequent products. The viscosity was marginally lower than the raw materials feed (Figure 6.1). It was also found that the refractive index (Figure 6.2a) and the density (Figure 6.5a) decreased, but increase after one hour of reaction. The reason for this is not clear.

A long reaction time could favour addition mechanisms and benefit the development of some intermolecular interactions and reactions. Also, it may allow the “stabilization” of some unstable species that are seeking for a more stable energy level during this process. Despite the low temperature at prolonged conversion there was an increase in the solids content. The solids content remained fairly constant until 8 hour reaction when it increases up to 2.40 wt %.

### **6.4.3 Compositional changes**

Refractive index, density and NMR can help to determine the aromaticity of visbreaking samples. All of them could differentiate products with a high aromatic content or high paraffinic content.

Regarding Figure 6.3b, a big change is observed at one hour reaction. The amount of aliphatic protons increases abruptly up to 96%. Throughout this work, hydrogen disproportionation has been linked to this increase. This step could be the responsible for the different free radical mechanisms that take place on thermal processes.

Taking a look to Figure 6.3a, it is easy to identify 4 peaks. The first section (from right to left) is related with the aliphatic (first two peaks) and benzylic (third peak) protons. The last peak is linked to the aromatic protons. Usually, the primary aliphatic protons peak is found around 0.9 ppm, it may refer to straight-chain alkanes or alkyl groups. The secondary aliphatic protons peak is associated with branched chains, it appears on the spectra at ~1.3 ppm. The peak found at 2.3 ppm is related with benzylic protons which is referring to benzylic aromatics. Lastly, a peak found around 7.3 ppm is related with aromatic and/or phenolic protons.

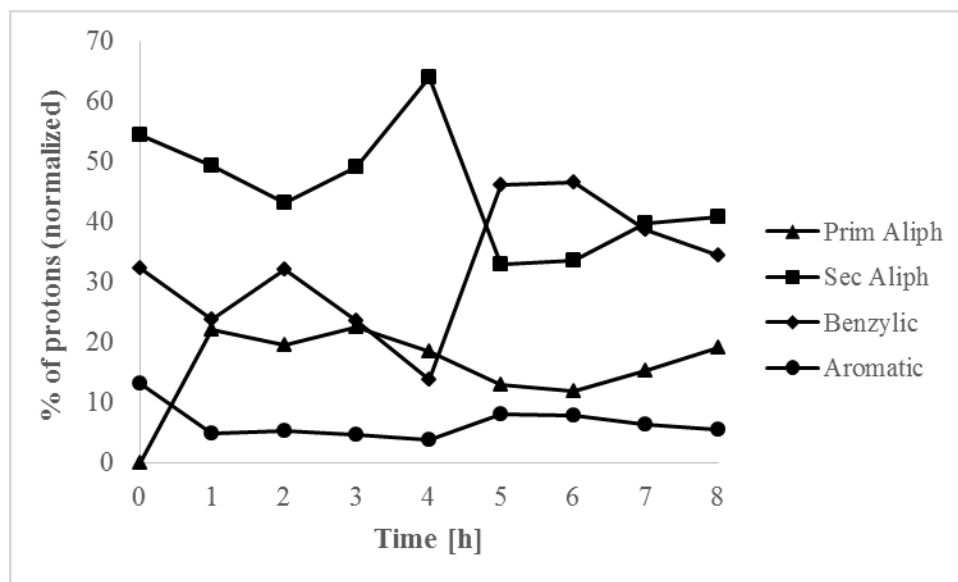


**Figure 6.9.** Area under the curve extracted from the NMR spectra, comparing the amount of the type of proton found in visbroken samples after 150 °C reaction

The distribution of protons in this set of experiments (Figure 6.9) is completely different to the other chapters. The changes are related with the secondary aliphatic and benzylic protons. However, primary aliphatic and aromatic protons also have changes. Abrupt decreases and increases are observed at 4 and 5 hour reaction. Perhaps, secondary aliphatic protons dominated the whole process since primary aliphatic protons are not observed. Regarding this, an overlapping can be hiding the peak related with primary aliphatic protons.

Figure 6.2a does not show a strong variation along with time. However, the analysis of Figure 6.2b allows to determine some changes based on the slope of refractive index vs measurement temperature. Samples after 2 and 6 hours reaction showed the most difference with respect to the other products. In general, refractive index results are similar to the Chapter 5 results. Hence, these values are higher than the results on Chapters 3 and 4. Usually, a higher refractive index suggests the presence of aromatic or heavier compounds.

An important variation in density is observed in Figure 6.4a. After one hour reaction, density drops up to 1.0054 g/cm<sup>3</sup> which can be considered very low compared with other products. But differences are more obvious in Figure 6.4b. Most of the slopes are equal, however one hour and six hour reaction products exhibit a different slope. There is not a deviation of the linear behaviour observed just a difference in slope.

#### 6.4.4 FT-IR

During visbreaking, some rearrangement and addition reactions can take place, which will cause some changes in composition. FT-IR could give information about the chemical nature of the compounds.

Most of the samples show a similar absorbance except the spectra for 8 hour reaction. The first peak is found at around  $2930\text{ cm}^{-1}$ , which corresponds to the stretching of methyl groups in aliphatic chains. It was followed by a peak at  $2853\text{ cm}^{-1}$  that is associated with methylene groups stretching on aliphatic chains. Two peaks are observed around  $1750$  and  $1600\text{ cm}^{-1}$ , which can be explained by a carbonyl group stretching and the vibration of a double bond (C=C) in a ring structure, respectively. The presence of methylene and methyl groups can be seen from the two peaks at  $1456$  and  $1375\text{ cm}^{-1}$  that are representative of these groups. Also, sulfur compounds can be observed when a peak around  $1050\text{ cm}^{-1}$  shows up, it is related with the stretching of the S=O bond. A group of peaks have been seen in all of the experiments are found at  $870$ ,  $814$ , and  $750\text{ cm}^{-1}$ . They correspond to with the out-of-plane deformation vibration of one isolated aromatic C-H bond, two or three adjacent aromatic C-H bonds and four aromatic adjacent aromatic bond, respectively [6] [7].

#### 6.4.5 Gaseous and solid products

The gaseous products generated from these reactions are mainly  $C_5$  and  $C_4$ , but  $C_1$  was found in at specific reaction times, 6 and 8 hours (Table 6.6). It is possible that this may be related with the solid content increase showed in Figure 6.7. The amount of nitrogen found on these samples is higher than on the previous chapters. The solubility is also affected by the low temperature, for example, the amount of nitrogen dissolved into bitumen.

It was suggested that the presence of solids tends to increase along with reaction time [8]. For the previous chapters, this was not true. However, Figure 6.9 agrees with this statement. Compared to previous chapters, the amount of solids generated from visbreaking at  $150\text{ }^\circ\text{C}$  is considerably lower with a maximum of  $2.4\text{ wt}\%$ .

The amount of asphaltenes obtained from these samples was as high as the set of experiments performed at  $200\text{ }^\circ\text{C}$  in Chapter 5. Two explanations could be possible: first, the addition mechanisms promoted by low temperatures can also benefit the development of asphaltenes; or

second, maltenes (resins) composition is changing and it could not avoid the aggregation process [9]. This may induce the asphaltene precipitation.

## 6.5 CONCLUSIONS

This work showed some similarities with Chapter 5 but some differences with Chapter 3 and 4 were noted.

- a) After performing visbreaking at 150 °C, it was found that viscosity cannot be decreased under these reaction conditions. As a result, viscosity has increased up to  $5.6 \times 10^3$  Pa.s which is higher than the initial viscosity measured to the Cold Lake bitumen feed. The only possible exception is the somewhat lower viscosity found after only 1 hour reaction time.
- b) It is possible that reaction time has a strong influence on the reactions that are taking place. Thermodynamically, addition reactions are favoured under low temperatures. Having longer reaction times could benefit polymerization processes.
- c) Based on the FT-IR spectra, the presence of some functional groups remain constant. Its intensities may vary. This suggests that bitumen does not experienced big changes; however, the changes can make a big difference to the bitumen properties.
- d) The distribution of hydrogen follows a different trend respect to previous chapters. In this case, secondary aliphatic and benzylic protons change abruptly between 4 and 5 hours reaction.
- e) A high formation of solids at 8 hour reaction could be related with the production of  $C_1$  in the gaseous phase.

### Literature cited

[1] ASTM D341-09. *Standard Practice for Viscosity-Temperature Charts for Liquid Petroleum Products*; ASTM: West Conshohocken, PA, 2009

[2] Schmidt, P. F. *Fuel Oil Manual. Volume 10*; Industrial Press, Inc.: New York, 1985, p.72.

[3] Speight, J. G., Ozum, B. *Petroleum Refining Processes*; Marcel Dekker: New York, 2002, p. 385

- [4] Speight, J. G., Ozum, B. *Petroleum Refining Processes*; Marcel Dekker: New York, 2002, p. 388
- [5] Speight, J. G. *Heavy Oil Production Processes*; Elsevier Science: Burlington, 2013. p. 135
- [6] Silverstein, R. M.; Bassler, G. C. *Spectrometric Identification of Organic Compounds*; 4th ed.; Wiley: New York, 1981.
- [7] Borrego, A. G.; Blanco, C. G.; Prado, J. G.; Diaz, C.; Guillen, M. D. <sup>1</sup>H NMR and FTIR Spectroscopic Studies of Bitumen and Shale Oil from Selected Spanish Oil Shales. *Energy Fuels* **1996**, *10 (1)*, 77–84.
- [8] Wiehe, I. A. *Process chemistry of petroleum macromolecules*; CRC Press: Boca Raton, FL, 2008, p. 142
- [9] Ghanavati, M.; Shojaei, M.-J.; Ahmad Ramazani, S. A. Effects of Asphaltene Content and Temperature on Viscosity of Iranian Heavy Crude Oil: Experimental and Modeling Study. *Energy & Fuels* **2013**, *27(1)* 7217–7232.

## 7. CONCLUSIONS

### 7.1 INTRODUCTION

Visbreaking can be considered a mature upgrading technology. It involves mild thermal cracking and the typical operating temperature range employed in industrial units is 430 to 490 °C. Previous studies in our group indicated that for oilsands bitumen it was possible to achieve a two order of magnitude viscosity reduction at milder conditions, namely, in the temperature range 340 to 400 °C. It was postulated that much of the viscosity reduction was due to deaggregation and not cracking, which implied that the same might be achieved at even lower temperatures. Visbreaking was not widely explored under low temperature conditions. There was a clear opportunity to expand knowledge in the field of thermal conversion of oil sands bitumen by studying and understanding of the nature of the transformations taking place over time when oil sands bitumen is exposed to low temperatures. An investigation of the thermal conversion of oil sands bitumen at low temperatures in the range 150-300 °C and reaction times of 1 to 8 hours was conducted. The two manipulated variables were temperature and reaction time.

### 7.2 MAJOR CONCLUSIONS

- a) Visbreaking was performed in order to reduce bitumen viscosity. Based on the results obtained in this work, the range of temperature used shows a discontinuity in the response of viscosity to thermal treatment at a temperature somewhere between 200 and 250 °C. The viscosity response of bitumen treated at 250 and 300 °C was completely different to that of bitumen treated at 200 and 150 °C. At 250 and 300 °C a viscosity decrease was achieved and a lower viscosity was obtained from products of visbreaking at 300 °C than 250 °C. On the other hand, a viscosity increase was evidenced in bitumen exposed to 200 and 150 °C. The highest product viscosities were obtained from samples of visbreaking at 200 °C.

- b)** The observed changes on bitumen after visbreaking can be explained in terms of free radical reactions. One of the factors that may favour these processes is hydrogen disproportionation. It was observed in all the experiments even at short reaction times.
- c)** In general, the amount of gaseous products formed during the reactions did not exceed 5 wt%. The presence of C<sub>1</sub> was predominantly observed when visbreaking was conducted at 300 °C and was much less evident at lower temperature conversion. C<sub>5</sub> was the main gaseous product for visbreaking at 250, 200 and 150 °C. The results suggest that the energy provided at 250 °C and lower temperature was not enough to overcrack the bitumen.
- d)** Reaction time and temperature are considered the most influential factors in determining visbreaking performance. Based on the results obtained in this work, it seems that the impact of temperature becomes less as temperature is decreased and reaction rate is slowed. This causes the influence of reaction time to be more pronounced at lower temperatures.
- e)** Performing visbreaking with longer reaction times benefitted free radical addition reactions (polymerization). Furthermore, the stabilization of larger molecules by inter- and intramolecular rearrangement could also take place at extended reaction times.
- f)** Asphaltene content was significantly lower in visbroken products obtained after reaction at 300 °C. On the other hand, a dramatically increase was observed in those products obtained in visbreaking performed at 250, 200 and 150 °C. A high asphaltene content could suggest compositional changes in bitumen as a consequence of a change in resins composition.
- g)** The viscosity changes obtained from visbreaking bitumen at 300 °C spanned orders of magnitude, yet, the asphaltenes content remained low and in a narrow range. The

molecules that constitute the asphaltenes content might affect bitumen viscosity, however, the results were clear that an increase on viscosity cannot be attributed solely to a high asphaltenes content.

- h) FT-IR was used to determine changes in bitumen. Spectra obtained did not show significant variations. However, conversion affected the presence of carbon double bonds. It is likely that thermal reactions at low temperatures could promote the formation of structures with carbon double bonds.
- i) Refractive index and density could be used to determine compositional changes. It was found that a decrease in these properties could be related with a reduction in the amount of aromatic hydrogen. As a consequence, it is probable that the presence of naphthenic molecules have increased.

### **7.3 FUTURE WORK**

This work provided interesting results. However, there are some points that could be studied in more detail.

- a) Visbreaking is mainly focused on liquid products. However, a solid fraction was obtained from this process. The solids fraction contained coke and other solids e.g. sand. An in-depth study could provide information about the actual amount of coke produced in this process, and it may also guide on the understanding of reaction mechanisms related to visbreaking.
- b) Visbreaking in a narrow temperature range should be studied. After performing visbreaking at 200 and 250 °C, it was found that the viscosity response of bitumen to the thermal treatment changed dramatically. This change could suggest a discontinuity that could be very useful for the understanding of bitumen behaviour.

- c) At 150 °C and 1 hour reaction time, a marginal decrease in bitumen viscosity was observed that was different to all other observations at 150 and 200 °C. Since visbreaking was not investigated at shorter reaction times than 1 hour, there is no information about the initial reactions and their impact on product properties. It might be worthwhile following up on this seemingly anomalous observation.
- d) Viscosity can be decrease for those reactions performed at 300 and 250 °C. However, products obtained from visbreaking at 200 and 150 °C show a tendency to increase viscosity. It is possible to determine a change on the viscosity response to the thermal treatment. For the first two temperatures (higher ones), the viscosity has the biggest reduction after 2 hours reaction.

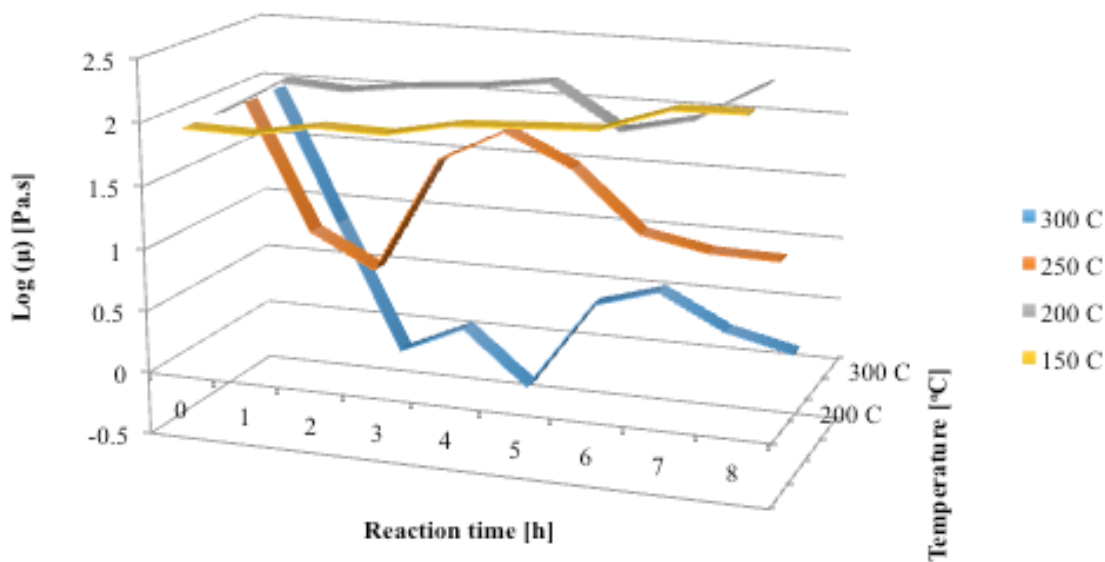


**Figure 7.1** Changes observed in Log ( $\mu$ ) along reaction time for the different reaction temperatures.

## 7.4 PRESENTATIONS

- Yañez, L.; De Klerk, A. Visbreaking of bitumen at low temperatures. Poster presentation: Helmholtz-Alberta Initiative 4<sup>th</sup> HAI Science Forum, Edmonton, Canada, September 29, 2014.

- Yañez, L.; De Klerk, A. Visbreaking oilsands bitumen at 300 °C. *Prepr. Pap.-Am. Chem. Soc., Div. Energy Fuels* **2015**, *60(1)*, 31-34.
- Yañez, L.; De Klerk, A. Visbreaking of oilsands bitumen at 250 °C. Poster presentation: 6<sup>th</sup> Faculty of Engineering Graduate Research Symposium (FEGRS 2015), Edmonton, Alberta, June 15-16, 2015.

## BIBLIOGRAPHY

ASTM D341-09. *Standard Practice for Viscosity-Temperature Charts for Liquid Petroleum Products*; ASTM: West Conshohocken, PA, 2009

ASTM D6560-12: *Standard test method for Determination of Asphaltenes in Crude Petroleum and Petroleum Products*; ASTM: West Conshohocken, PA, 2012.

Abou El Naga, H. H.; Abd El Aziem, M. W.; Mazin, A. S. The effect of the aromaticity of base stocks on the viscometric properties of multigrade oils. *Lubrication Sci.* **1998**, *10*, 343–363.

Ancheyta Juárez, J., Rana, M. S., & Trejo, F. Hydrocracking and Kinetics of Asphaltenes. In *Asphaltenes: Chemical Transformation during Hydroprocessing of Heavy Oils*; CRC Press/Taylor & Francis: Boca Raton, FL, 2009.

Ancheyta Juárez, J. *Modeling of processes and reactors for upgrading of heavy petroleum*; CRC Press: Boca Raton, 2013, p. 73.

Borrego, A. G.; Blanco, C. G.; Prado, J. G.; Diaz, C.; Guillen, M. D. <sup>1</sup>H NMR and FTIR Spectroscopic Studies of Bitumen and Shale Oil from Selected Spanish Oil Shales. *Energy Fuels* **1996**, *10* (1), 77–84.

Bulkowski, P. and Prill, G. *Abridged internal report on bitumen densities as function of temperature*. Internal report, Research Council of Alberta. Edmonton, Alberta. 1978.

Bunghez, I-R.; Ion, R-M.; Fierascu, R. C.; Radu, C.; Dumitriu, I.; Ion, M-L.; Neata, M.; Doncea, S-M. GC-MS and FTIR Analysis of Bitum/Kerogen as Organic Geochemistry Index. *Petroleum - Gas University of Ploiesti Bulletin, Technical Series* **2010**, *62* (3A), 163-168

Carrillo, J. A.; Pantoja E.; Garzón, G.; Barrios, H.; Fernandez, J.; Carmona, E.; Saavedra, J. Control of severity in visbreaking. *Prepr. Pap.-Am. Chem. Soc., Div. Energy Fuels* **2000**, *45*(3), 617-621.

Chopra, S. *Heavy Oils: Reservoir Characterization and Production Monitoring*; Society of Exploration Geophysicists: Tulsa, OK, 2010.

Cowan, B. P. *Nuclear Magnetic Resonance and Relaxation*; Cambridge University Press: New York, 1997.

Cronauer, D.; Snyder, R.; Painter P. Characterization of oil shale by FTIR spectroscopy. *Prepr. Pap.-Am. Chem. Soc., Div. Fuel Chemistry* **1982**, 27 (2), 122-131

De Klerk, A.; Gray, M. R.; Zerpa, N. Unconventional Oil and Gas: Oilsands, In *Future Energy: improved, sustainable and clean options for our planet*, 2ed; Letcher, T.M. Ed.; Elsevier: London, 2014, p. 95-116.

Evdokimov, I. N.; Losev, A. P. Effects of molecular de-aggregation on refractive indices of petroleum-based fluids. *Fuel* **2007**, 86, 2439-2445.

Flach, P. D. *Oil Sands Geology: Athabasca Deposit North*; Geological Survey Dept., Alberta Research Council: Edmonton, Alta., Canada, 1984.

Gary, J. H.; Handwerk, G. E. *Petroleum Refining: Technology and Economics*, 5ed; Taylor & Francis Group: Boca Raton, FL, 2007, p. 111-115.

Ghanavati, M.; Shojaei, M.-J.; Ahmad Ramazani, S. A. Effects of Asphaltene Content and Temperature on Viscosity of Iranian Heavy Crude Oil: Experimental and Modeling Study. *Energy & Fuels* **2013**, 27(1) 7217–7232.

Goual, L.; Firoozabadi A. Measuring Asphaltenes and Resins, and Dipole Moment in Petroleum Fluids. *AIChE J.* **2002**, 48, 2646-2663.

Gray, M. R. *Upgrading oilsands bitumen and heavy oil*; Pica Pica Press, an imprint of the University of Alberta Press, 2015.

Hardinger, S. "Infrared Spectroscopy". *Department of Chemistry and Biochemistry at University of California*, Los Angeles. 29 August **2006**. Visited 29 October 2015 <[http://www.chem.ucla.edu/harding/notes/notes\\_14C\\_IR.pdf](http://www.chem.ucla.edu/harding/notes/notes_14C_IR.pdf)>

Hein, F. J.; Berhane, H. *Cold Lake Oil Sands Area Formation Picks and Correlation of Associated Stratigraphy*; Alberta Geological Survey: Edmonton, 2006.

Huc, A. Y. *Heavy crude oils, from geology to upgrading: an overview*; Editions Technip: Paris, 2011.

- Jha, K. N.; Montgomery, D. S.; Strausz, O. P. Chemical composition of gases in Alberta bitumens and in low-temperature thermolysis of oil sand asphaltenes and maltenes. In *Oil sand and oil shale chemistry*; Strausz, O. P., Lown, E. M. Eds.; Verlag Chemie: New York, 1978, p.33-54.
- Joshi, J. B.; Pandit, A. B.; Kataria, A. B.; Kulkarni, R. P.; Sawarkar, A. N.; Tandon, D.; Yad, R.; Mohan, K. M. Petroleum Residue Upgradation via Visbreaking: A Review. *Ind. Eng. Chem. Res.* **2008**, *47*(23), 8960-8988.
- Karlsson, R.; Isacson, U. Application of FTIR-ATR to Characterization of Bitumen Rejuvenator Diffusion. *J. Mater. Civ. Eng.* **2003**, *15*(2), 157-165
- Lee, S., Speight, J. G., Loyalka, S. K. Handbook of Alternative Fuel Technologies; CRC Press: Boca Raton, 2015, p. 222.
- Majid, A.; Pihillagawa, I. Potential of NMR Spectroscopy in the Characterization of Nonconventional Oils; *Journal of Fuels* **2014**, *1*, 1–7.
- Manning, F. S.; Thompson, R. E. *Oilfield Processing of Petroleum*; PennWell Books: Tulsa, Okla., 1991, p. 19.
- Masliyah, J. H., Xu, Z., Czarnecki, J. A., Dabros, M. *Handbook on theory and practice of bitumen recovery from Athabasca Oil Sands*; Cochrane, Alta.: Kingsley Knowledge Pub., 2011-2013.
- Masson, J.-F.; Polomark, G. Bitumen Microstructure by Modulated Differential Scanning Calorimetry. *Thermochimica Acta* **2011**, *374* 105–114.
- McKetta, J. J. *Petroleum Processing Handbook*; M. Dekker: New York, 1992.
- McNab, J. G.; Smith, P. V. Jr; Betts, R. L. The evolution of petroleum. *Ind. Eng. Chem.* 1952, *44*, 2556-2563.
- Mehrotra, A. K. A generalized viscosity equation for liquid hydrocarbons: Application to oil-sand bitumens. *Fluid Phase Equil.* **1992**, *75*, 257-268.
- National Aeronautic and Space Administration. Air Viscosity. Visited online (January, 2016): <<https://www.grc.nasa.gov/www/BGH/viscosity.html>>

North, F. K. *Petroleum Geology*; Allen & Unwin: Boston, 1985, p.56.

Ovalles, C.; Rechsteiner, C. J. Application of NMR Technology in Petroleum Exploration and Characterization. In *Analytical methods in petroleum upstream applications*; CRC Press: Boca Raton, 2015

Parsons, A. F. *An introduction to free radical chemistry*; Blackwell: Oxford, 2000.

Sachanen, A. N.; Tilicheev, M. D. *Chemistry and Technology of Cracking*; Chemical Catalog Co.: New York, 1932.

Schmidt, P. F. *Fuel Oil Manual. Volume 10*; Industrial Press, Inc.: New York, 1985, p.72.

Speight, J. G. Heavy Feedstock Refining—The Future. In *Heavy And Extra-Heavy Oil Upgrading Technologies*; Gulf Professional Publishing: Oxford, 2013.

Speight, J. G. *Heavy Oil Production Processes*; Elsevier Science: Burlington, 2013. p. 135

Speight, J. G., Ancheyta Juárez, J. *Hydroprocessing of Heavy Oils and Residua*; CRC Press: Boca Raton, 2007, p. 45.

Speight, J. G., Ozum, B. *Petroleum Refining Processes*; Marcel Dekker: New York, 2002, p. 77.

Speight, J.G. *The Chemistry and Technology of Petroleum*, 4th ed.; Taylor & Francis Group: Boca Raton, FL, 2007.

Speight, J. G. Visbreaking: A technology of the past and the future. *Scientia Iranica* **2012**, *19* (3), 569-573.

Stangeby, P. C.; Sears, P. L. Yield of heated oil sand. In *Oil sand and oil shale chemistry*; Strausz, O. P., Lown, E. M. Eds.; Verlag Chemie: New York, 1978, p.101-118.

Strausz, O. P.; Lown, E. M. *The Chemistry of Alberta Oil Sands, Bitumens and Heavy Oils*; Alberta Energy Research Institute: Calgary, 2003.

Silverstein, R. M.; Bassler, G. C. *Spectrometric Identification of Organic Compounds*; 4th ed.; Wiley: New York, 1981.

*The Shell Bitumen Industrial Handbook*; Shell Bitumen: Chertsey, 1995, p.53.

ThermoScientific. Introduction to Fourier Transform Infrared Spectroscopy. *Molecular Materials Research Centre, Beckman Institute, California Institute Technology*. Visited November 6, 2015. <http://mmrc.caltech.edu/FTIR>

Tissot, B. P.; Welte, D. H. *Petroleum Formation and Occurrence*; 2nd, rev. and enl.; Springer-Verlag: Berlin, 1984, p.222.

Wang, L. Low temperature visbreaking. MSc thesis, University of Alberta, Edmonton, AB, Canada, 2013.

Wang, L.; Zachariah, A.; Yang, S.; Prasad, V.; De Klerk, A. Visbreaking oilsands-derived bitumen in the temperature range of 340-400 °C. *Energy Fuels* **2014**, *28*, 5014-5022.

Wang, L.; Zachariah, A.; Yang, S.; Prasad, V.; De Klerk, A. Visbreaking oilsands-derived bitumen in the temperature range of 340-400 °C. *Energy Fuels* **2014**, *28*, 5014-5022.

Wiehe, I. A. *Process chemistry of petroleum macromolecules*; CRC Press: Boca Raton, 2008, p. 369

Winter, H. H. Viscous Dissipation Term in Energy Equations. In *American Institute of Chemical Engineers, Modular Instruction*. R. J. Gordon, Ed.; *AIChE J*, New York, **1987**.

Yanez, L.; De Klerk, A. Visbreaking of Oil Sands bitumen at 300 °C. *Prepr. Pap.-Am. Chem. Soc., Div. Energy Fuels* **2015**, *60*(1), 31-34.

Zachariah, A. Low temperature pyrolysis and its application in bitumen processing. MSc thesis, University of Alberta, Edmonton, AB, Canada, 2014.

Zachariah, A.; Wang, L.; Yang, S.; Prasad, V.; De Klerk, A. Suppression of coke formation during bitumen pyrolysis. *Energy Fuels* **2013**, *27*, 3061-3070.

Zong-xian Wang; Ai-Jun Guo; Guo-he Que. Coke formation and characterization during thermal treatment and hydrocracking of Liaohe vacuum residuum. *Prepr. Pap.-Am. Chem. Soc., Div. Energy Fuels* **1998**, *43*(3), 758-764.

Zou, C. Heavy Oil and Bitumen, In *Unconventional Petroleum Geology*; Elsevier: Burlington, Mass., 2013, p. 307-335.

## APPENDICES

### APPENDIX A. Schematic reactor.

Micro reactors utilized for visbreaking reactions were obtained from Swagelok. They were built using Stainless Steel 316. The inner diameter is 2.7 cm and its length is 8.7 cm.

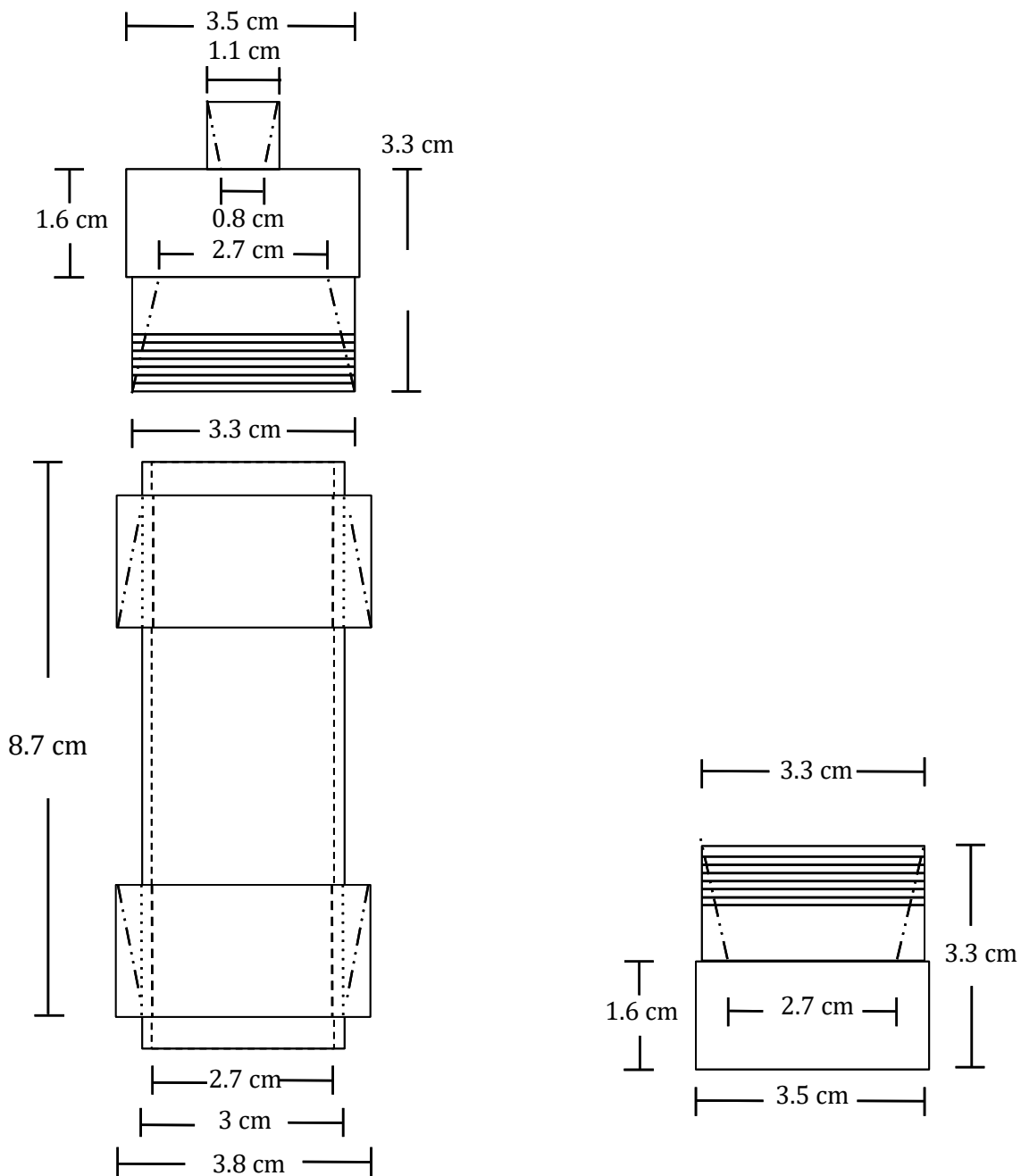
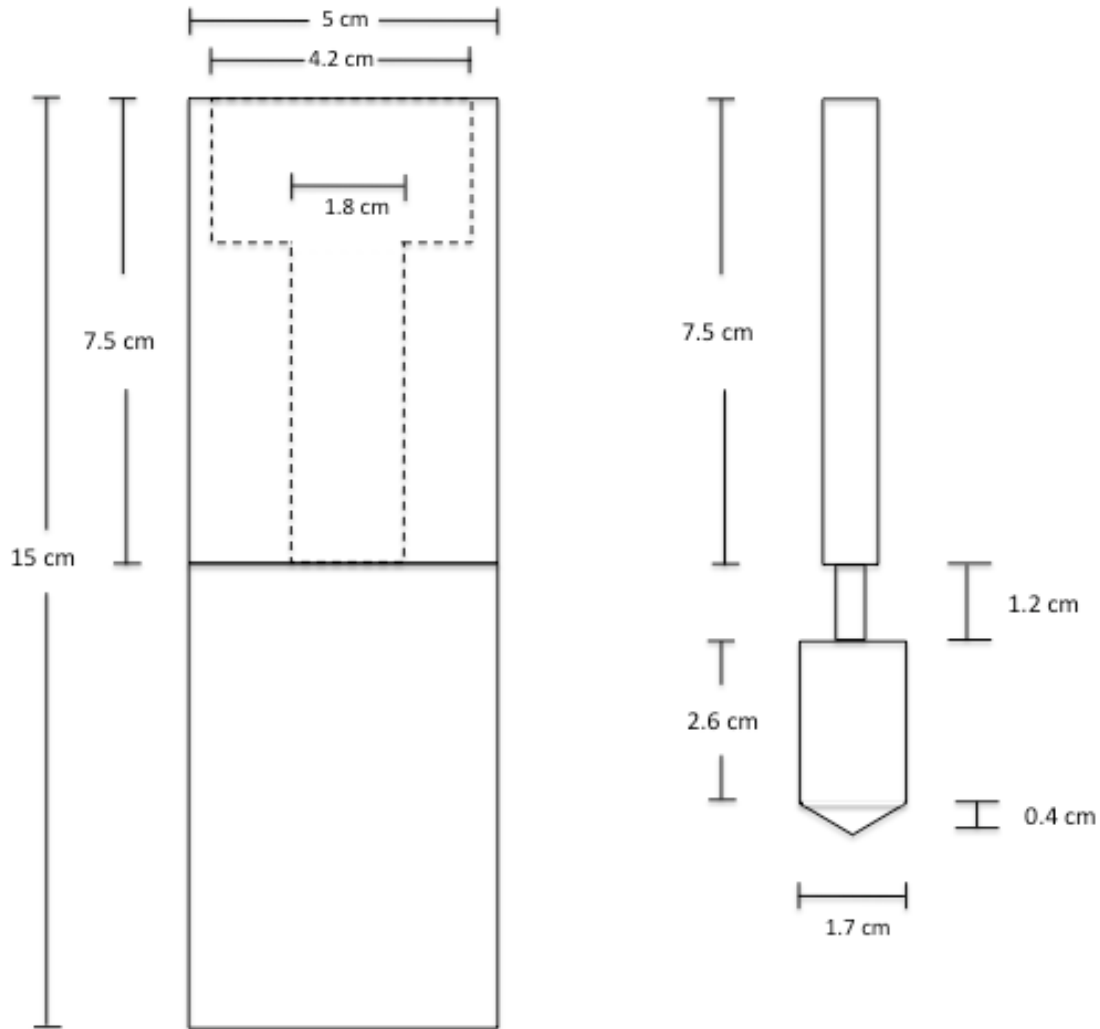


Figure A-1. Micro reactor used for visbreaking reactions.

**APPENDIX B.** Viscometer cell scheme.

The cell employed for performing viscosity measurements is shown in Figure B-1. This is a rotational rheometer operating under the Searle's principle (the measuring bob is rotating and the cup is still).



**Figure B-1.** Viscometer cell used to perform viscosity measurements in an Anton Paar RheoLabQC.

The measurement cup and bob coupled are shown in Figure B-2. The measuring bob can rotate inside the measuring cup where the sample is placed.

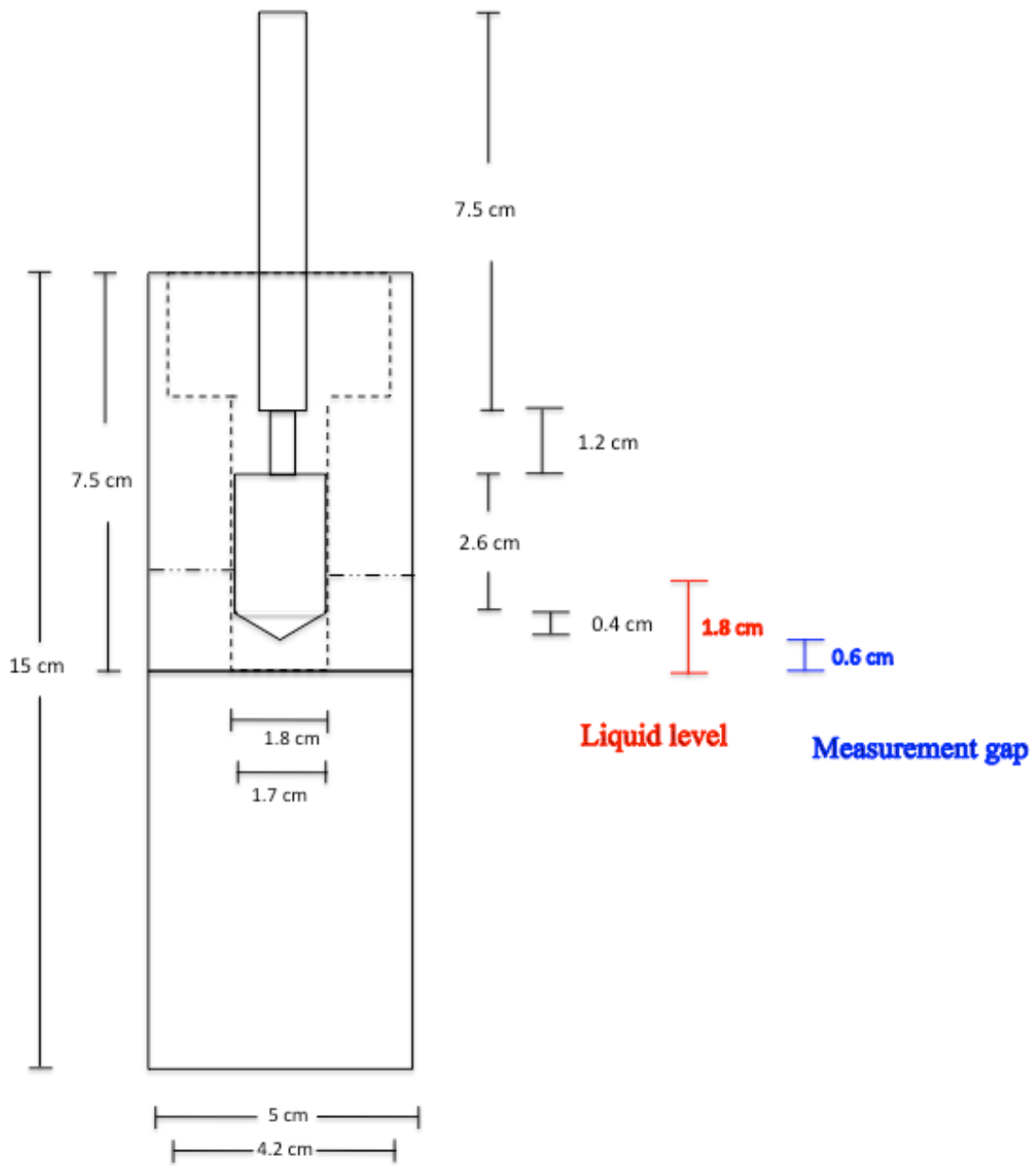


**Figure B-2.** Side view of the measurement cup and bob.

### APPENDIX C. Viscous heating.

Viscosity measurements can affect the fluid behavior. Shear forces face the internal resistance to flow of a substance, i.e. friction. The mechanical energy is transformed into internal energy (heat) [1]; as a consequence, the temperature can increase which will lead a viscosity decreasing.

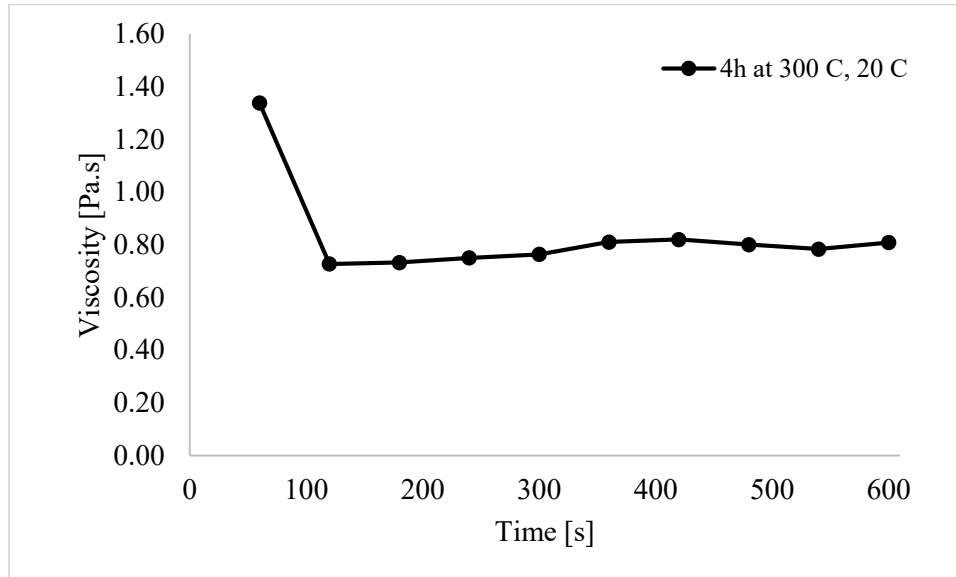


**Figure C-1.** Variation on viscosity along measurement time. Visbreaking sample obtained after 4 hours of reaction at 300 °C. Measurement temperature: 20 °C.

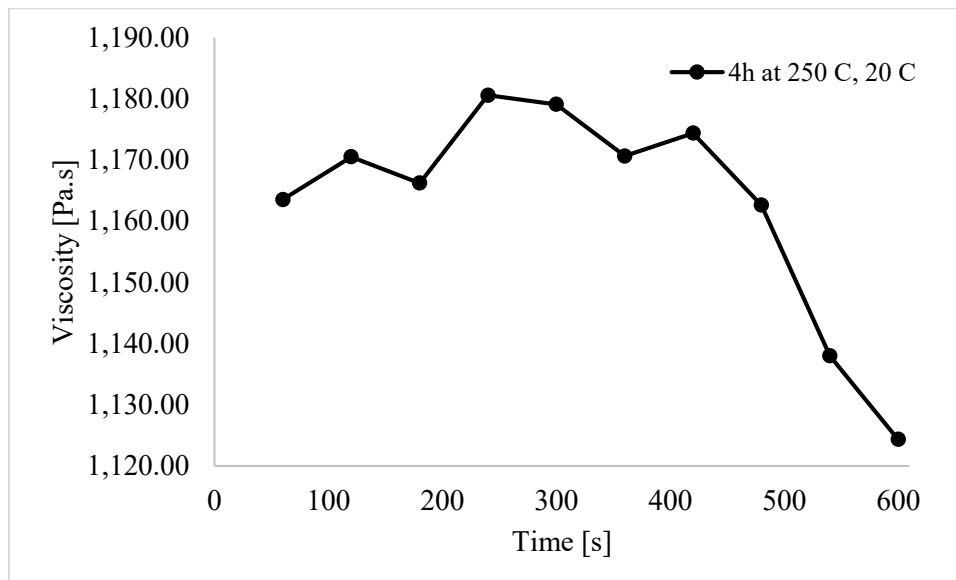


**Figure C-2.** Variation on viscosity along measurement time. Visbreaking sample obtained after 4 hours of reaction at 250 °C. Measurement temperature: 20 °C.

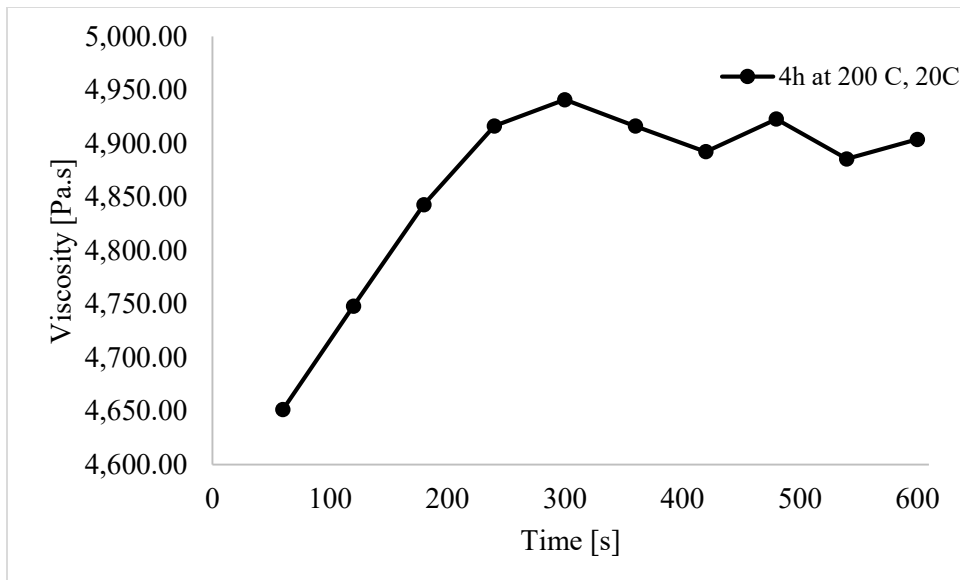


**Figure C-3.** Variation on viscosity along measurement time. Visbreaking sample obtained after 4 hours of reaction at 200 °C. Measurement temperature: 20 °C.

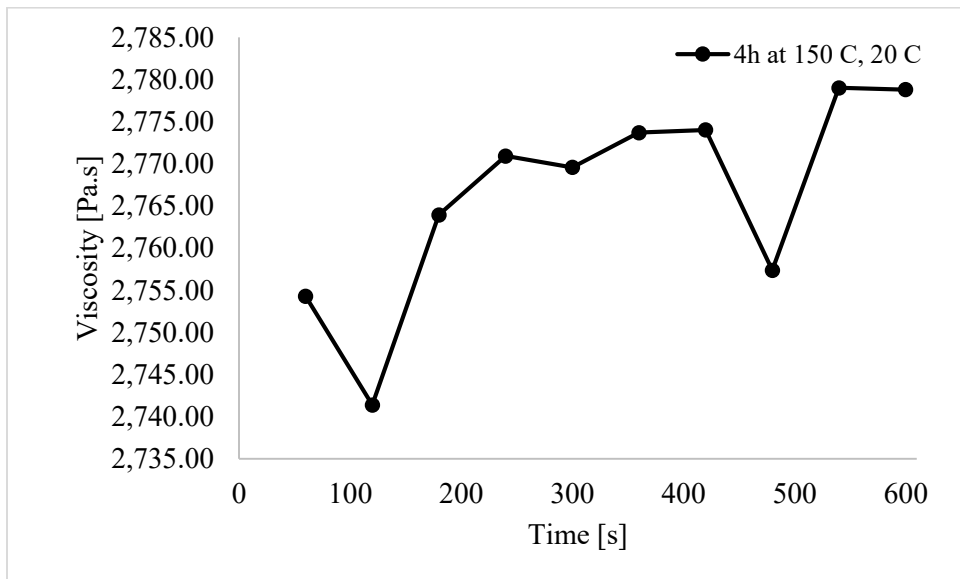
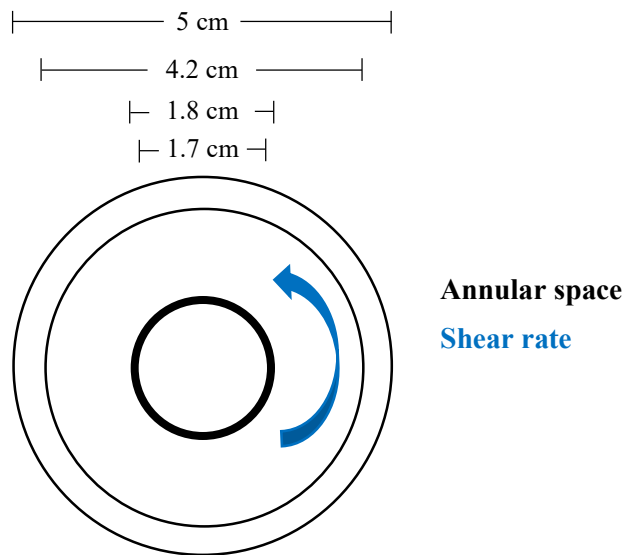


**Figure C-4.** Variation on viscosity along measurement time. Visbreaking sample obtained after 4 hours of reaction at 150 °C. Measurement temperature: 20 °C.

Figures C-1 and C-2 show a decreasing on viscosity, even though the shear rate was kept constant, the shear stress was varying which is reflected on the viscosity results. This behavior can be explained by the viscous heating.

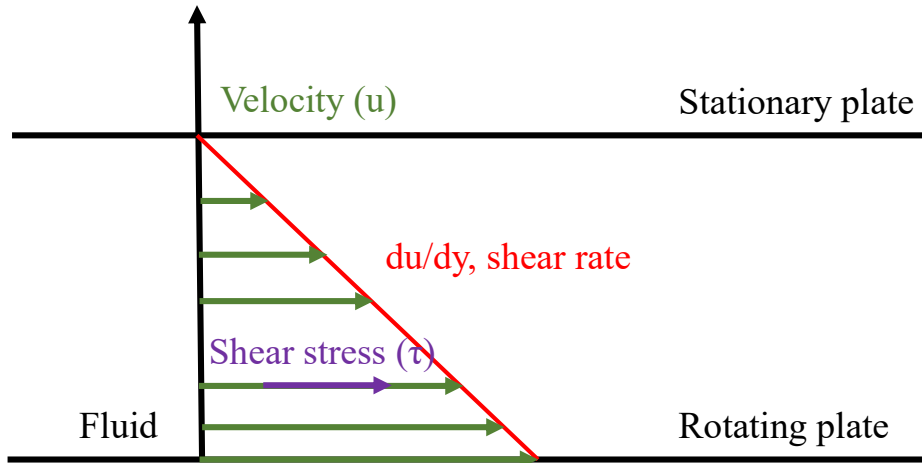
On the other hand, Figures C-3 and C-4 present a viscosity increase, which can be a hint to think about a non-Newtonian behavior. However some other factors could be affecting the viscosity response.

Figure C-5 shows a top view of the measurement system (RheoLab QC cup and bob) where the annular space corresponds to the fluid. The blue arrow is indicating the direction of the spin.



**Figure C-5.** Viscosity measurement scheme

In order to show how the measurement is performed, Figure C-3 presents a scheme of the configuration of the two concentric cylinders. The shear stress will follow the same direction as the angular velocity. On the other hand, the shear stress will be tangential to the flow. The viscosity value is the result of the torque measurement did by the equipment. It is important to note that the torque is the result of the force applied and the position where this force is applied.



**Figure C-3.** Schematic description of the forces included during a viscosity measurement. Based on [2]

### Literature cited

[1] Winter, H. H. Viscous Dissipation Term in Energy Equations. In American Institute of Chemical Engineers, Modular Instruction. Edited by R. J. Gordon. New York, 1987.

[2] National Aeronautic and Space Administration. Air Viscosity. Visited online (January, 2016): <https://www.grc.nasa.gov/www/BGH/viscosity.html>